HEPATITIS C VIRUS SUPPRESSES AUTOPHAGOSOME DEGRADATION BY ARL8B-MEDIATED LYSOSOMAL REPOSITIONING

By

© 2016

Kellyann Nadira Jones-Jamtgaard

Submitted to the graduate degree program in Microbiology, Immunology, and Molecular Genetics and the Graduate Faculty of the University of Kansas in partial fulfillment of the requirements for the degree of Doctor of Philosophy.

—————————————————————————

Chairperson Steven A. Weinman, M.D., Ph.D.

—————————————————————————

Wen-Xing Ding, Ph.D.

—————————————————————————

Michael J. Parmely, Ph.D.

—————————————————————————

Edward B. Stephens, Ph.D.

—————————————————————————

Thomas M. Yankee, Pharm.D., Ph.D.

Date Defended: December 16, 2016

The Dissertation Committee for Kellyann Nadira Jones-Jamtgaard

certifies that this is the approved version of the following dissertation:

HEPATITIS C VIRUS SUPPRESSES AUTOPHAGOSOME DEGRADATION BY ARL8B-

MEDIATED LYSOSOMAL REPOSITIONING

_____

Chairperson Steven A. Weinman, M.D., Ph.D.

Date approved: December 16, 2016

Abstract

HCV infection increases steady-state autophagosome numbers but the mechanism of this effect is poorly understood. Flux assays suggest that an increase in autophagosomes results from a block in the fusion of autophagosomes with lysosomes. The aim of this study was to determine how HCV prevents autophagosome degradation. Autophagy induction and flux were measured by a flux assay involving western blotting for LC3-II after addition of the lysosomal inhibitor, bafilomycin A1. Flux through the autophagy pathway is greatly diminished compared to uninfected cells. To determine if HCV suppressed autophagosome-lysosome fusion events, control and HCV-infected cells were transfected with tandem RFP-GFP-LC3, where the quenching of the GFP fluorescence indicates autophagolysosome formation. In HCV-infected cells, there was no loss of GFP fluorescence from puncta indicating lack of fusion between autophagosomes and lysosomes even under conditions that activate autophagy. We then assessed the activity and maturation of lysosomal hydrolases from HCV-infected cells and determined that HCV did not decrease global lysosomal proteolytic activity. We next performed fusion assays with isolated subcellular organelles to assess whether lack of fusion was intrinsic to autophagosomes and lysosomes themselves. Vesicles isolated from HCV-infected cells fused with each other normally in vitro suggesting that the cellular fusion defect resulted from trafficking rather than inability of vesicles to fuse. To test this hypothesis, we studied organelle positioning focusing on Arl8b, an Arf-like GTPase that specifically localizes to lysosomes. In control cells, Arl8b was primarily found in a perinuclear localization and co-localized with LC3-positive autophagosomes. In JFH-1-infected cells, Arl8b localization was more diffuse and peripheral and there was a complete failure of Arl8b to co-localize with LC3, even after autophagy induction. Since Arl8b has the ability to link lysosomes to the outwardly-directed

motor protein kinesin, we examined the effect of HCV on Arl8b itself. After HCV infection, mRNA and protein levels of Arl8b were both elevated three-fold. Lentiviral-mediated knockdown of Arl8b in infected cells restored autophagic flux to levels seen in control cells. In conclusion, HCV suppresses autophagic flux and increases the steady-state levels of autophagosomes by increasing the expression of Arl8b. This GTPase links lysosomes to kinesin, repositions them toward the cell periphery and suppresses their ability to fuse with autophagosomes. These trafficking changes may promote the HCV lifecycle.

Acknowledgements

I would like to thank all those who made my journey through graduate school and the completion of this dissertation a fulfilling experience. I would like to thank my advisor, Dr. Steven Weinman, for allowing me to complete my research in his laboratory and for providing me with support and guidance throughout this process. I would also like to thank all the members of the Weinman lab for their guidance, scientific expertise, and friendship. I am grateful to my committee members, Drs. Wen-Xing Ding, Michael Parmely, Edward Stephens, and Thomas Yankee, for challenging me to become a better scientist during the course of my PhD. I would also like to thank all the faculty, staff, and students in the Microbiology, Immunology, and Molecular Genetics department for being my scientific community.

My parents have always believed in me and done everything in their power to provide the best opportunities for me and I will be eternally grateful to them. I am thankful for every museum visit, DIY science experiment, my first microscope, and allowing me to take advantage of every educational and extracurricular opportunity open to me. This dissertation is dedicated to my parents and brother.

Science brought my husband and me together when we first met at the NIH and he has become my biggest cheerleader. Graduate school can be an isolating experience and I am so glad to have had my best friend with me the whole time. I am also thankful for my parents-in-law for making me feel at home in the Midwest especially when my parents could not be there due to distance.

I would also like to acknowledge the network of individuals who have been my support system, mentors, and sponsors throughout graduate school and who have always pushed me to be

Table of Contents

List of Figures

Abbreviations

ALR—Autophagic lysosome reformation

AMPK—Adenosine monophosphate-activated protein kinase

ATG—Autophagy-related Gene

BafA—Bafilomycin A1

BORC—Biogenesis of lysosome-related organelles complex-one related complex

DAA—Direct Acting Antiviral

DFCP1—Double FYVE domain-containing protein 1

EBSS—Earle's Balanced Salt Solution

EGFR—Epidermal growth factor receptor

ESCRT—Endosomal sorting complexes required for transport

FYCO1—FYVE and coiled-coil domain containing 1

GAP—GTPase-activating proteins

GDP—Guanine diphosphate

GEF—Guanine nucleotide exchange factor

GTP—Guanine triphosphate

HOPS—Homotypic fusion and protein sorting

HCV—Hepatitis C Virus

HDL—High density lipoprotein

IPS—Interferon-β promoter stimulator

IRES—Internal ribosome entry site

LC3—Microtubule-associated protein light chain 3

LDL—Low density lipoprotein

LDL-R—Low density lipoprotein receptor

LPS—Lipopolysaccharide

MAVS—Mitochondrial antiviral-signaling protein

mTOR—Mechanistic target of rapamycin

NEAA—Non-essential amino acids

NPC1L1—Niemann-Pick C1-Like 1

ORP1L—Oxysterol-binding protein-related protein 1L

PE—Phosphatidylethanolamine

PERK—Protein kinase-like endoplasmic reticulum kinase

PKA—Protein Kinase A

PI3K—Phosphoinositide 3-kinase

PI3P—Phosphatidylinositol 3-phosphate

PLA—Proximity Ligation Assay

SR-B1—Scavenger receptor class B type I

RIG-I—Retinoic acid-inducible gene-1

RILP—Rab interacting lysosomal protein

SCV—Salmonella containing vacuole

SIF—Salmonella induced filaments

SKIP—SifA and kinesin-interacting protein

SNARE—Soluble N-ethylmaleimide-sensitive fusion attachment protein receptor

Stx—Syntaxin

SVR—Sustained Virological Response

TFEB—Transcription factor EB

TRIF—TIR-domain- containing adapter-inducing interferon-β

ULK1—Unc-51 Like Autophagy Activating Kinase 1

UPR—Unfolded Protein Response

UTR—Untranslated Region

UVRAG—UV radiation resistance-associated gene

VLDL—Very low density lipoprotein

VPS—Vacuolar protein sorting

Chapter I: Introduction

Hepatitis C virus (HCV) is a single-stranded, positive sense RNA virus and a member of the *Flaviviridae* family. It was known that cases of hepatitis from blood transfusions were caused by an agent other than Hepatitis A or Hepatitis B viruses as early as the 1970s, however, neither antibodies nor antigens could be identified using conventional methods. In 1989, a cDNA clone derived from RNA was discovered after screening a library with serum from a patient with non-A, non-B hepatitis and this virus was named Hepatitis C (1). HCV is represented by six genotypes with genotype 1 accounting for most infections though genotype prevalence depends on geography (2).

HCV is a leading cause of liver disease and hepatocellular carcinoma worldwide. It is estimated that 130-170 million people globally are infected with almost half a million deaths from HCV-related complications yearly (3). Based on data from the National Health and Nutrition Examination Survey conducted from 2003-2010, the prevalence of chronic HCV in the United States is approximately 2.7 million people (4). If HCV infection becomes chronic, up to 30% of infected persons will go on to develop liver cirrhosis usually decades after initial infection and of those that develop cirrhosis, up to 4% per year will develop hepatocellular carcinoma (5).

Therapy for HCV infection has developed quickly in the twenty-five years since the discovery of the virus. Currently there are several available direct acting antivirals (DAA) that can be used in various combinations clinically to achieve a sustained virological response (SVR) in patients. SVR is defined as no detectable HCV RNA levels twelve or twenty-four weeks after the end of treatment. DAAs target either the viral protease NS3/4A, the viral RNA-dependent RNA polymerase NS5B, or the viral replication machinery through NS5A. Combinations of

DAAs with or without ribavirin can be used to achieve 98% SVR especially in patients with genotypes 1 and 2 (6). Ribavirin is a purine nucleoside analog that has been a longstanding part of HCV treatment prior to the advent of DAAs. It is possible that with increased screening for HCV and greater access to treatment regimens, the incidence of long-term deleterious effects from HCV infection will decrease substantially. However, there is still a need for a HCV vaccine and greater insight into the HCV immunological response will be needed to produce one (7).

Hepatitis C Virus Genome

The HCV genome is approximately 9.6kB in length and is translated into a ~3000 amino acid polyprotein that contains ten viral proteins. The open reading frame for the polyprotein is flanked by a 5' and 3' untranslated region (UTR). The 5' UTR contains the internal ribosome entry site (IRES) that is responsible for directing translation of the genome in a cap-independent manner (8). The endoplasmic reticulum signal peptidase cleaves the structural proteins, core, E1 and E2, as well as the viroporin, p7. Viral proteases, NS2/3 and NS3/4A, cleave the nonstructural proteins, NS2, NS3, NS4A/B, and NS5A/B (9).

Core, E1, and E2 make up the structural proteins that form the nucleocapsid and envelope proteins of the HCV virion. After cleavage by the signal peptidase, core protein is further processed into its mature form by signal peptide peptidase (10). Core is a multifunctional protein that also exists freely in the cell and associates with lipid droplets. Core protein association with lipid droplets appears to be critical for the production of infectious virus (11). E1 and E2 are glycoproteins that form the viral envelope and play a role in viral entry into the cell. Additionally, E1 and E2 are at the center of strategies around vaccine development since challenge with E1/E2 can elicit neutralizing antibodies.

Figure 1 HCV Viral Polyprotein. Schematic of the open reading frame of HCV showing the 9.6 kB RNA genome flanked by 5' and 3' UTR regions. The open reading frame encodes a 3000 amino acid polyprotein made up of ten structural and nonstructural proteins. The triangles show where the polyprotein is cleaved and whether the cleavage is mediated by host or viral protease.

structural proteins

nonstructural proteins

1

3011

5' UTR

core

E1

E2

p7

NS2

NS3

A

NS4B

NS5A

NS5B

3' UTR
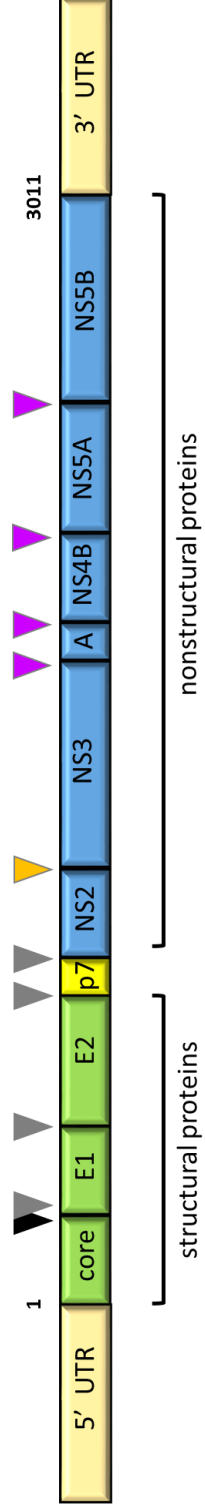
core cleavage by signal peptide peptidase

cleavage by signal peptidase

NS2-NS3 autocatalytic cleavage

NS3-NS4A viral protease cleavage

p7 is a viroporin that can form ion channels in membranes and is necessary for production of infectious virus. Our lab has previously studied the function of p7 and demonstrated that p7 could alkalinize acidic compartments within the cell raising the pH of vesicles to almost 6.0 compared with a pH of 4.0-4.5 in control cells. Additionally, either blocking p7 by using specific inhibitors could reduce the yield of infectious virus or alkalinizing vesicles pharmacologically could rescue virus production in a p7 channel-inactive mutant (12). p7 likely has other functions apart from its ion channel activity and may influence virion assembly through interactions with NS2 (13).

NS2, NS3, NS4A/B, and NS5A/B are the nonstructural proteins of HCV which function primarily in replication and assembly of the virus. NS2 is thought to play a role in virion assembly. NS2 can interact directly or in complex with p7, E1, E2, NS3, and NS5A (14, 15). NS2 localizes to ER-derived structures that may represent sites of virus assembly and mutations in viral proteins that affect NS2 localization impair infectious virus production. NS3 functions both as a protease in concert with NS4A and as a helicase to unwind RNA. In addition to cleaving the HCV polyprotein to produce the nonstructural proteins, the NS3/4A protease also functions in evasion of the host innate immune response. NS3/4A has been shown to cleave both MAVS, a mitochondrial antiviral signaling protein, and TRIF (Toll-IL-1 receptor domain-containing adaptor inducing IFN-β) to inhibit downstream production of interferon-β (16, 17). NS4B has been implicated in the formation of the membranous web which is thought to be the site of viral replication. Though its functions are not well characterized, NS4B has been shown to interact with a wide range of host proteins and may influence a diverse set of pathways including cellular stress by inducing the unfolded protein response (UPR), lipid metabolism, and cellular transformation (18). NS5A is a protein that can be heavily phosphorylated and aids in viral

replication and assembly. It has been shown that core protein and NS5A localize to lipid droplets and interact with HCV RNA-positive structures which may serve as a site for viral particle assembly (19). NS5B is the RNA-dependent RNA polymerase which is responsible for the key steps in HCV replication of making a negative-strand RNA intermediate from the positive-strand template and then converting the negative-strand RNA back to positive-strand RNA. Replication is error-prone due to lack of proof-reading capability by NS5B which generates a diversity of RNA genomes resulting in a quasispecies within an infected individual (9). NS5A and NS5B are also the main targets of commercially available DAAs to inhibit replication of the virus.

Hepatitis Virus Life Cycle

The HCV life cycle occurs completely in the cytosol of the cell. The main steps of the life cycle are binding of the virus and host cell entry, translation and polyprotein processing, RNA replication, virus assembly, and virus release from the host cell. Host tropism of HCV is limited to humans and chimpanzees with the hepatocyte being the primary cell type infected.

Host Cell Entry

HCV entry into cells is mediated by the glycoproteins E1 and E2 from the virus and CD81, SR-BI, claudin-1, and occludin are considered the essential host cell receptors/co-receptors. CD81 is the main HCV receptor and has been shown to bind directly to E2 (20). Normally, CD81 functions as a receptor for the B and T cell receptor complex and mediates vesicular fusion. It has been shown that HCV infection can be blocked by anti-CD81 antibodies and that cells can become permissive to HCV infection in cell culture by ectopically expressing CD81 (21, 22). SR-B1 (scavenger receptor call B type 1) also binds E2 and may act cooperatively with CD81 (23, 24). SR-B1 functions as a lipoprotein receptor and can bind

Figure 2 HCV Lifecycle. 1) The virus binds to receptors on the cell surface. The essential receptors are listed in the box. 2) After the virus is internalized by clathrin-mediated endocytosis, the RNA genome is released into the cytoplasm. The positive-stranded genome can be translated directly to produce the HCV polyprotein that is cleaved into the structural and nonstructural proteins or used for viral replication. 3) Viral replication takes place on a structure called the membranous web. The incoming RNA is a template to make negative-strand RNA which can then be used to make multiple copies of positive-strand RNA. 4) The RNA genome is then packaged into a viral particle containing a core capsid and envelope glycoproteins. Viral assembly takes place in proximity to lipid droplets. 5) The virions mature and then exit the cell through the secretory pathway.

CD81
SR-B1
Claudin-1
Occludin

RNA

(+)

②

①

HCV polyprotein

(-)

③ replication

(+)

membranous web

Lipid droplets

assembly ④

⑤
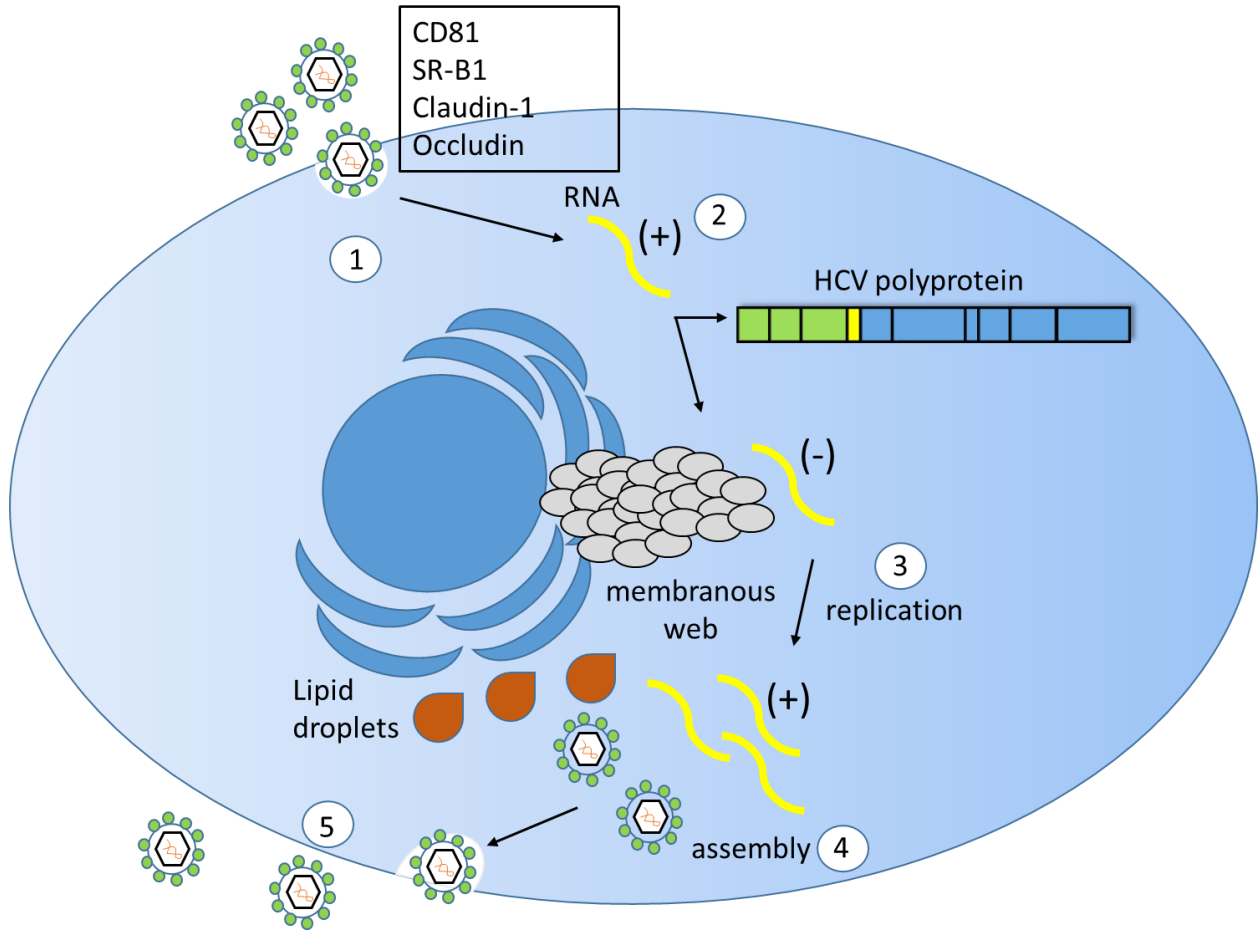
density lipoprotein (HDL), low density lipoprotein (LDL), and very low density lipoprotein (VLDL). Claudin-1 and occludin are tight junction proteins. It has recently been shown that an E1/E2 complex can interact with claudin-1 (25). Occludin can also interact with E2 and may play a role, like Claudin-1, in HCV entry at tight junctions (26). One hypothesis is that the CD81/SR-B1/virus complex migrates to the tight junctions where it can then interact with the tight junction proteins to promote entry as has been described for other viruses (27). While these four are considered the major receptors, others such as LDL-R (low density lipoprotein receptor), the lectins DC-SIGN and L-SIGN, and NPC1L1 (Niemann-Pick C1-like 1) cholesterol transporter, also aid in HCV entry into the cell (28-30).

Due to the restricted host tropism of HCV, there have been recent attempts to make a humanized mouse model to study infection by expressing various combinations of human CD81, SR-B1, Claudin-1, and occludin in the mouse liver. CD81 and occludin were sufficient to make the cells permissive to HCV and permissiveness increased when all four were expressed (31).

Once the virus binds to the host cell via its receptors, the virus enters by clathrin-mediated endocytosis and is trafficked by the early endocytic pathway. Then the genome is released into the cytosol through pH-dependent fusion between the envelope glycoproteins and endosome (32, 33).

RNA translation

Since the HCV genome is positive-stranded it can be used directly for translation after its release into the cytosol. As previously mentioned, the 5' UTR contains an IRES where the 40S ribosomal subunit will bind to initiate translation of the polyprotein. The polyprotein is then cleaved by cellular and viral proteases to generate the structural and nonstructural proteins required for HCV RNA replication and virus assembly.

RNA replication

Replication takes place in a complex called the membranous web. The membranous web is an alteration of ER-derived membranes that can be induced by expression of NS4B (34). The nonstructural proteins and viral RNA have been shown to localize in discrete foci in a membrane matrix by using a combination of immunofluorescence, fluorescence in situ hybridization, and electron microscopy in replicon-containing cells (35). Replicons are cells that express viral proteins and can support RNA replication but do not produce infectious virus (36). Though the exact function of the membranous web is unknown, it is thought to act as a physical scaffold to support the replication complexes.

The main steps of RNA replication are to 1) use the positive-strand RNA to serve as a template to make a negative-strand RNA intermediate and 2) make many copies of positive-strand RNA from the negative-strand. The positive-strand copies then can be used for making more viral proteins or packaging into new viral particles. The RNA replication process is primarily governed by the enzymatic activity of NS5B.

RNA replication also appears to be linked to host cellular lipid metabolism with HCV infection increasing the amount of intracellular lipids. It has been shown that HCV replication may take place on lipid rafts, specifically in association with calveolin-2, and an inhibitor of sphingolipid production also impaired HCV replication (37, 38). Additionally geranylgeranyl lipid, a product in the mevalonate pathway that synthesizes cholesterol, is required for efficient HCV replication since it post-translationally modifies FBL2, a host protein that interacts with NS5A (39).

HCV assembly and release

After replication, the positive-strand RNA genome must be packaged into a viral particle containing core, E1, and E2. Lipid droplets are an important component of HCV virus assembly. Core protein physically associates with lipid droplets and this interaction is crucial for infectious particle production (40). However, lipid droplets are most likely not the sites of viral particle assembly but rather bring core into close proximity to assembly sites on the ER where the E1E2 heterodimer is already localized. p7 and NS2 have been shown to re-localize core from lipid droplets to the ER and this change in localization correlates with increased virus production (41, 42). NS5A is also recruited to lipid droplets which may serve to tether sites of replication together in close proximity to sites of assembly (43). The phosphorylation state of NS5A may play an important role as a switch between its function in replication and assembly with the hyperphosphorylated form associated with virus assembly (44, 45). Additionally, though its exact function in assembly is unknown, NS3 has been shown to interact with core protein and mutations in its helicase domain impair virus assembly.

Lastly, virus particles are released from the cell through the secretory pathway. HCV virion maturation and eventual egress out of the cell seem to be regulated by the VLDL pathway. HCV virions produced in cell culture have a low buoyant density similar to VLDL and also associate with apolipoproteins, in particular apoE (46). The ESCRT (endosomal-sorting complex required for transport) pathway has also been implicated in release of HCV virions. The ESCRT pathway is important in endosomal protein sorting and the formation of multivesicular bodies and functions in exosome release. Dominant negative mutants of the ESCRT-III pathway impaired release of extracellular virus (47). Exosomes have also been shown to carry HCV RNA (48) and in a cell culture system could transmit infectious virus to naïve cells to start a productive infection (49). Lastly virion maturation and secretion may be pH-dependent since

alkalinization of vesicles by p7 is required for efficient virus production and intracellular virus is acid-sensitive (12).

Autophagy

Macroautophagy (hereafter referred to as autophagy) is a pathway that promotes cellular homeostasis and is especially crucial during times of cellular stress and/or starvation when a cell can "eat" parts of itself to provide amino acids and other cellular materials necessary for its survival. During autophagy, a cell can envelop organelles, unfolded proteins, pathogens, and other materials in a double-membrane structure called an autophagosome and target it for degradation by eventual fusion with a lysosome.

This pathway was first discovered in the 1950s by electron microscopy and Christian De Duve is credited with coining the term autophagy. Autophagy is governed by a set of autophagy-related genes (ATG) that are conserved across eukaryotes and were initially identified in yeast mutants during genetic screens. The most likely membrane source for autophagosomes is the ER. Autophagosomes are double-membraned structures that are 0.5-1.5um in size in mammals and the half-life of an autophagosome within the cell is approximately ten minutes (50).

Autophagy has been found to play roles in many areas that affect human health including cancer, neurodegeneration, pathogen clearance and immune response, and aging.

Sequestration

The early steps of autophagy involve nucleation and recruitment of ATG proteins, elongation of the autophagosomal membrane, and then its closure around cellular contents to form a complete autophagosome. Initiation begins with the recruitment of the ULK1 (uncoordinated-51-like kinase I) and the PI3K (phosphoinositide-3 kinase)-Beclin1 complexes to the nascent phagophore (51). ULK1, a serine/threonine kinase, is bound to mTOR (mechanistic

Figure 3 Overview of autophagy. ULK1 remains bound to lysosomally-localized mTOR when autophagy is inactive. When autophagy is stimulated, ULK1 is phosphorylated and is released from mTOR. The ULK1 and Beclin1-PI3K complexes localize near the nascent phagophore and initiate autophagosome biogenesis. The isolation membrane forms around the cargo to be degraded. LC3 is conjugated to PE by the ATG5-ATG12 complex which acts like an E3-ubiquitin ligase. LC3-PE decorates the inner and outer membranes of the autophagosome. Once the isolation membrane closes, the autophagosome matures by fusing with endosomes to form amphisomes or lysosomes to form autophagolysosomes. When fusion with a lysosome occurs, the hydrolases degrade the cargo and cellular materials are recycled.

ULK1

mTOR

Autophagy
inhibited

Autophagy
initiation

Beclin1 PI3K

mTOR

endosome

lysosome

ULK1

P

LC3-I

conjugation

ATG12
ATG16 ATG5

LC3-PE

autophagosome

amphisome

autophagolysosome

autophagolysosome
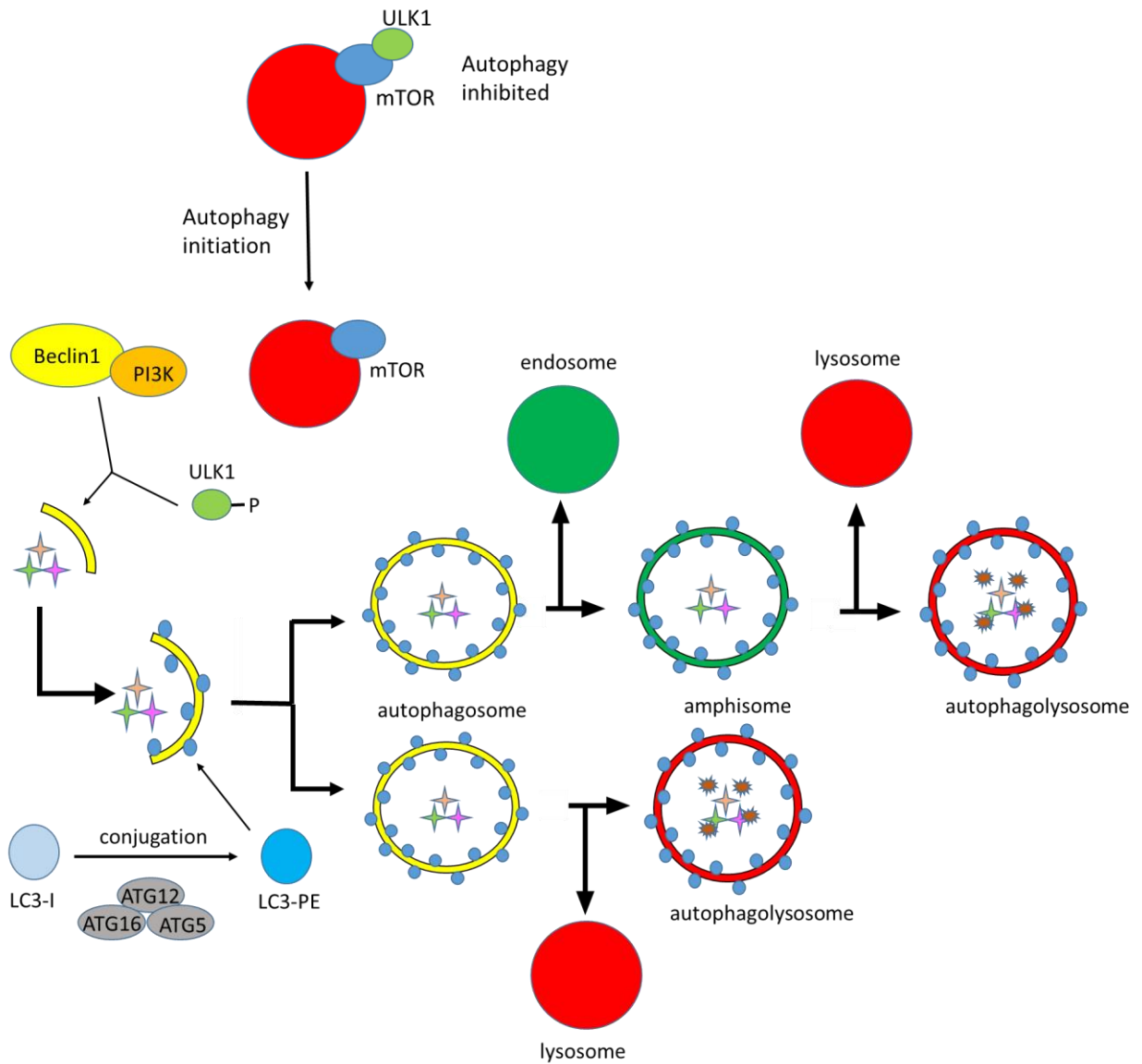
lysosome

autophagic cargo

LC3-II

lysosomal hydrolases

target of rapamycin) complex 1 (mTORC1) when nutrients are abundant within the cell. mTORC1, also a serine/threonine kinase, localizes to the lysosome through interaction with the Rag complex and inhibits autophagy by phosphorylating ULK1. Under nutrient-starvation conditions and autophagy induction, mTORC1 is inactivated and ULK1 is released (52, 53). Once ULK1 is released, it is phosphorylated by AMPK (AMP-activated protein kinase) to activate autophagy. ULK1 can bind to membranes and this may help recruit other ATG proteins and their binding partners to the site of autophagosome formation. The PI3K-Beclin1 and ULK1 complexes produce a pool of phosphatidyl-inositol-3-phosphate (PI3P) that is found in the autophagosomal membrane leaflets and also serves to recruit other autophagy effector proteins.

Once autophagy is initiated and the phagophore, denoting the site of autophagosome formation, is formed then the isolation membrane begins to elongate around the cargo that it will target for degradation. As previously mentioned autophagosomes most likely form from the ER. DFCP1 (double FYVE domain – containing protein 1) can bind to PI3P localizing to the ER during amino acid starvation where it also interacts with LC3 (microtubule-associated protein light chain 3). These cup-like DFCP1 structures, also called omegasomes, are thought to be the site of biogenesis for autophagosomes (54). The elongation step is dependent upon two ubiquitin-like conjugation systems: the ATG5-ATG12 and the ATG8-PE systems. ATG12 is conjugated to ATG5 via a lysine residue and then the ATG12-ATG5 complex binds to ATG16L which localizes it to the isolation membrane (55). ATG16L has been shown to directly bind to the ULK1 complex. The ATG12-ATG5 complex serves as the E3-ubiquitin ligase to attach ATG8 (also called LC3) to the lipid phosphatidylethanolamine (PE). PE is part of the composition of many intracellular membranes in the cell. LC3-PE (also referred to as LC3-II) decorates the isolation membrane and remains associated with the autophagosomal membrane as

it matures and then the LC3-II on the outside of the autophagosome is recycled once it is degraded by lysosomal fusion. The ATG12-ATG5 complex dissociates from the autophagosome before it closes. The exact steps required for elongation and closure are not clear but it has been shown that PI3P can form a cytosol-facing bud in membranes when clustered and that other ATG proteins seem to have the ability to sense membrane curvature and may help stabilize the isolation membrane as it elongates (56). Another hypothesis regarding membrane elongation is that LC3-containing membranes from other cellular locations can serve as additional membranes that tether and fuse with an elongating isolation membrane through LC3-interacting regions (57).

Autophagosome Transport to the Lysosome

Once autophagosomes are formed they must be transported to lysosomes for degradation. Maturation refers to the process by which autophagosomes acquire the proteins necessary to make them competent for fusion. Autophagosome maturation depends largely on the activity of GTPases. GTPases function by cycling between being bound to guanosine diphosphate (GDP) in its inactive form and to guanosine triphosphate (GTP) in its active form. GDP is dissociated from the GTPase by binding of a guanine nucleotide exchange factor (GEFs) which allows GTP to bind and facilitates recruitment of the GTPases to membranes where they can bind their effector proteins and carry out their function. GTPase-Activating proteins (GAPs) accelerate the hydrolysis of GTP to GDP inactivating the GTPase.

The most well-known family of GTPases involved in autophagy are the Rab proteins which regulate vesicular trafficking. Rab7 has been shown to play an important role in linking autophagy to the endo-lysosomal system. Rab7 is found on late endosomes, lysosomes, and autophagosomes though its presence on autophagosomes may be due to fusion events with late endosomes (58, 59). Maturation of the early endosome to a late endosome/lysosome is dependent

upon the switch from Rab5 to Rab7. Rab5 is found on early endosomes and is displaced by Mon1 which acts as a GEF for Rab7 recruiting it to the membrane through interaction with HOPS (homotypic fusion and protein sorting complex) marking the late endosome (60, 61). Autophagosomes can fuse with late endosomes to form an amphisome prior to fusion with a lysosome (62, 63). It is unknown what proportion of autophagosomes become amphisomes but it has been shown in hepatocytes that the majority of autophagosomes fuse with late endosomes before eventually fusing with lysosomes. It has been demonstrated that Rab7 co-localizes with LC3-positive structures that eventually become positive for LAMP-1 indicating fusion with a late endosome/lysosome. Knocking down Rab7 or expressing a dominant-negative version of Rab7 causes an accumulation of autophagosomes, reduced co-localization with LAMP1, and reduced degradation of long-lived proteins (64, 65). These studies and others have elucidated a role for Rab7 in the maturation of autophagic vesicles and fusion with late endosomes and lysosomes.

The functions that Rab7 carries out are due to which effectors are bound to it. Two proteins that regulates autophagosome maturation in coordination with Rab7 are Rubicon and UVRAG (UV-irradiation resistance-associated gene). Rubicon is an effector of Rab7 and can bind both Rab7 and UVRAG in different complexes. Rubicon sequesters UVRAG to prevent it from binding to the class C vacuolar protein sorting complex (C-VPS) which is part of the HOPS complex. Rab7 can compete with Rubicon-UVRAG binding through its own binding of Rubicon to free UVRAG. UVRAG is then free to interact with C-VPS and recruit this complex to autophagosomes. Rubicon negatively regulates endosomal maturation and endocytic pathways (66). UVRAG can also increase the association of Rab7 with autophagosomes and increase its activity thereby contributing to autophagosome maturation (67).

Another set of Rab7 effectors with opposing functions that are important for autophagy are RILP (Rab interacting lysosomal protein) and FYCO1 (FYVE and coiled-coil domain containing 1). RILP and FYCO1 bind to motor proteins and are responsible for moving vesicles along microtubules. Autophagy depends on an intact microtubule network since treatment of cells with vinblastine or nocodazole inhibits fusion of autophagosomes and endosomes (68). RILP binds to dynactin which recruits the dynein motor and can mediate minus-end transport of Rab7-containing vesicles towards the perinuclear region of the cell (69, 70). While this mode of transportation for late endosomes and lysosomes is well documented, it is not as clear whether autophagosome movement depends on Rab7-RILP. A recent study showed that autophagosome movement was dependent upon the Rab7 interaction with another effector, ORP1L (oxysterol-binding protein-related protein 1L) which is a cholesterol sensor. Under low cholesterol conditions, ORP1L prevents binding of RILP to dynactin resulting in more peripheral autophagosomes (71). FYCO1 binds to kinesin-1 and is found on Rab7-containing endosomes and lysosomes. FYCO1 can also bind to LC3 through an LC3-interacting region potentially linking autophagosomes to kinesin and moving them to the cell periphery (72).

Autophagosomes are formed at various sites throughout the cytosol and move towards the perinuclear region of the cell where lysosomes are predominantly found. While autophagosomes are able to move bidirectionally, their net movement tends to be towards the centrosome. This movement is dependent on dynein as inhibiting dynein by microinjection of antibody against dynein heavy chain or by treatment with an ATPase-inhibitor abrogates autophagosome movement towards the perinuclear region (73, 74). Once autophagosomes and lysosomes are in close physical proximity, fusion between the membranes occurs through tethers and SNARE (soluble N-ethylmaleimide-sensitive factor attachment protein receptor) proteins.

Tethering proteins bring membranes into close proximity prior to the engagement of SNARES. HOPS serves as a tether through its interaction with Rab7 to coordinate assembly of SNARE proteins on membranes (75). PLEKHM1 has been identified as a protein that binds Rab7, components of the HOPS complex, and LC3 and therefore may serve as an adaptor linking autophagosomal and lysosomal membranes (76). Membrane fusion is achieved by the interaction of four SNARES: the Qa, Qb, Qc SNARES on one membrane and the R-SNARE on the other (77). The SNARES involved in autophagy are Syntaxin-17 (Stx17) present on autophagosomes and VAMP7/8 on late endosomes/lysosomes. Stx17 is an ER-resident syntaxin and most likely appears on autophagosomes due to their ER membrane origin. Autophagosomes accumulate when Stx17 is knocked-down in cells indicating a role for Stx17 in autophagosome-lysosome fusion. SNAP-29, a Qbc SNARE protein, was also found to interact directly with Stx17 and is recruited to autophagosomes. Interactions between Stx17 and the lysosomal SNARE, VAMP8, were also found (78). Stx17 also can interact directly with the HOPS complex which may also serve to bring the autophagosome and lysosome together for fusion since knocking down HOPS subunits causes the accumulation of Stx17-positive autophagosomes (79).

Lysosomal Degradation of the Autophagosome

Fusion with a lysosome allows the contents of the autophagosome to be degraded and components to be recycled back to the cytosol. The degradative capacity of the lysosome depends upon proper acidification and proper expression of lysosomal proteases. Presenilin 1 targets the V0a1 subunit of the vacuolar ATPase to lysosomes which allows acidification by pumping protons into the lysosomal lumen. Presenilin 1-knockout cells were unable to degrade autophagosomes due to defects in proteolysis and acidification though fusion with lysosomes could still occur (80). Presenilin 1 mutations have been implicated in Alzheimer's disease and

autophagic defects are present in many neurodegenerative diseases. Cathepsins B, D, and L play important roles in autophagy. Cathepsin D deficient or cathepsin B and L double deficient mice show an accumulation of autophagosomes in their brains leading to death (81). Additionally, cathepsin L-deficient fibroblasts also accumulated autophagolysosomes which could not degrade their contents properly (82). After degradation, the products, for example amino acids, are recycled by lysosomal efflux transporters. For example, ATG22 was shown to be an amino acid effluxer in yeast, most likely for leucine, and that this recycling step at the end of autophagy was necessary for continued cell viability (83). Lysosomes are also recycled after their participation in autophagy by a process termed autophagic lysosome reformation (ALR). During ALR, mTOR is reactivated and LAMP-1 positive membranes form tubular structures that initially are not acidic and lack degradative capacity but after maturation, these tubules become fully functional lysosomes (84).

Arl8b

As previously discussed, an important aspect of autophagy maturation is organelle positioning and ensuring that autophagosomes are able to come into close spatial proximity with lysosomes for fusion to occur. An Arf-like GTPase that plays a main role in lysosomal positioning is Arl8b. Arl8b, as described above for Rab GTPases, cycles between GDP (inactive) and GTP (active) bound states. Arl8b was first characterized in 2006 and was found to bind to lysosomes as it co-localized with both CD63 and LAMP-2 positive vesicles (85). Arl8b did not co-localize with the early endosomal marker EEA1 and only partially co-localized with the late endosomal marker mannose-6-phosphate receptor. Tagged-Arl8b was also shown to affect the motility of lysosomes in transfected cells with an increase in peripheral lysosomes compared to untransfected cells (85, 86). Arl8b binds to the N-terminal portion of SKIP (SifA and kinesin-

interacting protein) and SKIP binds to kinesin-1 enabling plus-end transport of lysosomes to the periphery via microtubules (87).

Arl8b is post-translationally modified by acetylation on its N-terminus (87). While acetylation is important for associating Arl8b with membranes, it does not recruit Arl8b specifically to lysosomes. Recently, the BORC complex (biogenesis of lysosome-related organelles complex (BLOC)-one related complex) was identified as responsible for linking Arl8b to lysosomes (88). Knocking down members of the BORC complex altered the localization of Arl8b to a diffuse, cytosolic pattern instead of being associated with lysosomes.

Additionally, the HOPS complex can be recruited to lysosomes by Arl8b. The HOPS complex is a hexameric complex made up of vacuolar protein sorting (Vps) subunits 41, 11, 18, 39, 16, and 33a and Arl8b was found to directly interact with Vps41. Once Vps41 is localized to the lysosome, other Vps subunits can subsequently bind to complete the HOPS complex. Vps41 interacts with Vps18 which then allows the recruitment of Vps11 and 16. Vps11 can interact with Vps39 and Vps16 can interact with Vps33a (89). Knocking down Arl8b in cells causes various Vps subunits to no longer localize to lysosomes and be predominantly localized to the cytosol. It is believed that the Arl8b-SKIP-kinesin complex counteracts the Rab7-RILP-dynein complex with the latter moving lysosomes to the perinuclear region and the former to the periphery. Rab7-RILP has been shown to also interact with the HOPS complex and it has been suggested that there can be competition for HOPS binding between Arl8b-SKIP and Rab7-RILP (88). One theory is that by localizing HOPS to lysosomes, Arl8b may play a role in fusion of late endosomes and lysosomes.

In macrophages and dendritic cells, Arl8b has been implicated in the formation of lysosomal tubules which are formed upon stimulation with compounds such as

lipopolysaccharide (LPS). Lysosome tubules may play a role in retaining fluid-phase content from pinocytosis as well as phagosome maturation and acidification. LPS enhances localization of Arl8b on membranes in an mTOR-dependent manner. Treating cells with torin1, an mTOR inhibitor, in the presence of LPS returned the amount of membrane-associated Arl8b back to the basal levels (90, 91).

What are the consequences of moving lysosomes to the periphery? Lysosomes may be heterogeneous in both structure and function within the same cell. Peripheral lysosomes were found to be less acidic than perinuclear ones using fluorescein-dextran as a reporter of intraluminal pH (92). This alkalinization could be due to increased proton leakage and reduced vacuolar ATPase activity in peripheral lysosomes. There were also differences in Rab7 and Arl8b localization on lysosomes depending on their location. Peripheral lysosomes had increased Arl8b on their membranes and little Rab7 while perinuclear lysosomes contained more Rab7 which may indicate that the acquisition or depletion of Arl8b or Rab7 may play a role in lysosomal localization (92). There was also decreased cathepsin L activity in cells where peripheral localization of lysosomes was induced by dynamitin expression to break apart the dynein complex (92).

Another consequence of lysosomes moving to the periphery may be autophagy modulation. Autophagosomes and lysosomes fuse with each other in the perinuclear region of the cell (74). Arl8b overexpression decreased autophagic flux by decreasing co-localization between autophagosomes and lysosomes whereas Arl8b knockdown had the opposite effect enhancing autophagosome-lysosome fusion (93).

Role of Arl8b in pathogenesis

Arl8b has been shown to play a role in the pathogenesis of salmonella and tobamovirus through two different mechanisms. After invasion, *Salmonella* typhimurium occupies a vacuole termed the *Salmonella*-containing vacuole (SCV) that interacts with the endocytic pathway. The SCV does not fuse with lysosomes preventing degradation of the bacterium. SCVs eventually move to the cell periphery to enable cell-to-cell transfer. Arl8b was found to associate with SCVs in infected HeLa cells and was also localized to *Salmonella*-induced filaments (SIF) which are tubules formed by endosomal compartments (94). Knockdown of Arl8b kept SCVs in the perinuclear regions of cells and prevented them from moving to the periphery 24hrs post-infection as is usual. Additionally, Arl8b knockdown significantly decreased the amount of cell-to-cell spread of the bacterium.

Arl8b is highly conserved amongst eukaryotes and is found in plants and animals but not in yeast. The genus Tobamovirus contains positive-stranded viruses such as tomato mosaic virus and tobacco mosaic virus that infect plants. Tobamoviruses replicate on membranes that contain Arl8 and Tom1, a host protein that promotes viral replication by tethering viral proteins to membranes. Arl8 was found to be necessary for virus multiplication and negative-strand RNA synthesis (95). This suggests that Arl8 may help in the formation of tobamovirus replication complexes.

Autophagy and HCV

The earliest reports looking at the effect of HCV on autophagy found that upon virus infection, autophagosome formation is induced. Evidence of autophagy induction is typically shown by double-membrane vacuole formation in infected cells by electron microscopy, increased LC3-positive puncta in infected cells by immunofluorescence, and increased LC3-II levels by western blot when compared to uninfected cells (96, 97). Autophagy induction has

been observed in cells where HCV RNA was electroporated, during cell culture infection by virus-containing supernatant, and in replicon-containing cells.

It has been proposed that HCV induces autophagy through the UPR pathway. Knocking down parts of the UPR pathway in HCV-infected cells, for example using siRNA against PERK, could reduce the amount of LC3-II induced in infected cells (97, 98). The UPR represents a series of signaling pathways to alleviate ER stress induced by misfolded proteins. PERK (protein kinase-like endoplasmic reticulum kinase) alleviates ER stress by decreasing protein translation (99). One mechanism by which the UPR may induce autophagy in HCV-infected cells is via the AKT pathway. ER stress induced by HCV infection is able to inhibit AKT which leads to mTORC1 inhibition. mTORC1 inhibition leads to the upregulation of ULK1 activity inducing autophagy (100).

There is one report that argues HCV-induced autophagy is independent of the UPR. The authors show that the induction of autophagy appears to precede induction of the UPR in HCV-infected cells since LC3-II protein levels increase prior to induction of CHOP, a protein induced by ER stress. Additionally, subgenomic replicons expressing NS3-NS5B do not induce the UPR but do induce autophagy by increasing LC3-II in cells. Knocking down Ire1, a component of the UPR pathway, did not alter autophagy in HCV-infected cells and also did not decrease viral replication (101).

Initially, autophagy was suggested to only be required for the translation of incoming viral RNA but is dispensable in cells where replication has already been established. This was based on data that knockdown of autophagy proteins impaired the translation of electroporated HCV RNA but not in replicon cell lines where replication has already been established (102). However, this theory seems to be contradicted by the effects of autophagy inhibition on later step

in the HCV life cycle like replication and viral particle release that subsequent studies have shown. Nevertheless, it appears that HCV-induced effects on autophagy are important for early life cycle events as well as late ones.

Early events in autophagy are governed by the PI3K-Beclin1 complex as described earlier. It has been shown that knockdown of Beclin1 impairs HCV-induced autophagy (103) and knockdown of Vps34 (the class III PI3K) or pharmacologic inhibition of the activity of this PI3K inhibits HCV replication (104). The viral protein NS4B can interact with both Vps34 and Beclin1 (105). Interestingly NS4B, which forms the membranous web complex where viral replication occurs, was also found to induce autophagosome formation when ectopically expressed in cells (105). Therefore, there is speculation that autophagosomes induced by HCV infection could be the sites of viral replication. HCV membranous web complexes were isolated from JFH-1 replicon cells by fractionation and the fractions which were positive for LC3-II were also positive for NS3, NS5A, and HCV RNA (106). Additionally, LC3-positive puncta were found to co-localize with NS5A, NS5B, and HCV RNA by both immunofluorescence and electron microscopy and direct interactions were confirmed by immunoprecipitation (106, 107). However, there have also been studies that could not find any interactions between viral proteins known to be important for replication and autophagosomes (101, 102). Some of the discrepancies in these studies could be due to more transient associations of viral proteins with autophagy machinery that depend on stage of infection. For example, ATG5 was found to interact with NS5B by immunoprecipitation and co-localization by immunofluorescence at an early time point in infection but this association was abolished at later time points (108). NS5A also transiently co-localized with DFCP1, a marker of the omegasome, early in infection (104).

There is still controversy regarding whether autophagy induced by HCV goes to completion with autophagosomes fusing with lysosomes or if fusion and degradation are impaired. Long-lived protein degradation, which is a measure of autophagic degradation, was shown to be impaired in JFH-1 infected cells (97). Additionally, GFP-LC3 puncta did not co-localize with Lysotracker, a dye that stains acidic organelles, in JFH-1 infected cells whereas autophagy induced by nutrient starvation showed a high degree of co-localization between GFP-LC3 and Lysotracker in control cells.

However, other studies have showed complete maturation of the autophagosome into an autophagolysosome during HCV infection. Cells transfected with an RFP-GFP-LC3 plasmid showed predominantly red fluorescence after HCV infection indicating complete autophagy (100, 109). The RFP-GFP-LC3 plasmid is an indicator of autophagy progression. Intact autophagosomes appear yellow due to the presence of both fluorophores but once fusion with a lysosome occurs, red fluorescence remains while the GFP signal is quenched.

Recently, there is data to suggest a more nuanced view of autophagosome maturation in infected cells. There may be slowed maturation of autophagosomes in infected cells due to temporal regulation of Rubicon and UVRAG expression by HCV. As previously described, Rubicon negatively regulates autophagy by sequestering UVRAG and preventing autophagosome maturation. Once UVRAG is freed from Rubicon, it can then bind the HOPS complex and promote autophagosome maturation through Rab7. In a variant of JFH-1 that infects cells rapidly it appears that Rubicon is upregulated during early timepoints in infection causing autophagosomes to accumulate but at later timepoints, UVRAG expression is upregulated allowing autophagy to proceed to completion (110). The regulation of these proteins was shown to be tied to viral replication.

HCV-infected cells also decreased the amount of syntaxin 17 which would decrease autophagosome-lysosome fusion. Stx17 is the SNARE protein responsible for autophagosome-lysosome fusion. Overexpressing stx17 in HCV-infected cells decreased the release of viral particles which could be partially rescued by bafilomycin A1 treatment, which is a pharmacological way to block autophagosome-lysosome fusion (111).

Regardless, it is widely accepted that HCV relies on the induction of autophagy for its life cycle. Knocking down genes important for autophagy such as ATG7 (97, 112), ATG4B (102), Beclin1 (102, 112, 113), and LC3 (97) all impaired viral replication and infectious virus release. ATG7 helps to catalyze the ATG12-ATG5 conjugation reaction and ATG4B cleaves ATG8 to aid its conjugation with PE. Inhibition of the autophagy pathway by knockdown of Beclin1 or ATG7 abrogated extracellular release of HCV by an exosomal pathway (114). Exosomes from these autophagy knockdown cells are also less infectious.

Aspects of HCV infection in which autophagy may provide a pro-survival role are blocking the interferon-response and promoting cell survival. Knockdown of various autophagy genes was found to enhance the innate immune response to HCV infection as was demonstrated by the induction of interferon-stimulated genes (109, 113). HCV-infected cells that are knocked down for autophagy related genes, like Beclin1 or ATG7, undergo apoptosis at a higher rate than HCV-infected cells with normal autophagy machinery (113). This indicates autophagy may play a protective role for the virus during infection to promote viral persistence. Knockdown of autophagy also increased the amount of BST-2, also called tetherin, in HCV-infected cells (114). BST-2 is encoded by an interferon-inducible gene and is known to block release of other enveloped viruses.

The effects of HCV on autophagy may also influence how the disease progresses in chronically infected patients. A study looking at liver biopsies from fifty-six chronic hepatitis C patients found an increase in autophagic based on increased LC3-II levels by western blot and the presence of more autophagosomes by electron microscopy (115). There was no observed increase in mature lysosomes by electron microscopy in these samples leading to the conclusion that there may be a block in autophagosome degradation in chronic HCV.

Project Aims

Whether HCV-induced autophagy goes to completion is still controversial with evidence supporting both a lack of lysosome fusion or complete fusion. After our initial observation that infection with HCV virus caused a block in autophagic flux, we sought to characterize whether the block was caused by either (1) a trafficking defect where autophagosomes and lysosomes do not meet within a cell or (2) altered composition of autophagosomes or lysosomes within cells so that they are no longer competent for fusion. Once we determined that a trafficking defect was the reason for a block in fusion, we then set out to find a mechanism and began to explore the role of GTPases in HCV infection. The purpose of this dissertation was to explore the hypothesis that the HCV-induced block in autophagic flux is dependent upon Arl8b expression in infected cells.

Chapter 2 of this thesis explores the effect of HCV infection on the autophagic pathway and the potential roles for viral proteins in autophagic flux. Next, we looked at whether autophagosome-lysosome fusion was impaired in HCV-infected cells using subcellular fractionation coupled with an in vitro fusion assay and microscopy.

Chapter 3 of this thesis characterizes the effect of HCV infection on the expression and cellular localization of the Arf-like GTPase, Arl8b. The effect of organelle positioning on

autophagy is also explored by confocal microscopy looking at co-localization between autophagosomes and Arl8b-positive organelles. Lastly the effect of Arl8b knockdown on HCV-induced autophagy is tested.

Chapter 4 of this thesis examines the potential cooperativity between Arl8b and Rab7-RILP. Our lab recently demonstrated that HCV cleaves RILP breaking its linkage with dynein. It is known that the Arl8b and Rab7 complexes may be found on the same organelles and compete for HOPS binding.

This study is the first to demonstrate that an Arl8b-dependent mechanism governs autophagosome-lysosome fusion in HCV infection.

Chapter II: HCV infection causes a block in autophagosome-lysosome fusion

Introduction

Autophagy plays an important role in maintaining cellular homeostasis and protecting the cell from stress. Intracellular pathogens interact with the autophagy pathway, also termed xenophagy, either to exploit it to aid in their own pathogenesis or encounter it as a host defense mechanism. As a defense mechanism, intracellular pathogens are enveloped by the phagophore becoming trapped within the autophagosome and then degraded by fusion with the lysosome. For example, during autophagy induction by *Mycobacterium tuberculosis*, the phagosomes where the bacteria reside acquire lysosomal markers, such as hydrolases, and bacterial survival is reduced (116). Autophagy has also been implicated in various immune responses to pathogens such as pattern recognition receptor activation or antigen presentation. Autophagy is induced to restrict Rift Valley Fever virus by activating the toll-like receptor signaling adaptor MyD88 (117). EBNA1, a viral protein from Epstein-Barr virus, is processed through the autophagic pathway so that it can be presented to CD4+ T cells on MHC class II for immune surveillance (118).

However, many pathogens have evolved various mechanisms to either evade or exploit the autophagy pathway or its components to ensure survival and spread. Herpesviruses have evolved mechanisms to suppress autophagy. Herpes Simplex Virus-1, an alpha-herpesvirus, inhibits phosphorylation of eIF2α suppressing the UPR response leading to autophagy inhibition. Kaposi's sarcoma-associated herpesvirus, a gamma-herpesvirus, employs multiple methods to inhibit autophagy such as encoding a viral Bcl-2 protein that binds with high affinity to Beclin1 to prevent it from initiating autophagy or encoding a viral FLIP protein that directly interacts with ATG3 to prevent its interaction with LC3 impairing LC3-II membrane attachment (119). Viruses may utilize autophagy to provide membranes for replication, prolong the survival of

infected cells, aid in the maturation of infectious virus particles, and secrete viral particles. The mechanisms employed to accomplish these tasks are varied and can include interactions with the mTOR pathway, Beclin1, direct interactions with autophagy proteins, modulation of SNARE proteins, and others (120).

We sought to explore how HCV manipulates autophagy and what effect that could have on the viral life cycle. Since previous work in our lab has shown that the p7 viroporin can alkalinize acidic vesicles within cells and the earliest reports of the effect of HCV on autophagy suggested an incomplete autophagic response, we evaluated whether the observed loss of acidic compartments could play a role in the autophagic response during HCV infection. Therefore, we set out to determine whether HCV blocked autophagosome-lysosome fusion and ultimately were able to conclude that autophagic flux is inhibited during HCV infection. Next, we determined which viral proteins played roles in autophagic flux and what mechanism caused the failure of fusion between autophagosomes and lysosomes. The data presented in this chapter demonstrates that the lack of fusion between autophagosomes and lysosomes is likely due to a trafficking defect that prevents these organelles from contacting each other within the cell as opposed to a virally-induced change in organelle composition that renders them incompetent for fusion.

Materials and Methods

Cells and Culture Conditions

Huh-7.5 and Huh7.5-GFP-IPS cells were obtained from Charles Rice (Rockefeller Institute). These cell lines were cultured in Dulbecco's Modified Eagle Medium (DMEM) containing 4.5g/L glucose, L-glutamine, and sodium pyruvate, 10% fetal bovine serum (FBS), and 1% non-essential amino acids (NEAA). Cells were maintained at 37°C/5% CO_2.

The Super1a replicon cell line was obtained from Stanley Lemon (University of North Carolina School of Medicine). This cell line was grown in DMEM supplemented with 10% FBS, 1% NEAA, 2ug/mL blasticidin, and 200ug/mL G418. The cured cell line was acquired by treating the Super1a cells with 200 U/mL interferon-α for four weeks to eliminate the HCV genome. Cured cells were grown using the same media as Super1a cells without the G418. Cells were maintained at 37°C/5% CO_2.

A tetracycline-inducible Huh-7 cell line expressing core, E1, E2, p7, and NS2 was obtained from Kui Li (University of Tennessee Health Science Center). The cell line was cultured in DMEM containing 4.5g/L glucose, L-glutamine, and sodium pyruvate, 10% FBS, 1% NEAA, 2ug/mL tetracycline, and 200ug/mL G418. Cells were maintained at 37°C/5% CO_2. To induce expression of viral proteins, tetracycline was removed and media containing tetracycline-free FBS was used. Cells were washed daily with 1XPBS and media replaced. A tetracycline-inducible Huh-7 cell line expressing core protein alone (called L14) was also used in the same way as the core-NS2 cells.

A replicon cell line expressing NS3-NS5B from JFH-1 was made in our lab and grown in DMEM supplemented with 10% FBS, 1% NEAA, 2ug/mL blasticidin, and 200ug/mL G418.

Western blotting

Western blotting was performed using anti-LC3B, 1:1000 (Cell Signaling, Beverley, MA), anti-Cathepsin D, 1:500 (Santa Cruz Biotechnology, Santa Cruz, CA), anti-GAPDH, 1:1000 (Santa Cruz Biotechnology, Santa Cruz, CA), anti-core, clone C7-50, 1:1000 (Thermo Fisher Scientific, Waltham, MA), and anti-LAMP-2, clone H4B4, 1:2000 (DSHB, University of Iowa). Horseradish peroxidase-conjugated secondary antibodies were from Thermo Fisher

Scientific and IR-Dye conjugated secondary antibodies were from LI-COR Biosciences (Lincoln, NE).

HCV infection

JFH-1, a genotype 2a strain, was used for all experiments with HCV-infected cells. JFH-1 plasmid was obtained from Takaji Wakita (Tokyo, Japan). JFH-1 RNA was made as described in Kato et al (121). The JFH-1 plasmid was linearized with XbaI and this template was used to transcribe RNA using the T7 RiboMAX™ Express Large Scale RNA Production (Promega, Madison, WI). 10ug of JFH-1 RNA was used to electroporate $5x10^6$ Huh-7.5 cells. These cells were continuously passaged to allow the JFH-1 to become cell culture adapted. When greater than 75% of cells were infected, the cell culture supernatant containing virus was collected and stored at -80°C for future use. New stocks of virus were propagated by continuous cell culture infection with JFH-1 containing supernatant.

Huh-7.5 cells were infected with supernatant containing JFH-1 virus for twenty-four hours. Cells were passaged as necessary and infection was monitored by immunofluorescence for HCV core protein. JFH-1 infected cells were used in experiments when greater than 70% of the cells were infected.

Immunofluorescence

Huh-7.5 cells were plated on 12mm circular glass coverslips in 4-well plates. Cells were transfected with Lipofectamine LTX or Lipofectamine 3000 (Thermo Fisher Scientific). ptfLC3 plasmid (Addgene, Cambridge, MA) is the tandem RFP-GFP-LC3. For ptfLC3 experiments, twenty-four hours post transfection, cells were treated with either bafilomycin A1 (Sigma, St. Louis, MO) or Earle's Balanced Salt Solution (EBSS) for thirty minutes. Cells were fixed with 3% paraformaldehyde and permeabilized with acetone. Cells were blocked for one hour in

1XPBS containing 1% BSA and 1% EDTA at room temperature before being incubated with mouse anti-core clone C7-50, 1:300. The secondary antibody used was an AlexaFluor-647 conjugated donkey anti-mouse. Coverslips were mounted onto slides using Prolong Gold antifade mountant containing DAPI (Thermo Fisher Scientific).

Images were taken with a Nikon eclipse Ti PFS Quantitative Fluorescence Live-Cell and Multidimensional Imaging System equipped with a digital monochrome Coolsnap HQ2 camera (Roper Scientific, Tucson, AZ) using the MetaMorph software. Analysis to determine mean GFP/RFP ratio for RFP-GFP-LC3 transfected cells was done using CellProfiler cell image analysis software (www.cellprofiler.org).

Autophagy flux assay

Cells were treated with 100nM bafilomycin A1 for 4 four hours before being lysed with cell lysis buffer (20mM Tris-HCl (pH 7.5), 150mM NaCl, 1mM Na_2EDTA, 1mM EGTA, 1% Triton X-100) containing protease inhibitors. Cells treated with 0.1% DMSO were used as a negative control.

Lysosomal enzyme assays

For live cell imaging, Huh-7.5-GFP-IPS cells were plated on glass bottom Microwell dishes (Maktek, Ashland, MA) at 15,000 cells per dish. Bafilomycin A1 treatment was done at a concentration of 25nM overnight at 37°C/5% CO_2. Cells were treated with Magic Red Cathepsin B reagent (Immunochemistry Technologies, Bloomington, MA) at a 1X concentration in HEPES buffer (10mM HEPES, 133.5mM NaCl, 2.0mM $CaCl_2$, 4.0mM KCl, 1.2mM $MgSO_4$, 1.2mM NaH_2PO_4, 11mM glucose; pH 7.4) for one hour at 37°C/5% CO_2. Nuclei were stained with 1ug/mL Hoechst stain in HEPES buffer for twenty minutes at 37°C/5% CO_2. Live cell imaging was done using a Nikon eclipse Ti PFS Quantitative Fluorescence Live-Cell and

Multidimensional Imaging System equipped with a digital monochrome Coolsnap HQ2 camera. Fluorescence images were collected using Metamorph software at wavelengths of 560nm excitation/607nm emission for the Cathepsin B substrate.

For the plate reader assay, Huh-7.5 cells were plated in 96-well plates with clear bottoms at 10,000 cells per well. Cells were treated with Magic Red Cathepsin B reagent for two hours at 37°C/5% CO_2. Cells were washed twice with HEPES buffer and lysed with 1XRIPA buffer for five minutes at 4°C. Fluorescence measurements were taken at room temperature in a Fluostar Optima plate reader (BMG Labtech, Durham, NC) at excitation/emission wavelengths of 584/620nm.

To assess cathepsin D processing, Huh-7.5 cells were treated with 25nM bafilomycin A1 overnight at 37°C/5% CO_2. Cells were trypsinized, washed, and resuspended in 2mL homogenization buffer (0.25M sucrose, 6mM EDTA, 20mM HEPES-NaOH; pH 7.4) and homogenized with a dounce homogenizer with loose-fitting pestle. Homogenate was centrifuged at 3000xg for ten minutes at 4°C to collect the heavy membrane pellet. The 3000xg pellet was resuspended in 100uL homogenization buffer containing protease inhibitors for western blot.

Subcellular fractionation

Fractionation was carried out as described in Koga et al (122). Briefly, approximately 200 million Huh-7.5 cells were collected and ruptured by nitrogen cavitation in a nitrogen bomb (Parr Instrument Company, Moline, IL) for seven minutes at a final pressure of 35psi in a volume of 1mL 0.25M sucrose. Disrupted cells were centrifuged at 2000xg for five minutes at 4°C to remove intact cells and nuclei. Supernatant containing organelles was centrifuged at 17,000xg for twelve minutes at 4°C to separate organelles (pellet) from cytosol and ER fractions (supernatant). The pellet was resuspended in 0.25M sucrose and mixed with 85.6% Nycodenz

(Accurate Chemical, Westbury, NY) and placed in the bottom of an ultracentrifuge tube. On top of the homogenate, 26% Nycodenz, 24% Nycodenz, 20% Nycodenz, and 15% Nycodenz was layered. Gradients were spun at 104,333xg for three hours at 4°C in a SW41Ti swinging bucket rotor. Autophagosomes were collected from the interface between 15-20% Nycodenz and lysosomes were collected between 24-26% Nycodenz. Fractions were washed with 0.25M sucrose and autophagosomes and lysosomes were resuspended in 100uL 0.25M sucrose with protease inhibitors for use in the in vitro fusion assay.

In vitro fusion assay and Flow cytometry

In vitro fusion assay was carried out as described in Koga et al (122). Briefly, isolated autophagosomes were incubated with anti-LC3-PE antibody (Cell Signaling) at a 1:50 dilution and isolated lysosomes were separately incubated with anti-LAMP-2-APC (BD Biosciences, San Jose, CA) at a 1:20 dilution in 0.25M sucrose. Antibodies were incubated with organelles for thirty minutes at room temperature. Organelles were washed with 0.25M sucrose to remove any unbound antibody. Organelles were resuspended in 5uL fusion buffer (10mM HEPES, 10mM KCl, 1.5mM $MgCl_2$, 1mM DTT, and 0.25M sucrose) per reaction and 5uL of autophagosomes were combined with 5uL lysosomes. 5uL of reaction buffer (0.25M sucrose, 3mM ATP, 3mM GTP, 0.16mg/mL creatine phosphokinase, 8mM phosphocreatine, and protease inhibitors) was added to the autophagosome-lysosome mixture and the fusion reaction was carried out at 37°C for thirty minutes. The total volume of the reaction was brought up to 100uL with 0.25M sucrose and 100uL of 2% paraformaldehyde was added for fixation. Fixed samples were subjected to flow cytometry using a LSR II instrument (BD Biosciences).
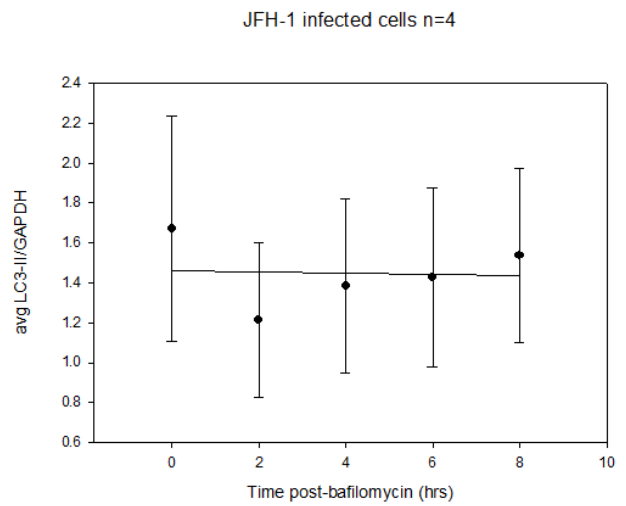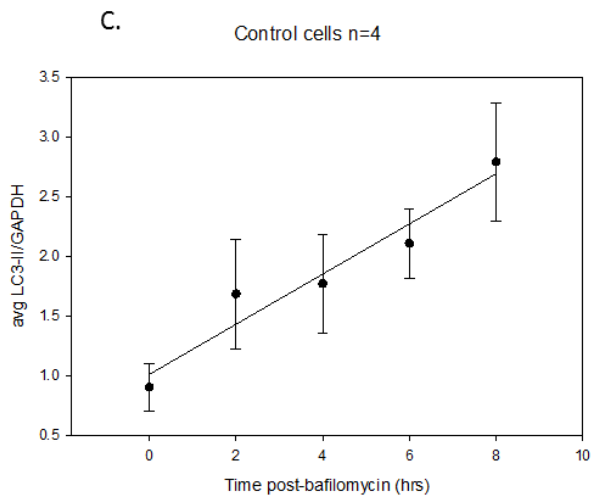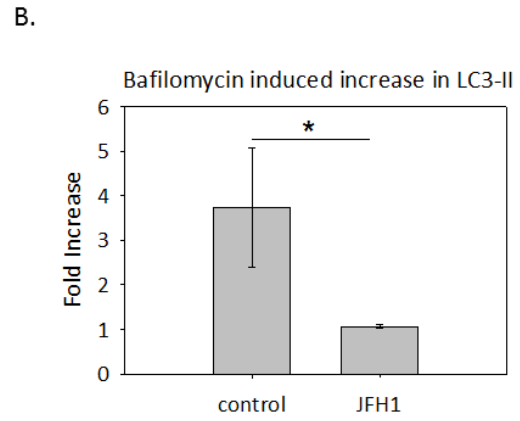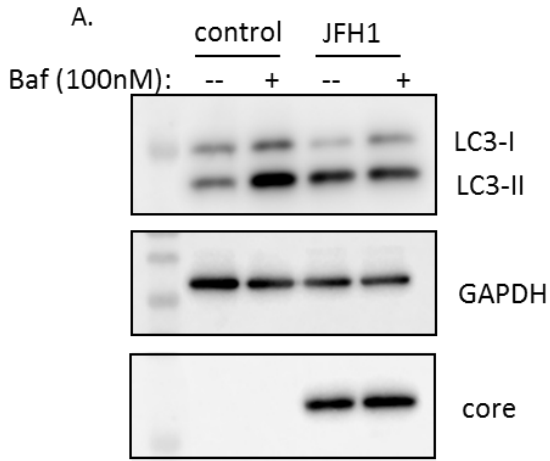
Results

JFH-1 infection leads to altered autophagic flux

To better understand the effect of HCV on autophagy, we assessed autophagic flux in JFH-1-infected human hepatoma Huh-7.5 cells. The ability to study the effect of HCV infection has been greatly enhanced by the advent of a cell-culture system using an isolate from a Japanese patient with fulminant HCV-associated hepatitis developed in 2005 (123). This cell-culture system allows for the study of the entire HCV life cycle within cells. Huh-7.5 cells are a Huh-7 clone that is more permissive for HCV replication due to a point mutation in the retinoic acid-inducible gene-1 (RIG-I) which is a double-stranded RNA sensor (124, 125). To assess autophagic flux, lysosomal inhibitors were used to allow the accumulation of autophagosomes. Bafilomycin A1 was used to prevent the degradation of autophagosomes by inhibiting the vacuolar type H^+-ATPase which results in alkalization of the lysosome (126). When bafilomycin A1 is added to cells undergoing normal, basal autophagy, autophagosome and lysosome fusion is inhibited and autophagosomes will accumulate. This accumulation can be monitored by western blot by an increase in LC3-II which decorates autophagosomes.

Huh-7.5 cells were treated with 100nM bafilomycin A1 for four hours. In uninfected cells, there was an approximate four-fold increase in LC3-II levels in bafilomycin-treated cells compared to cells treated with DMSO only (Figure 4A, B). As previously described, during JFH-1 infection, the basal level of autophagy is increased compared to uninfected cells indicated by the increase in LC3-II in the untreated infected sample. However, treating JFH-1 infected cells with bafilomycin A1 does not further increase the level of LC3-II which would suggest that while HCV may initially induce autophagy, viral infection also prevents degradation of

Figure 4 HCV infection causes a block in autophagic degradation. Huh-7.5 cells were infected with JFH-1, HCV genotype 2a, and then treated with bafilomycin A1 (BafA). *A)* Huh7.5 cells were treated with BafA for 4hrs prior to SDS-PAGE analysis. Western blot was done with anti-LC3 antibody, anti-GAPDH antibody as a loading control, and anti-core antibody to monitor HCV infection. *B)* Densitometry analysis of the changes in LC3-II levels, normalized to GAPDH levels, as determined from western blotting. Quantification of western blots (n=5) was done using ImageJ software. The difference between control and JFH-1 was statistically significant (p=0.029) as indicated by the Mann-Whitney Rank Sum test. *C)* Huh7.5 cells were treated with BafA for indicated time points and LC3-II levels were determined by immunoblotting. Plots represent the quantification (n=4) of the fold increase in LC3-II levels, normalized to GAPDH levels, as determined from western blotting. For control samples, there is a positive correlation between LC3-II levels and length of treatment time by calculating the linear regression. There is no significant correlation for the JFH-1 samples.

A.

control   JFH1

Baf (100nM):   --   +   --   +

LC3-I
LC3-II

GAPDH

core

B.

Bafilomycin induced increase in LC3-II

*

Fold Increase

control   JFH1

C.

Control cells n=4

avg LC3-II/GAPDH

Time post-bafilomycin (hrs)

JFH-1 infected cells n=4

avg LC3-II/GAPDH

Time post-bafilomycin (hrs)

autophagosomes. This would indicate that JFH-1 infection can impair autophagic flux in Huh-7.5 cells.

Next, we treated cells with bafilomycin A1 at different timepoints up to eight hours. In control cells, there was a statistically significant time-dependent increase in LC3-II levels (Figure 4C). The slope of the line reflects the autophagy initiation rate. LC3-II decorated autophagosomes are intermediate structures and their steady-state abundance reflects a balance between rates of formation and destruction via lysosomal fusion (127). In JFH-1-infected cells, there was an absence of a time dependent accumulation of LC3-II under the same conditions. The slope of the line is not significantly different from zero. Using ANOVA, there was a significant difference (p=0.0290) between the accumulation of LC3-II in control cells compared to JFH-1 infected cells. This analysis reveals that the initial increase in autophagy observed in a cell culture model of HCV infection is due primarily to a suppression of LC3-II degradation and not from an increase in autophagy initiation.

The effect of autophagic flux was also examined in replicon cells. The Super1a replicon cells used in this study contain the full-length genome from HCV strain H77c, a genotype 1a virus. As mentioned previously, replicon cells lines can replicate viral RNA but do not produce infectious viral particles (128). Cured cells were compared to full-length Super1a replicons. Cured cells treated with bafilomycin A1 displayed an increase in LC3-II levels as expected (Figure 5). The Super1a cells did not show an increase in LC3-II after bafilomycin A1 treatment. Autophagic flux in the replicon cell lines reflected what was observed during JFH-1 infection in cells.

Figure 5 Full-length replicon shows block in autophagic degradation. Huh7 cells either cured of the HCV genome or expressing the full length H77c HCV genome were treated with bafilomycin A1 (BafA) for 4 hours before cell lysates were collected for western blot. Western blot was done with anti-LC3 antibody, anti-GAPDH antibody as a loading control, and anti-core antibody to show HCV protein expression.
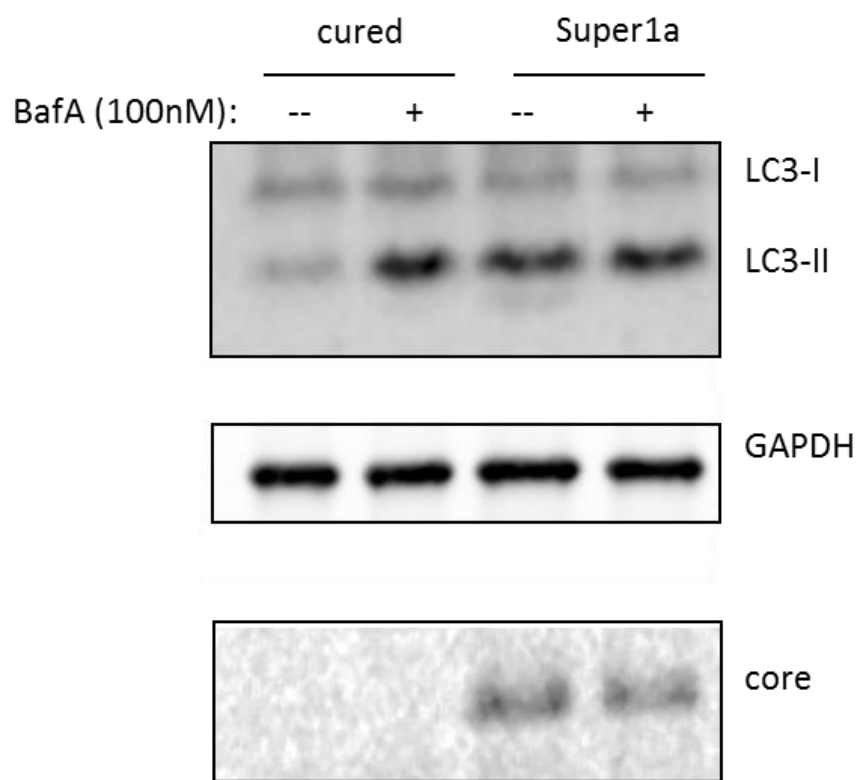
Effect of viral proteins on autophagic flux

Next the role of viral proteins in blocking autophagic flux was examined. The first set of proteins tested were core, E1, E2, p7, and NS2 using a tet-inducible Huh-7 cell line. Seven days after protein expression was induced by tetracycline removal, autophagic flux was assessed. In cells cultured with tetracycline where viral proteins were not expressed, LC3-II levels increased after bafilomycin treatment as expected. After expression of core, E1, E2, p7, and NS2 was induced, there was no increase in LC3-II levels after bafilomycin treatment similar to what was seen during JFH-1 infection (Figure 6A). This represented the subset of viral proteins that were sufficient to inhibit autophagic flux in Huh-7 cells. Expression of core alone could not cause the block in flux since LC3-II levels increased after treatment with bafilomycin in the presence of core (Figure 6B). Expression of NS3, NS4A/B, and NS5A/B did not seem responsible for the impaired flux because, when expressed via a replicon system, bafilomycin treatment could result in an increase in LC3-II levels (Figure 6C). The inability to increase LC3-II levels after bafilomycin treatment caused by JFH-1 infection was narrowed down to expression of E1, E2, p7, or NS2.

We were unable to further exclude any other viral proteins and to definitively conclude which protein or proteins were responsible for the impaired autophagic flux. We employed several methods to express viral proteins in Huh-7.5 cells including lipofectamine-based transfection, baculovirus transduction, lentivirus transduction, and creation of stable-cell lines. However, experiments were hampered by very low levels of protein expression. For example, we made lentiviral constructs expressing tagged-versions of p7, NS2, and p7-NS2 together. After transduction in Huh-7.5 cells, the presence of mRNA for the viral proteins was detected but protein expression could not be seen by western blot (data not shown).

Figure 6 Viral proteins and autophagy. Cells were treated with bafilomycin A1 for four hours before cell lysates were collected for western blot. Western blot was done with anti-LC3 antibody, anti-GAPDH antibody as a loading control, and anti-core or NS3 antibody to monitor viral protein expression. *A)* Tet-regulated Huh-7 cells expressing core, E1, E2, p7, and NS2 (CNS2) viral proteins *B)* Tet-regulated Huh-7 cells expressing core protein and *C)* Replicon cells expressing NS3, NS4A/B, and NS5A/B.
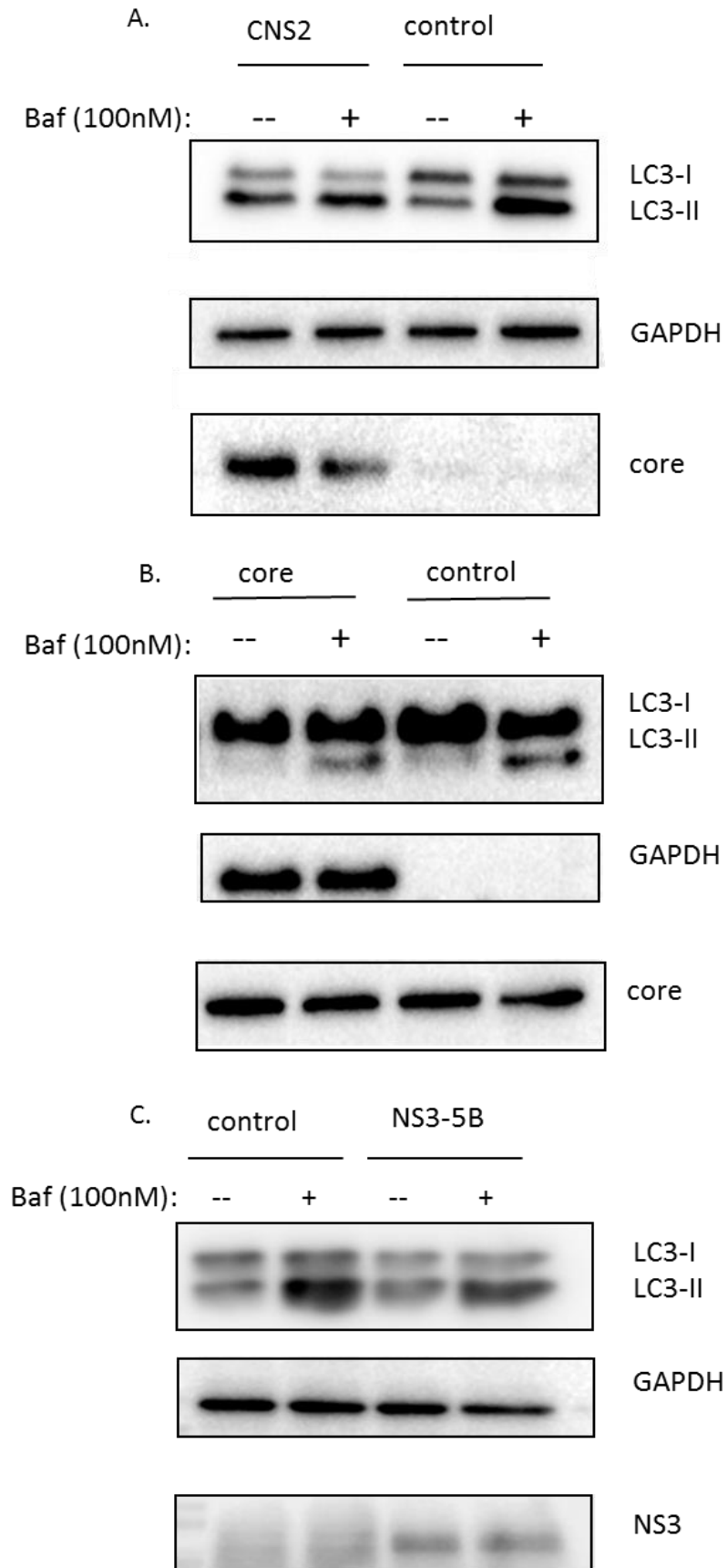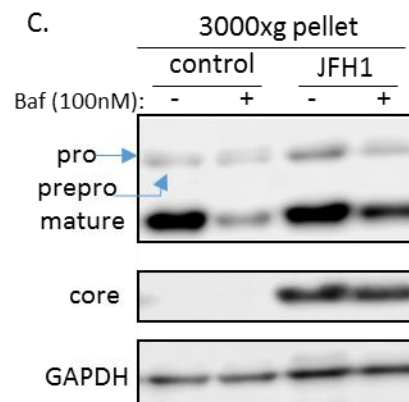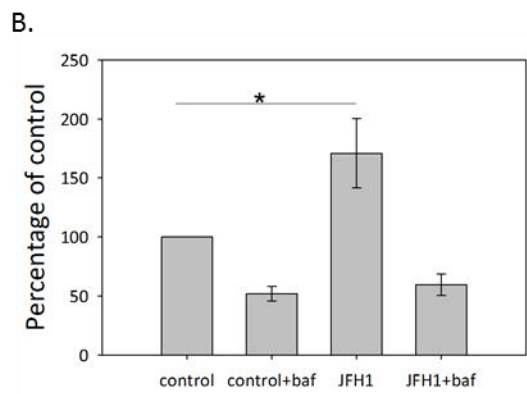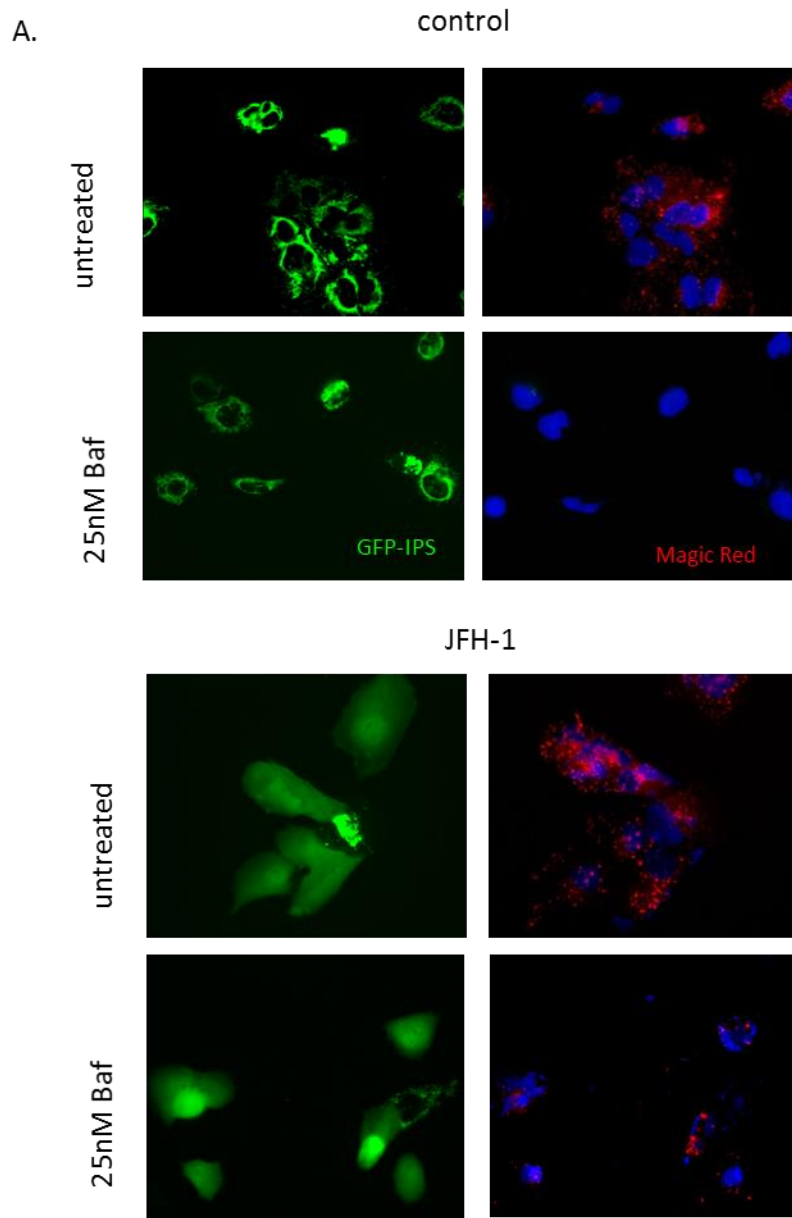
JFH-1 infection does not alter cathepsin B and D activity

Previously Wozniak *et al* demonstrated that the HCV p7 protein inhibits the acidification of intracellular compartments in infected cells (12). Fusion of autophagosomes occurs with acidified organelles either endosomes to form amphisomes or lysosomes to form autophagolysosomes. It is possible that fusion is occurring but due to defects in acidification or impaired lysosomal hydrolase activity, degradation of autophagosomes does not occur.

We explored whether the block in degradation indicated by the autophagic flux assay was due to increased vesicular pH altering fusion with autophagosomes. To measure lysosomal activity, we monitored the proteolytic function of cathepsins during JFH-1 infection. Cathepsin B, a cysteine protease, localizes to lysosomes in its mature form. Procathepsin B is trafficked to the lysosome through binding to the mannose-6-phosphate receptor and undergoes autocatalytic proteolytic cleavage resulting in production of its mature form (129). Cathepsin B activity was measured using a substrate, Magic Red(z-Arginine-Arginine)$_2$, that generates fluorescence upon enzymatic cleavage (130). Huh-7.5 cells transduced with EGFP-IPS (IFN-β promoter stimulator-1) were used to monitor infection. Upon HCV infection, the GFP signal will appear diffuse in the cytosol when the viral NS3 protease cleaves the IPS tethered to the mitochondrial membrane. The GFP will remain localized to mitochondria in uninfected cells. Using live cell imaging, uninfected cells displayed red fluorescence indicating the cleavage of the Magic Red substrate by active cathepsin B (Figure 7A). Bafilomycin A1 treatment can inhibit the generation of red fluorescence by alkalinizing the lysosome. JFH-1 infected cells are also able to generate fluorescence by cathepsin B cleavage illustrating that HCV infection does not inhibit cathepsin B activity. (Figure 7A & B).

Figure 7 HCV does not suppress cathepsin B and D activity. Huh-7.5-GFP-IPS or Huh-7.5 cells were treated with 25nM BafA overnight. Cells were then treated with Magic Red Cathepsin B reagent in HEPES buffer. *A)* Live cell imaging of GFP-IPS cells was done using a Nikon eclipse Ti PFS Quantitative Fluorescence Live-Cell and Multidimensional Imaging System equipped with a digital monochrome Coolsnap HQ2 camera. Fluorescence images were collected using Metamorph software at wavelengths of 560nm excitation/607nm emission for the Cathepsin B substrate. Nuclei were stained with Hoechst stain. Representative images are shown. *B)* Huh-7.5 cells were incubated as described, washed twice with HEPES buffer and lysed with RIPA buffer for 5min at 4°C. Fluorescence measurements were taken at room temperature in a Fluostar Optima plate reader at excitation/emission wavelengths of 584/620nm. * $p<0.001$ by the Mann-Whitney Rank Sum test. *C)* Huh-7.5 cells were treated with 25nM BafA overnight. The 3000xg pellet from the post-nuclear homogenate was resuspended in homogenization buffer with protease inhibitors for analysis by SDS-PAGE. Western blotting was done for anti-cathepsin D, anti-core, and anti-GAPDH. Western blot shown is representative of three experiments.

A. control

untreated

25nM Baf

GFP-IPS

Magic Red

JFH-1

untreated

25nM Baf

B.

C.

3000xg pellet

control   JFH1

Baf (100nM):   -   +   -   +

pro

prepro

mature

core

GAPDH

We also measured the activity of another enzyme, cathepsin D. The maturation of this aspartic enzyme from its preprocathepsin form to procathepsin D to its mature form is highly dependent on the acidic environment of the lysosome (131). The 28-kDa mature form of cathepsin D was present in equivalent amounts when comparing uninfected and JFH-1-infected cells indicating efficient enzyme maturation in both conditions (Figure 7C). Treatment of cells with bafilomycin A1 was able to reduce the appearance of the mature form of cathepsin D in both control and infected cells.

We were unable to find evidence that JFH-1 infection decreases the maturation of proteases or inhibits their proteolytic activity.

Defects in autophagosome fusion during HCV infection are due to trafficking

Since HCV infection did not alter global lysosomal proteolytic activity, the HCV-induced defect in autophagosome degradation might be due to a lack of fusion between autophagosomes and lysosomes. A defect in fusion could be due to an altered composition of the autophagosome preventing fusion even if the organelles encounter each other or a defect in trafficking within HCV-infected cells preventing the autophagosomes from contacting lysosomes. To differentiate between these two possibilities, we performed an in vivo assay using an RFP-GFP-LC3 reporter plasmid as well as an in vitro fusion assay with isolated organelles.

To explore whether trafficking is altered in HCV infected cells, Huh-7.5 cells were transfected with the RFP-GFP-LC3 plasmid and left untreated, treated with EBSS, or treated with bafilomycin A1. EBSS treatment activates autophagy by simulating nutrient starvation by amino acid deprivation. Autophagosome formation is marked by yellow fluorescence due to the co-localization of the RFP and GFP signals of the LC3-II on the autophagosomal membrane. Autophagosome fusion with a lysosome to form an autophagolysosome causes quenching of the
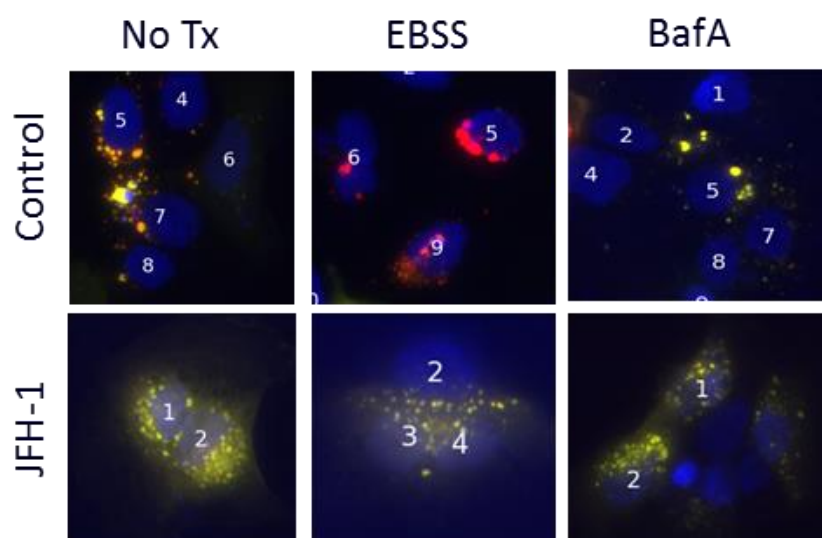
GFP fluorescence and its eventual degradation and only the RFP fluorescence is visible as it is more resistant to the acidic environment of the lysosome. GFP has a pKa value of 6.0 whereas RFP has a pKa value of 4.5. If fusion does not occur, autophagosomes will remain yellow. The characteristics and use of this plasmid are described in Kimura *et al* (132).

Uninfected Huh-7.5 cells had a mean green-to-red ratio of approximately 0.7 where a ratio of 1 means equal green-to-red signal. Treatment with bafilomycin increased this ratio whereas EBSS treatment decreased it (Figure 8A, B). This corresponds to the visual observation that bafilomycin made puncta appear more yellow in control cells while EBSS treatment caused puncta to be redder as the GFP signal was quenched in the lysosome. Similar to bafilomycin, HCV infection increased the ratio of green to red fluorescence of whole cells (Figure 8B) and prevented the formation of red puncta by EBSS (Figure 8A). These results indicate that HCV infection decreased autophagosome-lysosome fusion events even under conditions stimulating autophagy

Autophagosomes and lysosomes were isolated from Huh-7.5 cells using a discontinuous Nycodenz gradient and the identities of the fractions were confirmed by western blot for organelle markers (Figure 9A&B). LC3-II protein was found in the autophagosome and autophagolysosome fractions. LAMP-2 protein was a little more promiscuous which was also observed in the original paper detailing the method. Western blotting for cathepsin D showed more mature protein in the lysosomal fraction (data not shown). Autophagosomes and lysosomes were differentially labeled with fluorescent primary antibodies and used for an in vitro fusion assay where fusion events were measured by flow cytometry (Figure 9C&D). Autophagosomes and lysosomes from uninfected cells and JFH-1-infected cells were able to fuse with each other at similar rates (Figure 9E). As a control for no fusion, organelles were either fixed with

Figure 8 HCV suppresses fusion of autophagosomes and lysosomes in Huh-7.5 cells. Huh-7.5 cells transfected with RFP-GFP-LC3 plasmid were treated with either BafA or EBSS. Cells were fixed with 3% paraformaldehyde and permeabilized with acetone. Cells were stained with anti-core antibody followed by an AlexaFluor 648-conjugated secondary antibody. DAPI was used to stain nuclei. Single wavelength fluorescence images were acquired using Metamorph software at 560nm excitation/607nm emission for TxRed (RFP), 485nm excitation/525 emission for FITC (GFP), 650 excitation/684nm emission for CY5 (HCV core), and 387 excitation/440 emission for DAPI. *A)* Representative images of transfected control and JFH-1 infected cells are shown *B)* Analysis was carried out using CellProfiler software to determine the mean integrated intensity of the GFP/RFP ratio per cell. A total of 367 cells were analyzed. Box plots were created using R software and show the treatment groups analyzed. The differences between all groups are statistically significant by the Kruskal-Wallis test.

A.

	No Tx	EBSS	BafA
Control			
JFH-1			

B.

GFP/RFP ratio for cells

No Tx EBSS BafA No Tx EBSS BafA

control JFH-1
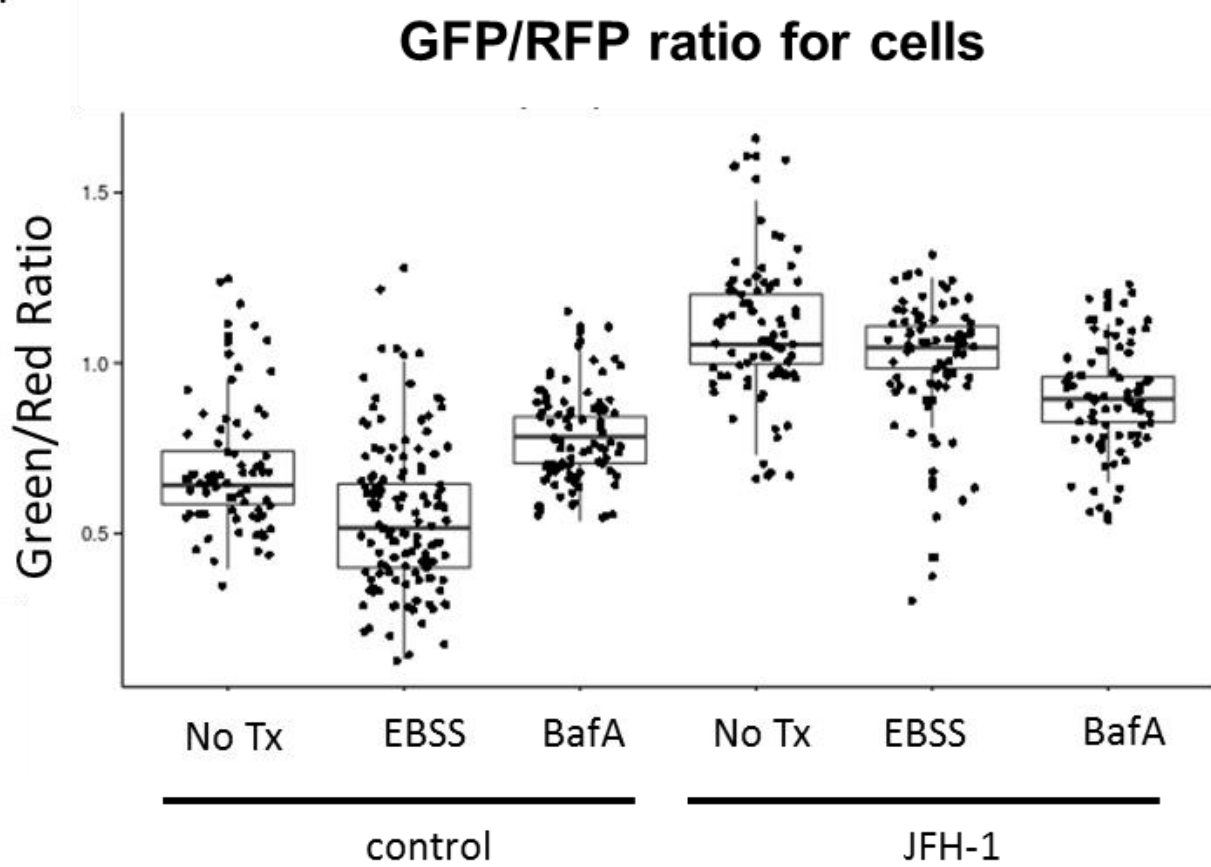
Figure 9 Autophagosomes and lysosomes from HCV-infected cells can fuse in vitro. Huh7.5 cells were fractionated on a discontinuous Nycodenz gradient. *A)* Representation of the Nycodenz gradient and where the organelle fractions are located. *B)* Organelle fractions from the Nycodenz gradient were collected and subjected to SDS-PAGE analysis. Western blotting was done using anti-LC3 antibody (autophagosome marker) and anti-LAMP-2 (lysosome marker). *C)* Flow cytometry of individual vesicle fractions. Autophagosomes were incubated with anti-LC3-PE antibody (1:50) while lysosomes were incubated separately with anti-LAMP-2-APC (1:20). 2% paraformaldehyde was added for fixation. PE- and APC-positive organelles were analyzed by flow cytometry using a BD LSR II instrument. *D)* Labelled autophagosomes and lysosomes were mixed together in reaction buffer for fusion to occur. Controls for "no fusion" were incubated at 4°C and had no ATP or GTP added to the reaction. 2% paraformaldehyde was added for fixation. Fusion is indicated by organelles that are both PE- and APC-positive. *E)* The bar graph illustrates the percentage fusion of autophagosomes and lysosomes from control and JFH-1-infected cells when compared to their "no fusion" controls. This graph is representative of three independent preparations and flow cytometry experiments. Differences between control and JFH-1 were not significant.

A.

Nycodenz gradient

B.

C.

D.

E.
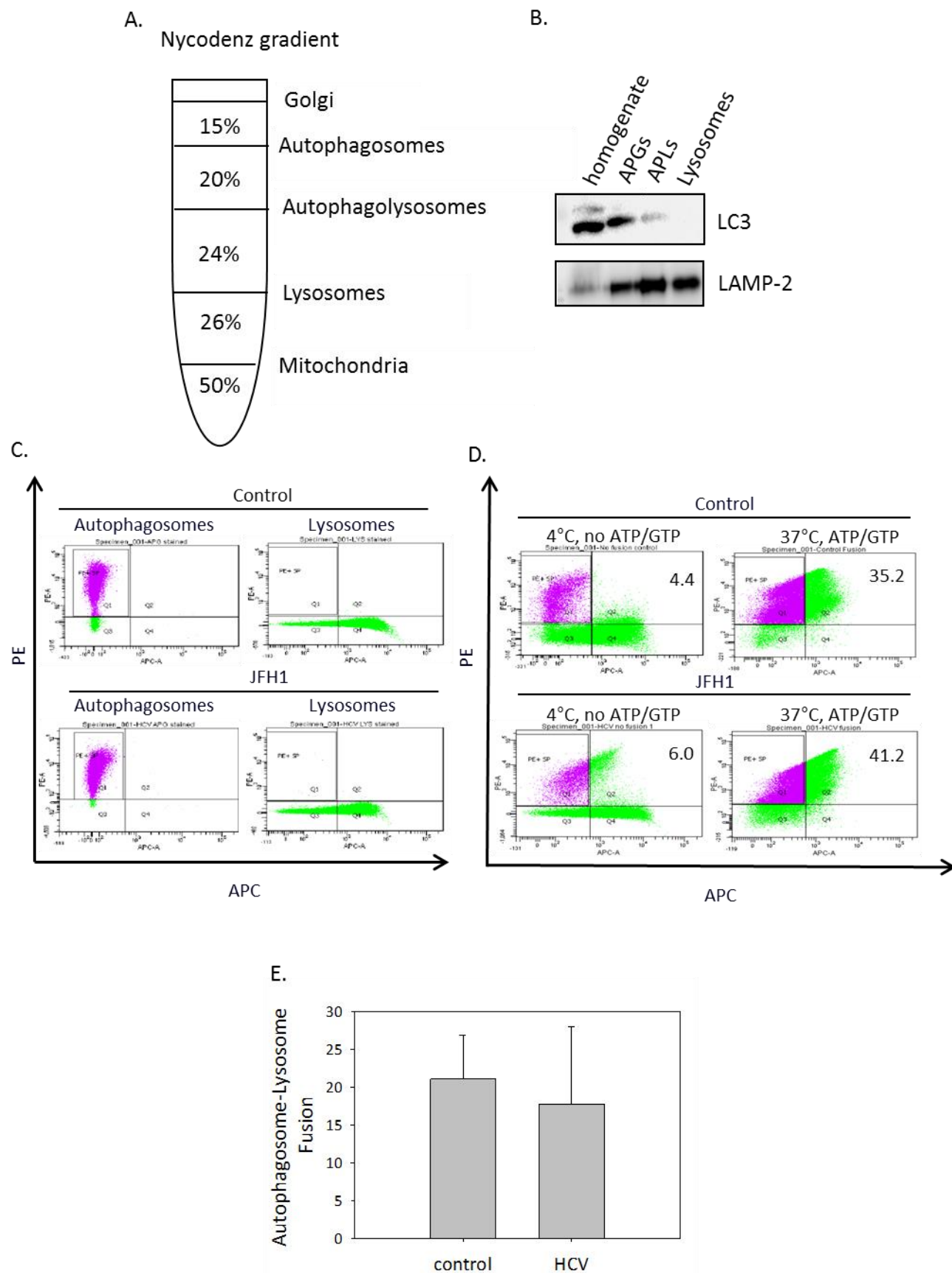
paraformaldehyde immediately or were held at 4°C without ATP or GTP in the fusion buffer (Figure 9D). This suggests that HCV infection does not alter the ability of autophagosomes and lysosomes to fuse with each other and the fusion defects observed result from alterations in trafficking.

Discussion

From these experiments, we concluded that JFH-1 infection blocks fusion of autophagosomes and lysosomes. We demonstrated a fusion defect in two ways. First, bafilomycin treatment is unable to increase LC3-II levels in infected cells and second, autophagosomes are not degraded in JFH-1 infected cells and therefore remain yellow using the tandem RFP-GRP-LC3 plasmid.

Besides a block in fusion with lysosomes, this data also suggests that after an initial induction of autophagy, JFH-1 infection may block autophagy initiation. If autophagy was constantly being induced during infection, then it would be expected that LC3-II levels would continue to increase after being treated with bafilomycin at different time points as new autophagosomes form within the cell. However, autophagy initiation is also blocked in JFH-1 infected cells since LC3-II does not increase over the eight-hour time course. There is evidence that HCV infection may regulate autophagosome maturation in a temporal fashion by upregulating Rubicon or UVRAG at either early or late timepoints in infection (110). Additionally, there is a report that HCV infection upregulates Beclin1 as well as mTOR activity. While it has been suggested that upregulation of mTOR activity may not affect HCV-induced autophagy negatively, it is possible that upregulating mTOR activity could be a mechanism to blunt the initiation of HCV-induced autophagy at later stages in infection. This may lead to an accumulation of autophagosomes within the cell that the virus utilizes for viral replication. The

half-life of an autophagosome is approximately ten minutes so it would be interesting to determine whether JFH-1 infection increases the stability of autophagosomes. This could be done by using a photo-activatable PAGFP-LC3 which allows labeling of autophagosomes at a specific time point. These autophagosomes could then be followed by live-cell imaging to see how long they persist (133). Unfortunately, conventional methods of examining protein half-life by cycloheximide treatment must be used with caution in autophagy studies since cycloheximide inhibits autophagy.

Since the autophagosomes in HCV-infected cells remain yellow using the RFP-GFP-LC3 tandem plasmid indicating a block in fusion, there is also the possibility that fusion occurs but the degradative capacity of the lysosome is impaired. However, we showed that cathepsin B and D activity and processing is not impaired by JFH-1 infection. This was surprising given previous findings regarding the role of p7 in altering lysosomal pH. It cannot be ruled out, however, that HCV infection does not affect a subset of lysosomes since the methods used to measure proteolytic activity are looking at global lysosomal activity within the cell. Previous studies have shown subpopulations of lysosomes exist in cells and can carry out different functions. For example, only a subset of lysosomes has been shown to participate in chaperone-mediated autophagy (134). Additionally, lysosome positioning within the cell may determine their function as well. If there are changes to the composition of organelles within HCV-infected cells, those alterations do not prevent autophagosome-lysosome fusion as was shown by using isolated organelles in an in vitro fusion assay.

We also observed a block in autophagic flux in replicon cells. This suggests that viral replication and viral protein expression are sufficient to block autophagosome-lysosome fusion. While we were unable to determine which viral proteins were responsible for inhibiting

autophagosome-lysosome fusion, we narrowed it down to E1, E2, p7, and/or NS2. E1 and E2 have been implicated in the induction of the UPR response during HCV infection due to their maturation in the ER. p7 was shown to induce apoptosis in cells but did not activate autophagy despite being able to bind to Beclin1 (135). While NS2 has not been implicated in HCV-induced autophagy, it has roles in viral assembly and infectious particle production and can interact with many other viral proteins. Some preliminary data from our experiments suggests that expression of a HA-tagged NS2 may be able to decrease autophagic flux but not to the same levels seen in JFH-1 infection (data not shown).

From this data, we concluded that JFH-1 infection in Huh-7.5 cells blocks autophagosome-lysosome fusion due to a defect in trafficking. Isolated autophagosomes and lysosomes from HCV-infected cells remain fusion competent.

Chapter III: HCV infection overexpresses Arl8b expression to alter autophagy

Background

Intracellular trafficking is important for the health of cells. Membrane and vesicular identity, trafficking, signaling, and regulation are determined by GTPases. GTPases can belong to multiple families with the most well-studied being the Ras superfamily, which includes the Rab, Arf, Ran, Ras, and Rho families. Additionally, phosphoinositides also contribute to membrane identity. Phosphoinositides can recruit GAPs and GEFs regulating GTPase activity and also act as effectors or co-receptors of small GTPases (136). For example, Rab5 can interact with phosphoinositide-3-kinases to generate phosphatidylinositol-3-phosphate on endosomes which in turn helps recruit effectors such as EEA1 (137). Membrane fusion and cargo movement is accomplished by binding of tethering factors to GTPases which contributes to specificity of fusion and may also coordinate the binding of the correct SNAREs for docking (138).

After concluding that impaired fusion between autophagosomes and lysosomes in HCV infection was likely due to a trafficking defect, the next step was to identify factors that could be responsible. One GTPase that we focused on was Arl8b due to its potential role in regulating autophagy by controlling lysosomal positioning. As previously mentioned, Arl8b localizes specifically to lysosomes. Lysosomes are emerging as critical organelles in signaling and regulation and not simply "suicide bags" as first described by Christian de Duve in the late 1950s. The biosynthesis of lysosomes is regulated by TFEB (transcription factor EB). TFEB is held in an inactive phosphorylated state in the cytosol and upon activation, it is translocated to the nucleus where it induces the transcription of genes related to lysosomal hydrolases, lysosomal membrane proteins, and lysosome biogenesis regulators (139). A recent study also

showed that TFEB is also linked to autophagy and its upregulation can induce both autophagy-related gene transcription and autophagosome formation (140). Lysosomal hydrolases are then acquired by trafficking via the mannose-6-phosphate receptor. Lysosomes can fuse with multiple types of organelles and in the case of autophagy are recycled by autophagic lysosome reformation.

Arl8b is recruited to lysosomes via the BORC complex and binds to kinesin-1 through the effector SKIP to control microtubule-dependent movement of lysosomes to the cell periphery. Positioning of lysosomes by Arl8b seems to be important for, not only autophagy, but also for cell spreading and motility (88), lytic granule transport (141), and invasion and protease secretion in prostate cancer (142). Changes to the lysosome, either their positioning or function, have not been implicated in HCV infection. Our previous data showed no HCV-induced defects in lysosomal hydrolases and no changes to lysosome composition that would inhibit fusion with autophagosomes. However, we decided to focus on exploring whether HCV infection altered Arl8b expression and localization and what effect Arl8b knockdown would have on autophagy.

Materials and Methods

Cells and Culture Conditions

Huh-7.5-RFP-NLS-IPS cells were obtained from Charles Rice. This cell line was cultured in Dulbecco's Modified Eagle Medium (DMEM) containing 4.5g/L glucose, L-glutamine, and sodium pyruvate, 10% FBS, and 1% NEAA. Cells were maintained at 37°C/5% CO_2.

293FT cells were purchased from Thermo Fisher Scientific. This cell line was cultured in DMEM containing 4.5g/L glucose, 6mM L-glutamine, 1mM sodium pyruvate, 10% FBS, 1% NEAA, and 500ug/mL G418. Cells were maintained at 37°C/5% CO_2.

Western blotting

Western blotting was performed using anti-LC3B, 1:1000 (Cell Signaling), anti-GAPDH, 1:1000 (Santa Cruz Biotechnology), anti-core, clone C7-50, 1:1000 (Thermo Fisher Scientific), and anti-Arl8b, 1:1000 (Proteintech, Rosemont, IL). Horseradish peroxidase-conjugated secondary antibodies were from Thermo Fisher Scientific and IR-Dye conjugated secondary antibodies were from LI-COR Biosciences.

Immunofluorescence

Huh-7.5 cells were plated on 12mm circular glass coverslips in 4-well plates. Cells were transfected with Lipofectamine 3000 (Thermo Fisher Scientific). Plasmids used were Arl8b wildtype-GFP, Arl8bQ75L-GFP, and Arl8bT34N-GFP in a pcDNA3.1/CT-GFP-TOPO backbone (gifts from Don J. Mahuran, University of Toronto). Cells were fixed with 4% paraformaldehyde and blocked for one hour in 1XPBS containing 1% BSA and 1% EDTA at room temperature. For staining with anti-LAMP-2, clone H4B4, 1:500 (DSHB, University of Iowa), cells were permeabilized with acetone for five minutes. For staining with anti-LC3B, 1:400 (Cell Signaling), cells were fixed and permeabilized with ice-cold methanol for ten minutes. JFH-1 infection was monitored by staining for anti-core, clone C7-50, 1:300 (Thermo Fisher). Secondary antibodies used were AlexaFluor-conjugated (Thermo Fisher Scientific) and Phalloidin-647 (Abcam, Cambridge, MA) was used to stain actin. Coverslips were mounted onto slides using Prolong Gold antifade mountant containing DAPI (Thermo Fisher Scientific).

Confocal images were taken on a Leica TCS SPE confocal configured with a Leica DM550 Q upright microscope.

Real time quantitative PCR

RNA was isolated from Huh-7.5 cells using TRI reagent (Thermo Fisher Scientific) followed by cDNA synthesis using the High Capacity cDNA Reverse Transcription Kit (Thermo Fisher Scientific). qPCR reactions were set up using iQ SYBR Green (BioRad, Hercules, CA) on a CFX96 Real Time system on a C1000 Thermal Cycler (BioRad). The following primers were used for Arl8b, forward primer: 5'-GCGGTATTGCAGAGGAGTCA-3' and reverse primer: 5'-CCAAGCACTAGCACTGGAA-3', and GAPDH, forward primer: 5'-GGAGCGAGATCCCTCCAAAAT-3' and reverse primer: 5'-GGCTGTTGTCATACTTCTCATGG-3'. Primers were validated using a temperature gradient cycling protocol to identify the appropriate melting temperature and run on agarose gels to ensure only one PCR product was present.

shRNA mediated knockdown of Arl8b

MISSION Arl8b shRNA (clone ID NM_018184.2-671s21c1) and TRC2 pLKO.5-puro non-Target shRNA control plasmid (SHC216) were obtained from Sigma-Aldrich. 293FT cells were transfected with MISSION plasmids, psPax2, and pMDG.2 vectors at a ratio of 1ug:0.75ug:0.25ug using X-tremeGENE HP transfection reagent (Roche Indianapolis, Indiana) to produce lentivirus. Lentivirus was collected after 24-48 hours. Huh-7.5 cells were transduced with lentivirus and 8ug/mL polybrene for 48 hours. Cells were selected with 3ug/mL puromycin and maintained with 1ug/mL puromycin.

Results

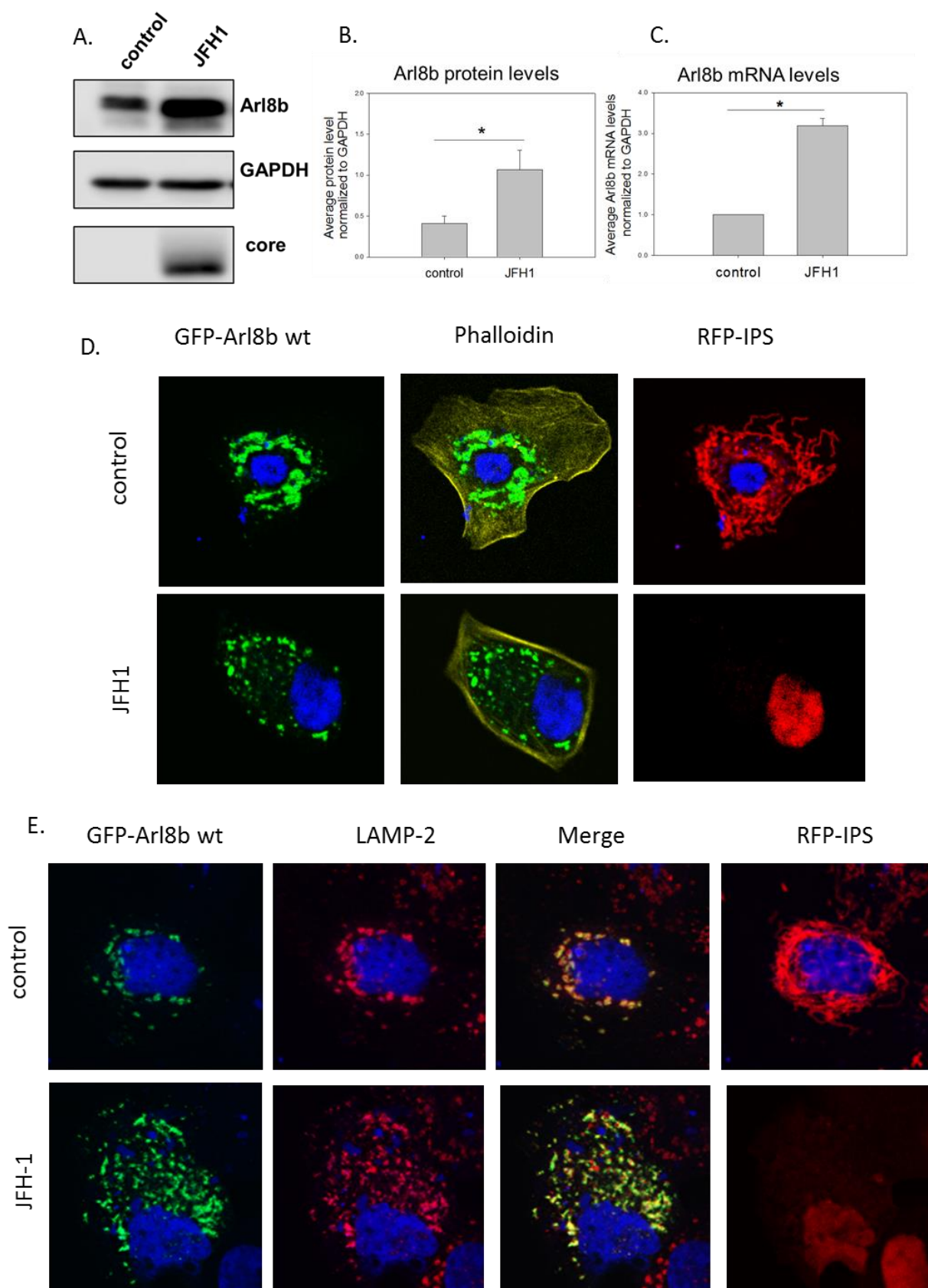### HCV infection alters the lysosomal Arf-like GTPase, Arl8b

In trying to identify potential proteins involved in autophagosome-lysosome fusion, we focused on Arl8b. We found that during HCV infection, both Arl8b protein and mRNA levels

are elevated approximately three-fold indicating that HCV alters Arl8b at a transcriptional level (Figure 10A-C). Next, we examined the localization of Arl8b-positive organelles during infection. Uninfected and HCV-infected Huh-7.5-RFP-NLS-IPS cells were transfected with the wildtype Arl8b-GFP plasmid. After transfection with Arl8b, uninfected cells displayed large, circular structures that were usually in the perinuclear region with some vesicles in the periphery (Figure 10D). These vesicles co-localized with LAMP-2 indicating that the expressed protein was indeed decorating lysosomes (Figure 10E). Similar results were obtained when expressing the constitutively active version of Arl8b with a Q75L mutation which remains locked in a GTP-bound state. When the dominant-negative Arl8b T34N mutant is expressed that remains bound to GDP, there are punctate structures that are most likely aggresomes but do not co-localize with LAMP-2 (86) (Figure 11B). Wildtype Arl8b-positive structures also co-localized with cathepsin D in fixed cells and Magic Red substrate, indicating cathepsin B activity, in live cells further identifying them as acidified lysosomes (Figure 11A).

HCV-infected cells displayed a dramatically altered localization of Arl8b-positive vesicles dispersed throughout the cell periphery (Figure 10D). There was no longer a perinuclear clustering as seen in control cells. HCV infection does not alter the identity of the Arl8b-positive vesicles as they still co-localize with LAMP-2 (Figure 10E). These findings suggest that HCV-induced increase in Arl8b results in an increased peripheral lysosomal positioning.

Figure 10 Arl8b expression is increased and its localization altered by HCV infection.

Huh7.5 cells were infected with JFH-1, HCV genotype 2a A) Cells were lysed and western blotting was done using anti-Arl8b antibody, anti-GAPDH antibody as a loading control, and anti-core antibody to monitor HCV infection. B) Densitometry analysis of the changes in Arl8b levels, normalized to GAPDH levels, as determined from western blotting. Quantification of western blots (n=3) was done using Licor Odyssey software. C) Quantification of Arl8b mRNA levels normalized to GAPDH from n=3 experiments D) Arl8b-GFP was transfected into Huh7.5-RFP-NLS-IPS cells and stained with Phalloidin-647 to define cell boundaries. Infection was monitored by the RFP signal. Nuclei were stained with DAPI. Fluorescence images were collected using LasX software. Representative images are shown. E) Arl8b-GFP was transfected into Huh7.5-RFP-NLS-IPS cells and stained with anti-LAMP-2. Nuclei were stained with DAPI. Fluorescence images were collected using LasX software. Representative images are shown.

A.

B. Arl8b protein levels

C. Arl8b mRNA levels

D. GFP-Arl8b wt   Phalloidin   RFP-IPS

control

JFH1

E. GFP-Arl8b wt   LAMP-2   Merge   RFP-IPS

control

JFH-1

Figure 11 Arl8b expression in Huh7.5 cells. *A)* Huh7.5 cells were transfected with wildtype Arl8b-GFP and either incubated with Magic Red substrate (upper panel) or fixed and stained for cathepsin D (lower panel). Nuclei were stained with DAPI. Fluorescence images were collected using Metamorph software. Representative images are shown. *B)* Cells were transfected with Arl8bQL-GFP or Arl8bTN-GFP, fixed, and stained for LAMP-2. Nuclei were stained with DAPI. Fluorescence images were collected using LasX software. Representative images are shown.

A.

Arl8bwt-GFP   Magic Red   Merge

Arl8bwt-GFP   Cathepsin D   Merge

B.

Arl8bQL-GFP   LAMP-2   Merge

Arl8bTN-GFP   LAMP-2   Merge
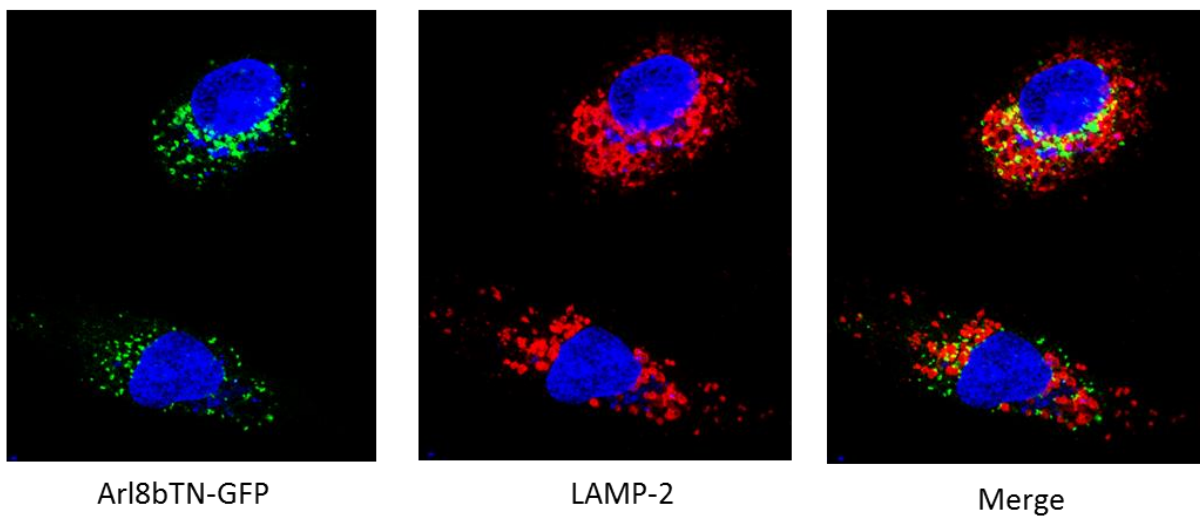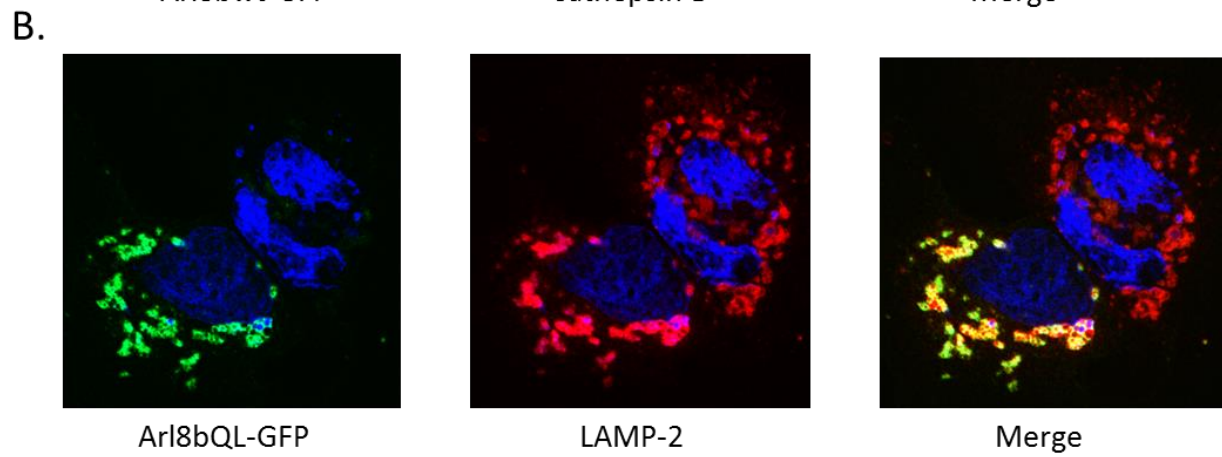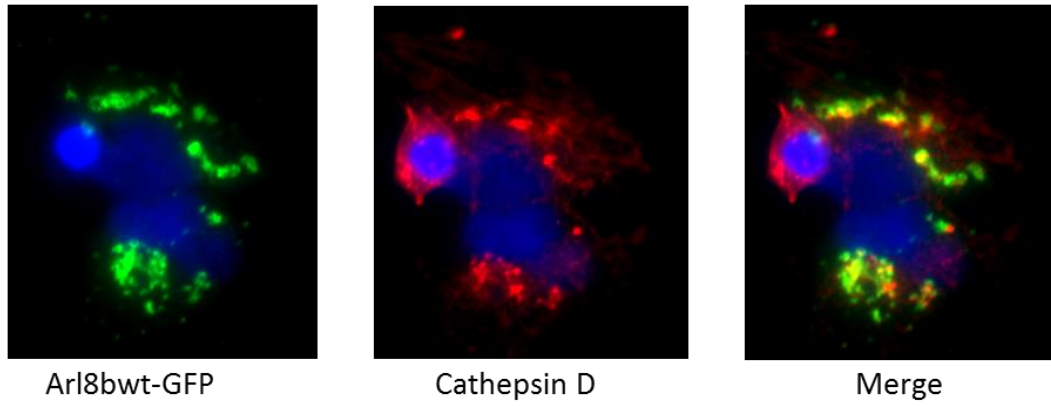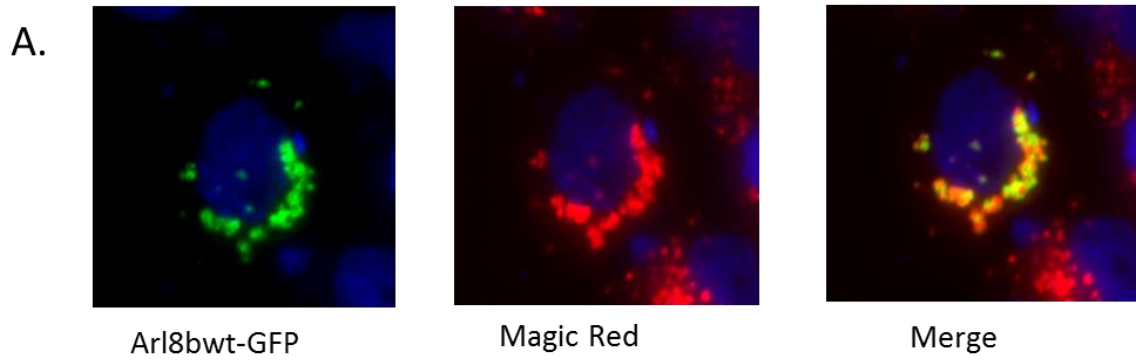
Impaired autophagic flux in HCV infection is due to an Arl8b-dependent mechanism

We wanted to see what effect lysosomal positioning had on fusion with autophagosomes. Control and JFH-1 infected Huh-7.5 cells were transfected with wildtype Arl8b-GFP and the cells were stained for the presence of endogenous LC3. In uninfected Huh-7.5 cells, Arl8b-positive vesicles once again were found primarily in the perinuclear region in large puncta and co-localized with LC3-positive vesicles indicating autophagosome-lysosome fusion (Figure 12A). Autophagosome-lysosome fusion occurs in the perinuclear space. In HCV-infected cells, Arl8b-positive vesicles were dispersed into the periphery as previously shown and the amount of co-localization with LC3-positive puncta drastically decreased (Figure 12A). This data agrees with previous observations that there is a decrease in the amount of fusion between lysosomes and autophagosomes in HCV infected cells. Cells were also treated with EBSS to simulate amino acid starvation and activate complete autophagy. In control cells, Arl8b-positive lysosomes and autophagosomes displayed a high degree of co-localization while EBSS treatment did not enhance autophagosome-lysosome fusion in JFH-1 infected cells (Figure 12B).

Next, we determined if knocking down Arl8b in HCV-infected cells could alter autophagic flux. It has been shown that knocking down Arl8b in cells results in increased fusion of autophagosomes and lysosomes thereby increasing autophagic flux (93). By transducing Huh-7.5 cells with a lentivirus expressing an Arl8b shRNA and selecting cells with puromycin, we obtained cells that had a greater than 80% knockdown of Arl8b by western blot for protein levels. We also transduced and selected for cells expressing a nontarget shRNA which had comparable levels of Arl8b expression to non-transduced Huh7.5 cells (Figure 13A). Knocking down Arl8b did not seem to have an effect on the ability of cells to be infected by JFH-1 virus. Autophagic flux in HCV-infected Arl8b knockdown cells was then measured by

Figure 12 Arl8b co-localization with LC3 is decreased by HCV infection. Huh7.5 cells were infected with JFH-1 virus. A) wildtype Arl8b-GFP was transfected into cells, fixed with methanol, and stained with anti-LC3 and anti-core antibodies. Fluorescence images were collected using LasX software. Nuclei were stained with DAPI stain. Representative images are shown. B) Cells were treated as in panel A except they were also treated with EBSS for thirty minutes prior to fixation.

A.

core

merge

LC3

GFP-Arl8b wt

control

JFH-1

EBSS

B.
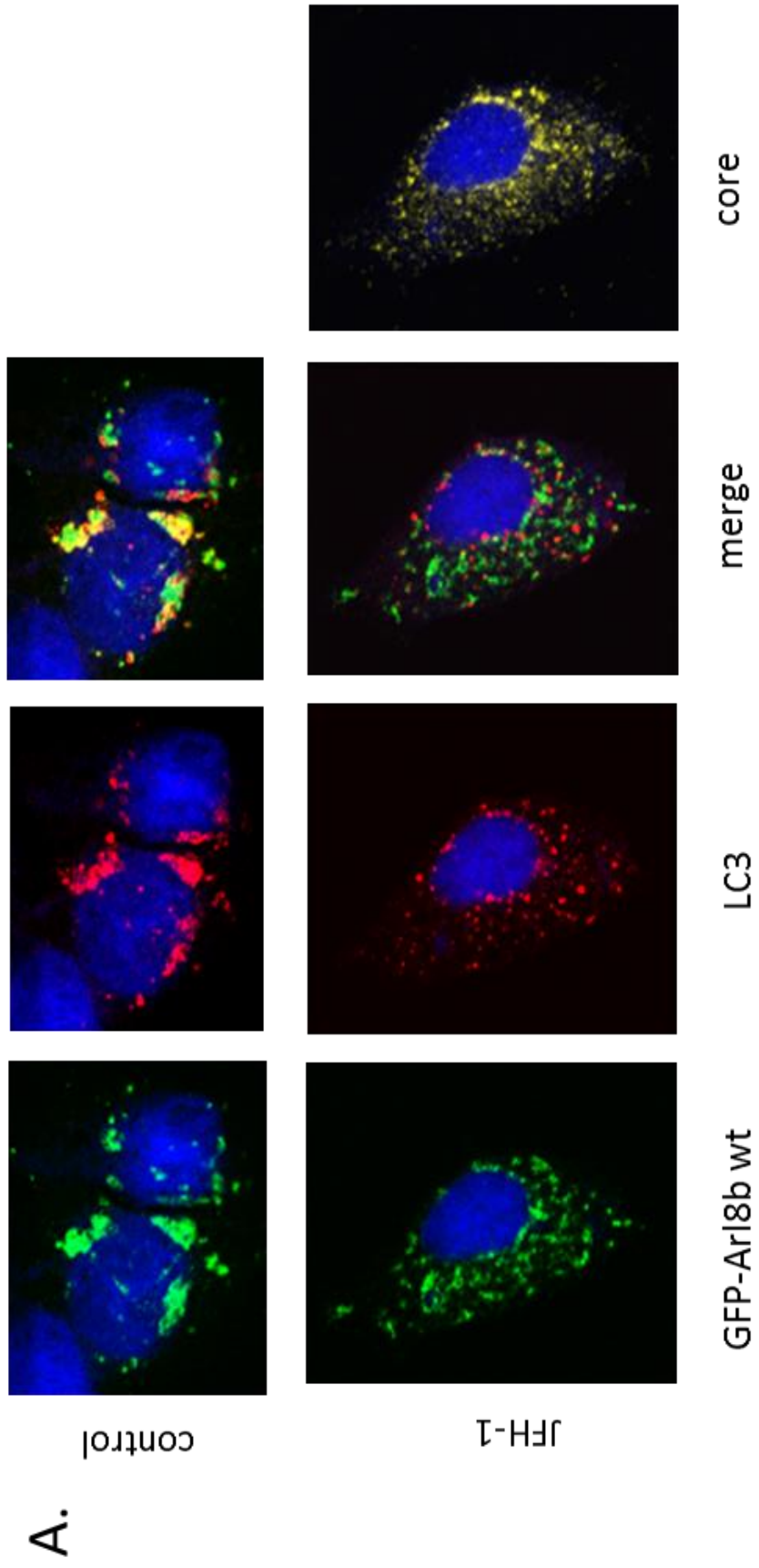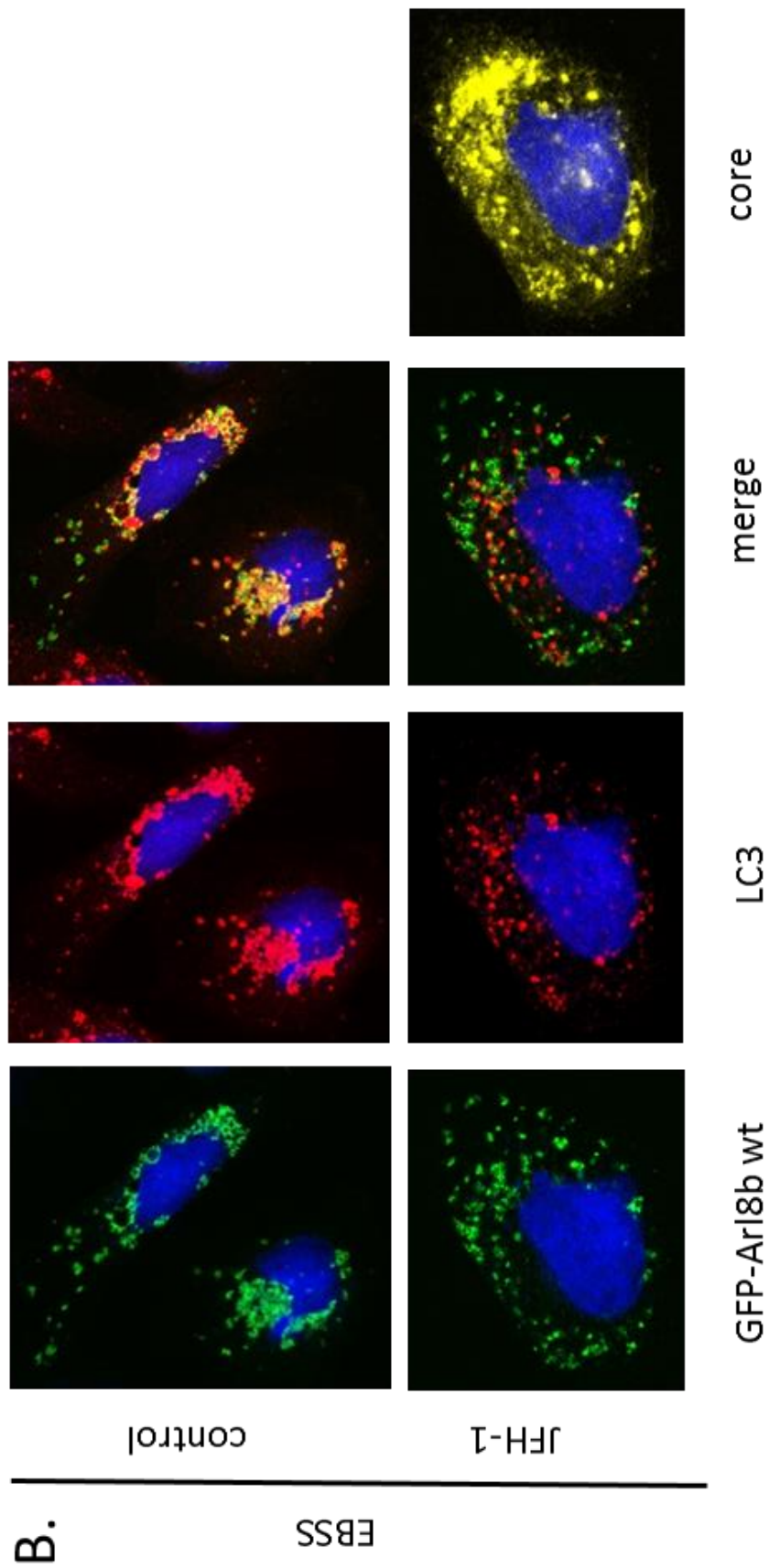
Figure 13 Arl8b knockdown restores autophagic flux in HCV-infected cells. Huh7.5 cells were transduced with lentivirus expressing an Arl8b or nontarget shRNA *A)* Cells were lysed and western blotting was done using anti-Arl8b antibody and anti-GAPDH antibody as a loading control. *B)* Cells were infected with JFH-1 and treated with 100nM bafilomycin A1 for four hours. Western blotting was done using anti-LC3 antibody, anti-GAPDH antibody as a loading control, and anti-core to detect HCV infection. *C)* Densitometry analysis of the changes in LC3-II levels after bafilomycin treatment, normalized to GAPDH levels, as determined from western blotting. Quantification of western blots (n=3) was done using Licor Odyssey software.

Huh7.5   nontarget shRNA   Arl8b shRNA

Arl8b

GAPDH

	nontarget shRNA				Arl8b shRNA			
	control		JFH1		control		JFH1	
BafA(100nM):	--	+	--	+	--	+	--	+

LC3-I
LC3-II

GAPDH

core
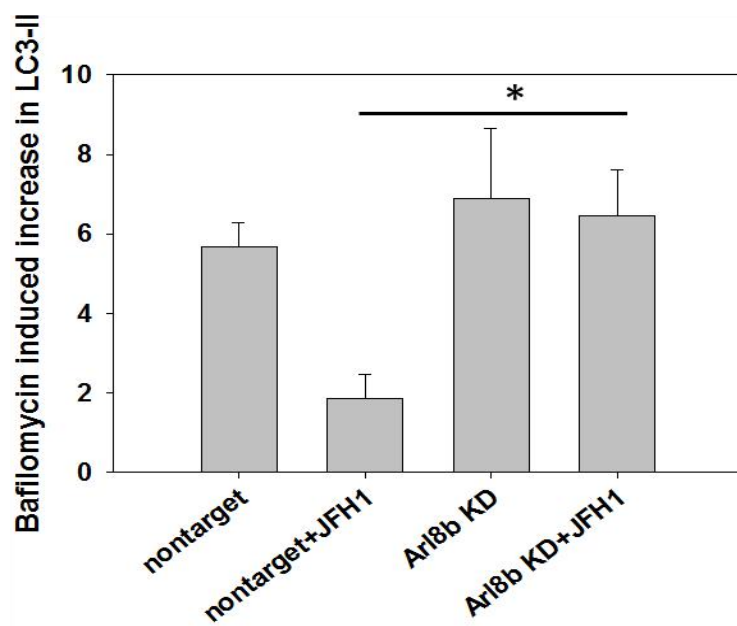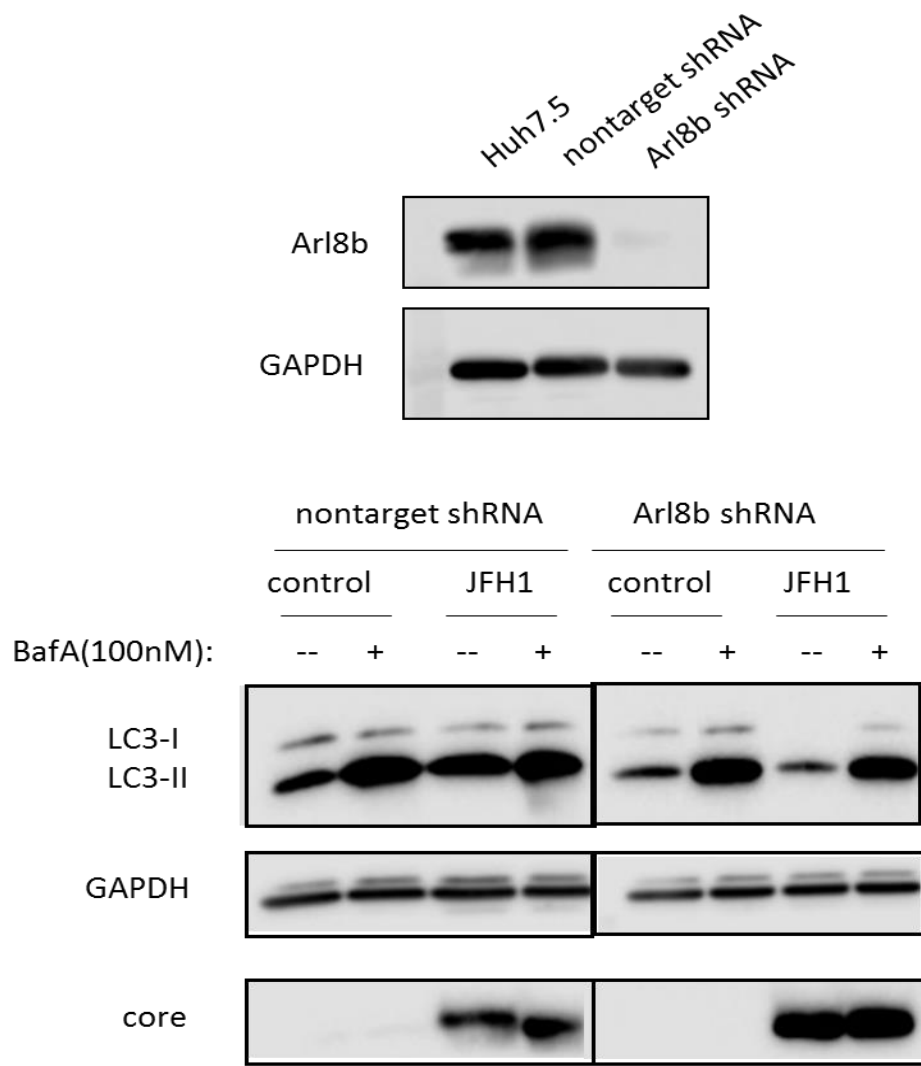
treating cells with bafilomycin A1 to block lysosomal fusion as in Figure 4A. In agreement with our hypothesis, knocking down Arl8b in HCV-infected cells could restore autophagic flux to similar levels seen in uninfected cells with almost a six-fold increase in LC3-II levels after bafilomycin A1 treatment (Figure 13C&D). Autophagic flux remained impaired in HCV-infected nontarget shRNA-expressing cells when compared to uninfected cells as was previously demonstrated. The difference in autophagic flux between JFH-1 infected non-target cells and JFH-1 infected Arl8b knockdown cells was statistically significant.

Discussion

From these experiments, we concluded that upon HCV infection, Arl8b protein levels are increased and this leads to a dispersal of lysosomes into the cell periphery. This altered lysosomal positioning reduces fusion with autophagosomes allowing them to persist within HCV-infected cells. Knocking down Arl8b was sufficient to restore autophagosome-lysosome fusion in HCV-infected cells indicating it is a key player in the mechanism of how HCV impairs autophagic trafficking.

Previous studies reported that Arl8b protein overexpression forced lysosomes into the cell periphery, however, in our cell-culture system using Huh-7.5 cells, we consistently observed the majority of Arl8b-positive lysosomes in the perinuclear region. While there were some Arl8b-positive puncta that could be found in the periphery, there was always a concentration of puncta in the perinuclear region. When the same transfection and fixation protocol was used in HeLa cells, Arl8b was more peripheral when compared to Huh-7.5 cells (data not shown) leading to the conclusion that there may be cell type-specific differences in localization when Arl8b is exogenously introduced rather than an artifact of the transfection technique used.

While an increase in Arl8b expression does not necessarily mean an increase in activity, this data suggests that since lysosomes are more peripheral in HCV infected cells there may be an increase in linkage to kinesin through Arl8b. One way to more directly measure Arl8b activity would be to look at binding to its effector SKIP and whether there was more binding during HCV infection. We tried to do this by purifying the portion of SKIP corresponding to the first 300 amino acids that binds to Arl8b as a GST fusion protein and then looking for binding of Arl8b in cell lysates. Unfortunately, endogenous Arl8b bound nonspecifically to the GST protein only negative control and could not confirm specific binding to the SKIP construct.

While the main function of Arl8b is associated with lysosomal movement, we also cannot rule out that Arl8b may have other functions during HCV infection. As previously mentioned, Arl8 plays a role in the tobamovirus replication complex in plants. We did explore the effect of Arl8b knockdown on infectious virus production by electroporating a JC1-luc virus into non-target and Arl8b knockdown Huh-7.5 cells and then infecting naïve Huh7.5 cells with extracellular virus. JC1-luc is a virus that contains a luciferase reporter to allow for monitoring translation of the viral genome. Preliminary results showed that there was less extracellular virus from Arl8b knockdown cells compared to the non-target expressing cells though the decrease was not statistically significant (data not shown). A more extensive analysis of the effect of the loss of Arl8b on HCV infection would have to be undertaken looking at various steps in the life cycle including viral replication and particle production.

This data suggests that pathogens may alter lysosomal positioning as part of their pathogenesis. Viruses may prevent their destruction by evading fusion with lysosomes while others may need to fuse with the endo-lysosomal compartment for their life cycle or use lysosomal membranes for replication. While this is the first report of lysosomal positioning being

altered during HCV infection, this has been reported for other viruses. For example, dynein binds to the hexon capsid of adenovirus in order to move it towards the perinuclear region of the cell where viral replication takes place in the nucleus. The protein kinase A (PKA)–dependent mechanism that modulates dynein for virus binding also moves late endosomes and lysosomes to the cell periphery due to dynein displacement from RILP. This raises the possibility that adenovirus may utilize acidic compartments in the periphery to induce rapid acidification of virus-containing compartments for release into the cytosol (143). Our data shows that during HCV infection, lysosomal movement to the periphery serves to impede autophagosome-lysosome fusion. If HCV uses autophagosomal compartments for viral replication and/or assembly, then preventing fusion with lysosomes may prevent degradation of intracellular virus in autophagolysosomes.

Chapter IV: Potential cooperativity between Rab7 and Arl8b

Introduction

Arl8b resides on lysosomes and links this organelle to kinesin for anterograde movement to the cell periphery. The opposing dynein force is primarily controlled by the Rab7 GTPase and its effector RILP. The Rab7-RILP complex localizes to late endosomes and lysosomes and binds to the dynein complex (70, 144). RILP binds directly to p150glued (also called dynactin) which then binds to the ~1.2 megadalton dynein complex comprised of multiple subunits (69). RILP has been implicated in proper late endosomal structure and function. Knockdown of RILP decreased the number of intraluminal vesicles in late endosomes and delayed EGFR (epidermal growth factor receptor) degradation (145). Intraluminal vesicles are part of the multivesicular bodies which transport membrane proteins to lysosomes for degradation. RILP plays a role in endosomal maturation by binding to Vps22 and Vps36, two components of the ESCRT-II pathway (146). Additionally, RILP directly binds to members of the HOPS complex which implicates it in tethering vesicles for fusion though this interaction may be independent of Rab7 (147, 148). RILP can also bind to Rab24 and Rab34, both involved in endosomal/lysosomal function.

While Rab7 is a well-known regulator in autophagosome maturation, the specific role of RILP in autophagy is less understood. Autophagy leading to the degradation of lipid droplets, termed lipophagy, in hepatocytes appears to be regulated by Rab7 and impaired RILP binding of microtubules caused decreased association of both multivesicular bodies and lysosomes with lipid droplets (149). It was also shown that Rab7-RILP and LC3 could co-localize indicating the presence of Rab7-RILP on autophagosomes and modulating RILP levels affected autophagosome localization. This study also found roles in autophagic flux for additional Rab7

binding proteins, ORP1L, a cholesterol sensor, and PLEKHM1, which interacts with HOPS and contains a LC3-interacting region (71). A different study, however, indicated that the retrograde transport of lysosomes for fusion with autophagosomes was Rab7-RILP independent and instead was dependent upon the TRMPL1-ALG-2 complex where ALG-2 binds directly to dynein-dynactin (150).

Correct cellular function depends upon proper transport of organelles using molecular motors to move along the cytoskeleton. Dynein and kinesin move vesicles along microtubules in a bidirectional manner by saltatory movement where they are pulled in both directions but there is net movement in one direction depending on the stimuli. There are two main theories governing how bidirectional movement is accomplished: 1) a tug-of-war when both motors are active and compete to move cargo and 2) coordination when motors are not active at the same time so that one motor is dominant. The tug-of-war option is the most readily accepted with support from both in vivo and in vitro experiments. Kinesin produces about 6 piconewtons (pN) of force whereas dynein upon binding to dynactin and its adaptor bicaudal-D2 produces about 4.3 pN of force making it possible that one dynein motor can resist and potentially overcome the force of kinesin (151). In reality, the model is likely more complex than the tug-of-war due to the "paradox of codependence" where it has been observed experimentally that inhibiting one motor can also inhibit movement in the opposite direction (152).

Our lab has studied the effect of HCV infection on the Rab7-RILP complex. Wozniak et al. found that HCV infection can induce the cleavage of RILP which abolishes its interaction with dynein (153). This cleavage is important to produce infectious virus and overexpressing the C-terminal portion of RILP, which binds to Rab7 but not dynein, during HCV infection can increase the amount of extracellular virus compared with infection alone.

There are some conflicting data on whether or not Arl8b and Rab7-RILP are found on the same vesicles (147, 154). It is known that Arl8b and RILP can both recruit the HOPS complex and may compete with each other for HOPS binding (155). Therefore, we explored the relationship between Rab7 and Arl8b during HCV infection.

Materials and Methods

Immunoprecipitation

Huh7.5 cells were transfected with GFP-Rab7Q67L or Arl8bQ75L-GFP using Lipofectamine 3000 (Thermo Fisher Scientific). Forty-eight hours post-transfection, cells were scraped in a hypotonic lysis buffer (10mM HEPES pH7.5, 10mM NaCl, 1mM KH_2PO_4, 5mM $NaHCO_3$, 1mM $CaCl_2$, 0.5mM $MgCl_2$, 5mM EDTA, 10mM sodium pyrophosphate, 1mM Na_3VO_4, 1mM PMSF, protease inhibitor). Cells were incubated on ice for thirty minutes and then homogenized with a dounce homogenizer. A post-nuclear homogenate was prepared by centrifuging homogenate at 800xg for fifteen minutes at 4°C. 500ug of homogenate was used per immunoprecipitation (IP) reaction and 2ug rabbit anti-GFP (Thermo Fisher Scientific) or 2ug of anti-rabbit IgG (Thermo Fisher Scientific) as a negative control were used. IP reactions were rotated overnight at 4°C. The next day, 50uL of sheep anti-rabbit IgG Dynabeads M-280 (Thermo Fisher Scientific) was added to each IP reaction and rotated for four hours at 4°C. Beads were washed with hypotonic buffer three times before being boiled and loaded on an SDS-PAGE gel.

To evaluate the effect of detergent on IP reactions, an NP-40 based buffer (20mM Tris pH 8.0, 137mM NaCl, 10% glycerol, 1% NP-40, 2mM EDTA, 2mM Na_3VO_4, protease inhibitor) was also used. Cell lysates were incubated on ice for thirty minutes before being clarified at

14000xg for fifteen minutes at 4°C. IP reactions were done the same way as with the hypotonic buffer.

Membrane fractionation

At six days post-JFH-1 infection, control and infected Huh-7.5 cells were scraped into hypotonic lysis buffer. Cells were incubated for thirty minutes on ice before homogenizing them with a dounce homogenizer. Cells were centrifuged at 800xg for fifteen minutes at 4°C to collect a postnuclear homogenate. The homogenate was centrifuged at 20,000xg for twenty minutes at 4°C to collect a membrane fraction and supernatant. The membrane pellet was washed twice with hypotonic buffer centrifuging at 20,000xg between each wash. The membrane pellet was resuspended in RIPA buffer prior to loading on a SDS-PAGE gel.

Western blotting

Western blotting was performed using anti-LC3B, 1:1000 (Cell Signaling), anti-GAPDH, 1:1000 (Santa Cruz Biotechnology), anti-core, clone C7-50, 1:1000 (Thermo Fisher Scientific), anti-JL-8, 1:2000 (Clontech, Mountain View, CA) to recognize GFP, anti-RILP H-85, 1:500 (Santa Cruz Biotechnology), anti-FLAG M2, 1:2000 (Sigma Aldrich), anti-dynamitin, 1:500 (Abcam), anti-p150glued, 1:500 (BD Bioscience) and anti-Arl8b, 1:1000 (Proteintech, Rosemont, IL). Horseradish peroxidase-conjugated secondary antibodies were from Thermo Fisher Scientific.

Immunofluorescence

Huh-7.5 cells were plated on 12mm circular glass coverslips in 4-well plates. Cells were transfected with Lipofectamine 3000 (Thermo Fisher Scientific). Plasmids used were Arl8b wildtype-GFP, pDestmCherry-FYCO1, pEGFP-NI-FYCO1, and pTre2-Bla-RILPΔ1-216-FLAG.

The FYCO1 plasmids were a gift from Terje Johansen (University of Tromsø, Norway) and the RILP plasmid was made by Ann Wozniak (University of Kansas Medical Center). Cells transfected with RILPΔ1-216-FLAG were fixed with methanol/acetone for five minutes prior to staining. Staining for FLAG was done with a rabbit anti-FLAG antibody, 1:200 (Sigma Aldrich). Cells transfected with FYCO1 were fixed with 4% paraformaldehyde and permeabilized with acetone for five minutes. For staining with anti-LC3B, 1:400 (Cell Signaling), cells were fixed and permeabilized with ice-cold methanol for ten minutes. Cells were blocked for one hour in 1XPBS containing 1% BSA and 1% EDTA at room temperature. JFH-1 infection was monitored by staining for anti-core clone C7-50, 1:300 (Thermo Fisher). Secondary antibodies used were AlexaFluor-conjugated (Thermo Fisher Scientific). Coverslips were mounted onto slides using Prolong Gold antifade mountant containing DAPI (Thermo Fisher Scientific).

Confocal images were taken on a Leica TCS SPE confocal configured with a Leica DM550 Q upright microscope. Images were taken with a Nikon eclipse Ti PFS Quantitative Fluorescence Live-Cell and Multidimensional Imaging System equipped with a digital monochrome Coolsnap HQ2 camera (Roper Scientific, Tucson, AZ) using the MetaMorph software.

RILP manipulation

RILP shRNA plasmids were purchased from Origene (Rockville, MD). Huh7.5 cells were transfected with empty vector, scrambled shRNA, or RILP shRNA with Lipofectamine LTX. Transfected cells were selected using 3ug/mL puromycin. Clones were picked and expanded and RILP expression was analyzed by RT-PCR and western blot.

pTre2-Bla-HA-RILP and pTre2-Bla-RILPΔ1-216 were transfected into Huh-7.5 cells using Lipofectamine 3000. Cells were treated with 5ug/mL blasticidin for six days to kill any untransfected cells and then split into two wells of a 6-well plate for bafilomycin A1 treatment. Tet-regulated Huh-7.5 cells stably expressing pTre2-Bla(HA-ncRILP-FLAG) were infected with JFH-1 virus overnight. ncRILP is a non-cleavable RILP and was made by mutating amino acids 81-85 within the RILP sequence to alanine. The next day, HA-ncRILP-FLAG expression was induced with tetracycline-free media. A set of JFH-1 infected cells was left uninduced by leaving tetracycline in the media as a control. At time of bafilomycin A1 treatment, cells had been infected for six days and HA-ncRILP-FLAG had been induced for five days.

Results

Membrane-bound components of dynein complex are reduced during HCV infection

After the observation that HCV decreases full-length RILP through cleavage, we sought to identify how motor protein binding to Rab7 complexes is affected. During infection, the cleaved portion of RILP is also eventually degraded. The RILP cleavage product remains bound to Rab7 so it is unclear whether other Rab7 effectors are able to bind bringing new molecular motors to Rab7-positive organelles. Multiple methods exploring the Rab7-RILP-dynein interaction during HCV infection were employed. Immunoprecipitation procedures were done using a GFP-tagged Rab7Q67L protein. Rab7Q67L was used to enhance the amount of GTP-bound Rab7 within the cell. Using a hypotonic buffer to keep organelles intact, we identified an interaction between Rab7 and RILP (Figure 14A). Unfortunately, an interaction of Rab7 with motor proteins could not be identified through immunoprecipitation by western blot for components of dynein or kinesin complexes under any condition tested. Additionally, performing the reciprocal IP for dynein or kinesin could not demonstrate an interaction with Rab7 (data not shown). We also unsuccessfully tried to find an

Figure 14 Dynein-associated proteins are decreased on HCV-infected membranes. A) Huh7.5 cells were transfected with GFP-Rab7QL and a GFP antibody was used for immunoprecipitation using magnetic dynabeads. Beads were boiled and loaded onto an SDS-PAGE gel and probed for the presence of GFP and RILP. B) Huh7.5 cells were infected with JFH-1 and fractionated into a membrane fraction and supernatant fraction at 20,000xg. Fractions were run on an SDS-PAGE gel and probed for RILP, p150glued, dynamitin, GAPDH as a loading control, and core to monitor infection. C) Densitometry was done using Odyssey LICOR software and expressed as the ratio of protein in control cells (n=3).
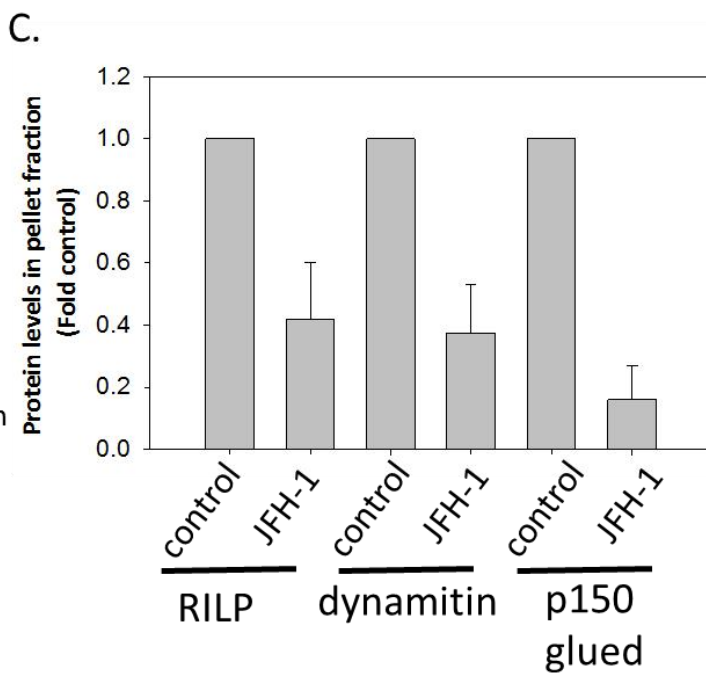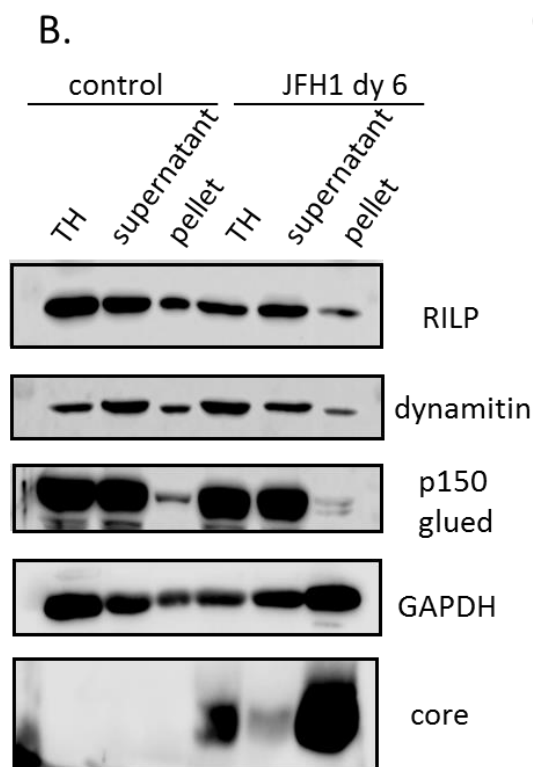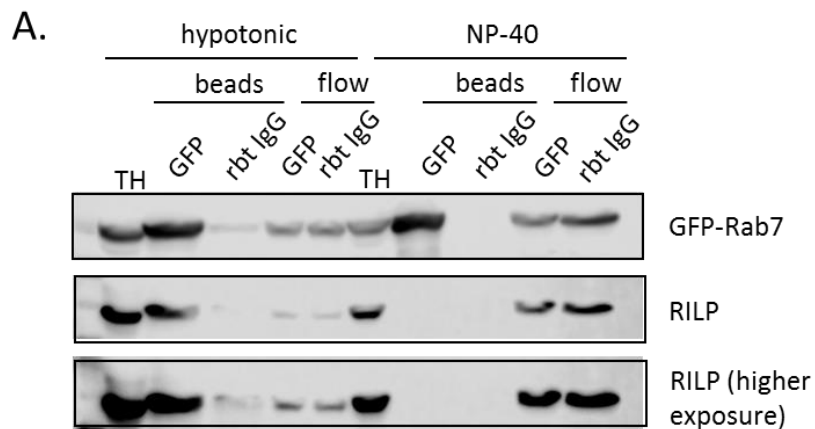
interaction between Rab7 and dynein or kinesin using a proximity-ligation assay (PLA) which produces a fluorescent signal if the interaction is within 40nm. A different group reported previously that they were also unable to identify interactions between RILP and motor proteins using multiple techniques such as yeast-two hybrid and co-IP (70).
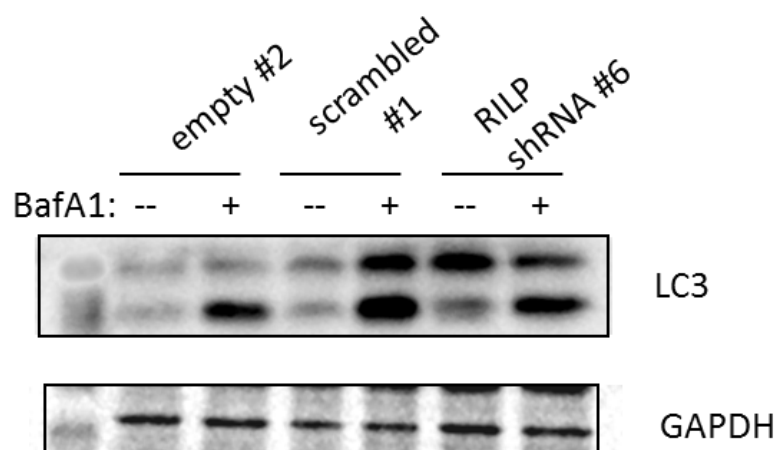
Next, we decided to look at the presence of dynein complex motor proteins on membranes from HCV-infected cells. If the portion of RILP that binds to dynein is cleaved, then it would be expected that the presence of proteins associated with the dynein complex would be decreased on membranes. JFH-1 infected cells were homogenized in a hypotonic buffer to keep organelles intact and total homogenate, supernatant, and membrane pellet were run on a SDS-PAGE gel. A 20,000xg pellet should contain most organelles except for ER based on subcellular fractionation techniques used previously. RILP was decreased in the pellet fraction from HCV-infected cells as would be expected from our lab's previous data. Dynamitin (also called p50) and p150glued were also decreased in the membrane fraction from HCV-infected cells (Figure 14B&C). Dynamitin and p150glued are both components of the eleven-protein dynactin complex which is a cofactor of the dynein complex (156). Dynactin bridges RILP to dynein. This result suggests that HCV-infection decreases dynein binding to organelles.

Effect of RILP mutants on autophagic flux

Since Rab7-RILP has been reported to reside on autophagosomes/amphisomes, we explored whether the changes in RILP induced by HCV-infection could affect autophagy. To do this we measured autophagic flux in cells where full-length RILP was partially knocked down and in cells where RILPΔ1-216-FLAG or HA-ncRILP-FLAG were expressed. If RILP plays a major role in autophagic flux in HCV infection, then we would expect that either decreasing RILP protein or expressing the cleaved RILP that HCV produces would be sufficient

Figure 15 RILP knockdown or RILP mutant expression does not alter autophagic flux. A) Huh7.5 cells were transfected with empty, nontarget, and RILP shRNA plasmids and selected with puromycin. Level of RILP knockdown was confirmed by western blot using anti-RILP antibody and anti-GAPDH as a loading control and RT-PCR using GAPDH as a control. B) Huh7.5 cells from panel A were treated with 100nM bafilomycin A1 for four hours. Western blotting was done using anti-LC3 antibody and anti-GAPDH antibody as a loading control. C) Huh7.5 cells were transfected with HA-RILP or RILPΔ1-216-FLAG, selected with blasticidin, and treated with 100nM bafilomycin A1 for four hours. Western blotting was done using anti-LC3 antibody, anti-GAPDH antibody as a loading control, and anti-HA or anti-FLAG antibody for levels of transfected plasmid. D) Tet-regulated Huh7.5 cells were induced to express ncRILP and infected with JFH-1 virus. Cells were treated with 100nM bafilomycin A1 for four hours. Western blotting was done using anti-LC3 antibody, anti-GAPDH antibody as a loading control, anti-HA for levels of ncRILP expression, and anti-core to monitor HCV infection.

A.

	empty		scrambled		RILP	
	#2	#3	#1	#2	#1	#6

RILP

GAPDH

Gene Expression

empty 2   empty 3   RILP 1   RILP 6   scram 1   scram 2

empty #2   scrambled #1   RILP shRNA #6

BafA1:   --   +   --   +   --   +

LC3

GAPDH
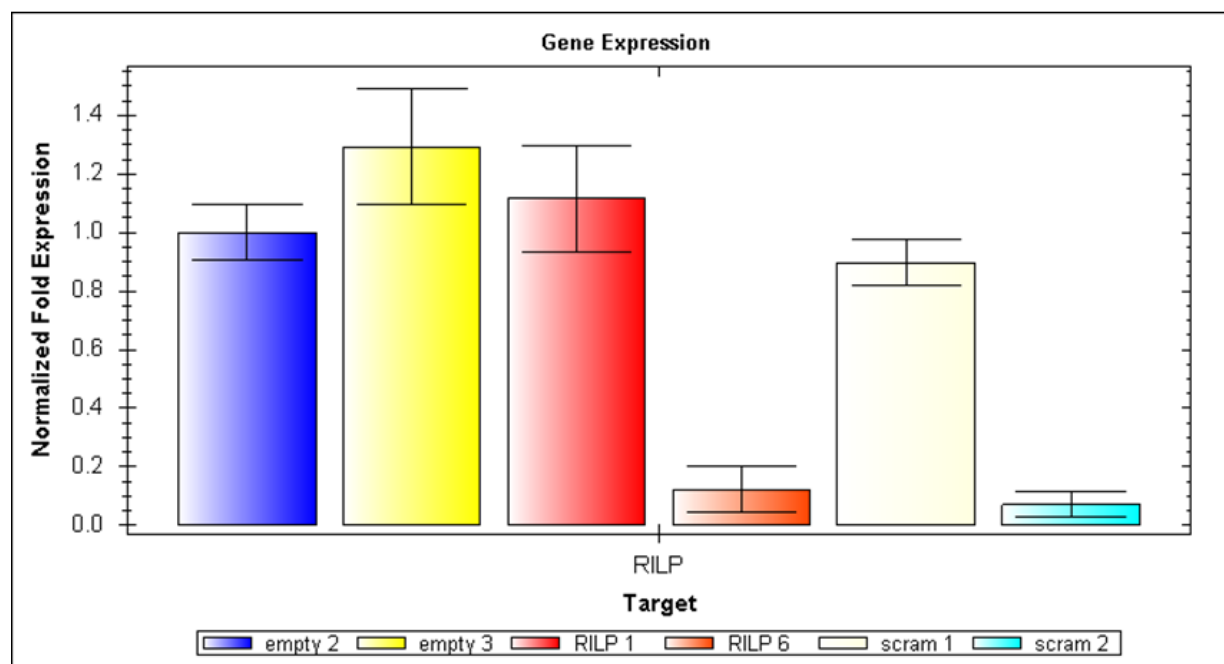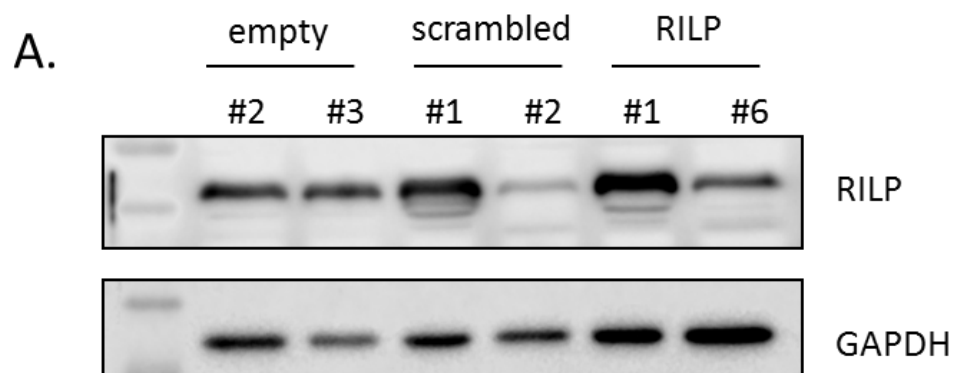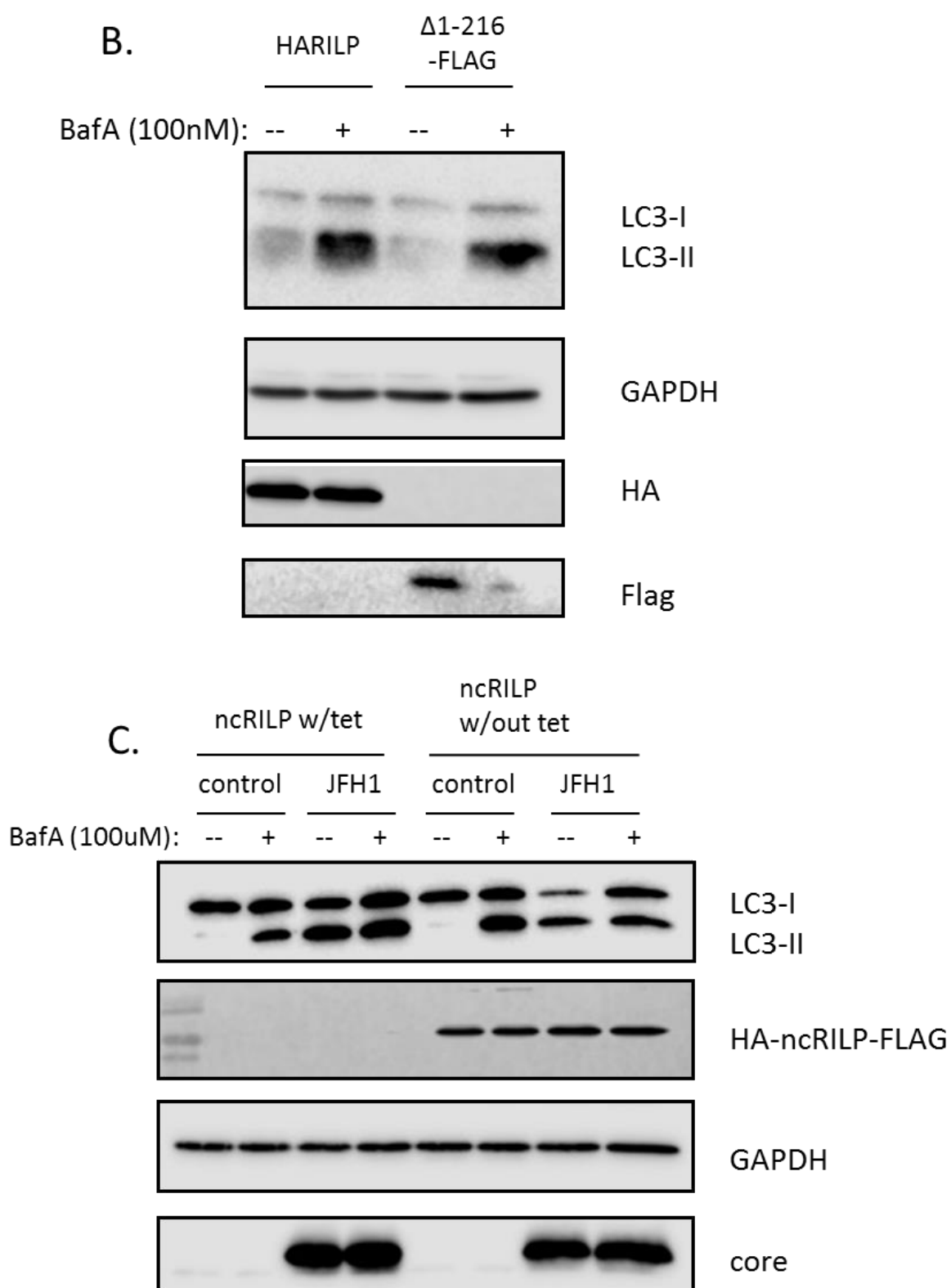
to produce a block in autophagy. Conversely, expressing a non-cleavable form of RILP should restore autophagic flux in JFH-1 infected cells if cleaving RILP serves to alter autophagy. Using a RILP shRNA plasmid could decrease RILP levels by greater than 60%. Knockdown of RILP or expression of RILPΔ1-216-FLAG could not reproduce the defect in autophagic flux seen in HCV infection alone (Figure 15B&C). Expression of ncRILP during HCV infection could not correct the defect in autophagic flux raising LC3-II levels after bafilomycin A1 treatment (Figure 15D). ncRILP expression did decrease LC3-II levels during HCV infection suggesting that it might suppress autophagy induction.

Arl8b and Rab7 occupy the same vesicles

Since Arl8b and Rab7 are both reported to reside on lysosomes, we looked at whether they could be found on the same vesicles in Huh7.5 cells. Performing co-IP using cells transfected with Arl8bQL-GFP and homogenized in a hypotonic buffer, the presence of Arl8b, RILP, Rab7, and LAMP-2 could be identified (Figure 16A). This would indicate that Arl8b and Rab7-RILP complexes reside on the same organelles and since they are LAMP-2 positive, they likely represent lysosomes. When RILPΔ1-216-FLAG is co-transfected with wildtype Arl8b-GFP in Huh-7.5 cells, there are vesicles that are positive for both Arl8b and the RILP mutant but the co-localization is not perfect (Figure 16B). There are vesicles that are positive for only Arl8b or RILP. This is not surprising considering that Rab7-RILP is also found on late endosomes and amphisomes where Arl8b is not known to be present. Additionally, expressing the N-terminally truncated RILP alone did not seem to be sufficient to rearrange Arl8b-positive organelles to the periphery as seen in JFH-1 infected cells. This would suggest that other changes during viral infection are necessary for the changes observed in Arl8b localization.

Figure 16: Arl8b and Rab7-RILP co-localize on a subset of vesicles. A) Huh7.5 cells were transfected with Arl8bQL-GFP, lysed in a hypotonic buffer, and an anti-GFP antibody was used to immunoprecipitate vesicles. The vesicles were loaded onto an SDS-PAGE gel and probed with anti-GFP, anti-RILP, anti-Rab7, and anti-LAMP-2. B) Huh7.5 cells were transfected with wildtype Arl8b-GFP and RILPΔ1-216-FLAG. Dashed lines represent cell boundaries as defined by Phalloidin-647 staining. Nuclei were stained with DAPI. Images were collected using LasX software and representative images are shown.

A.

Merge

RILPΔ1-216-FLAG

Arl8b-GFP
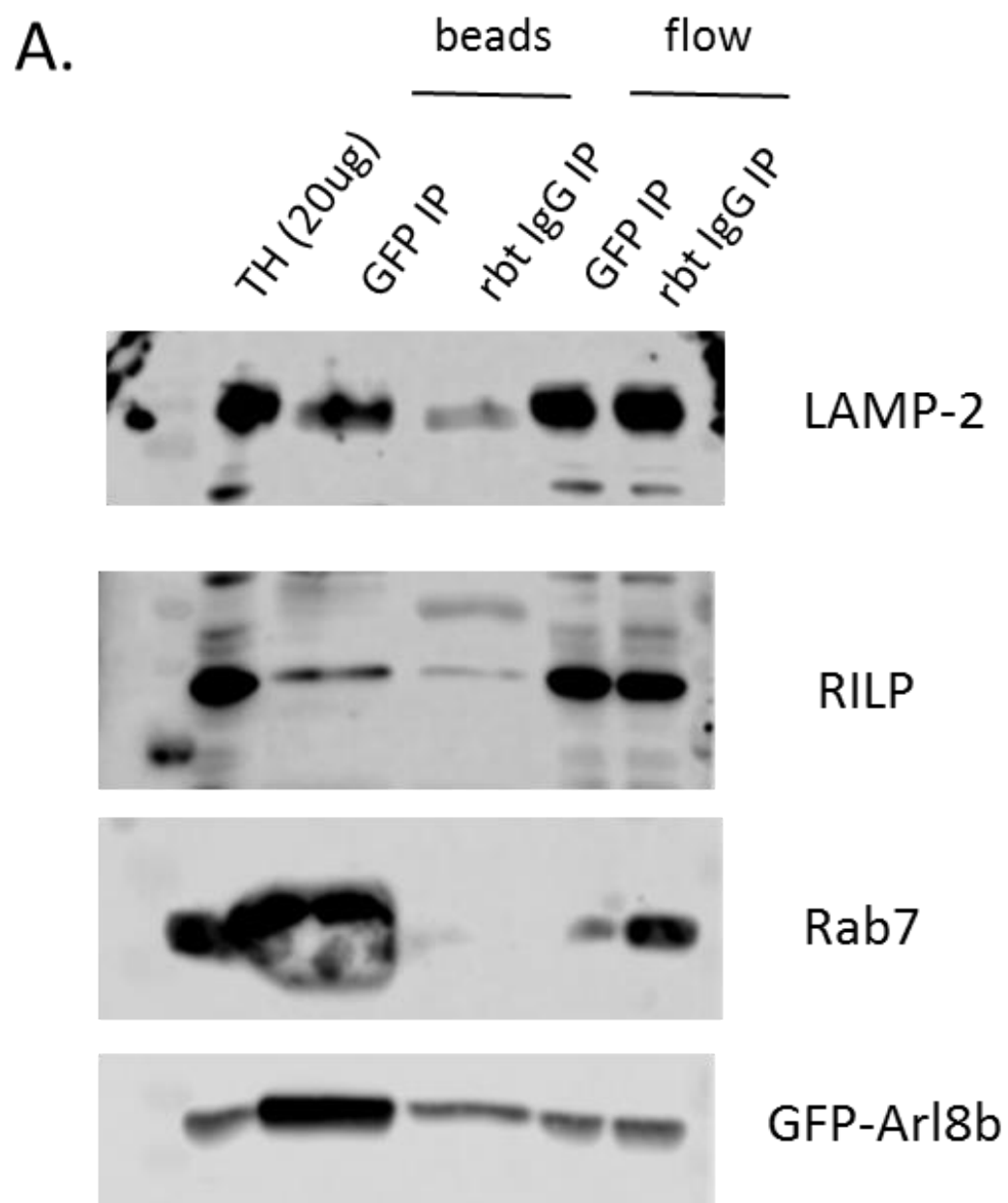
B.
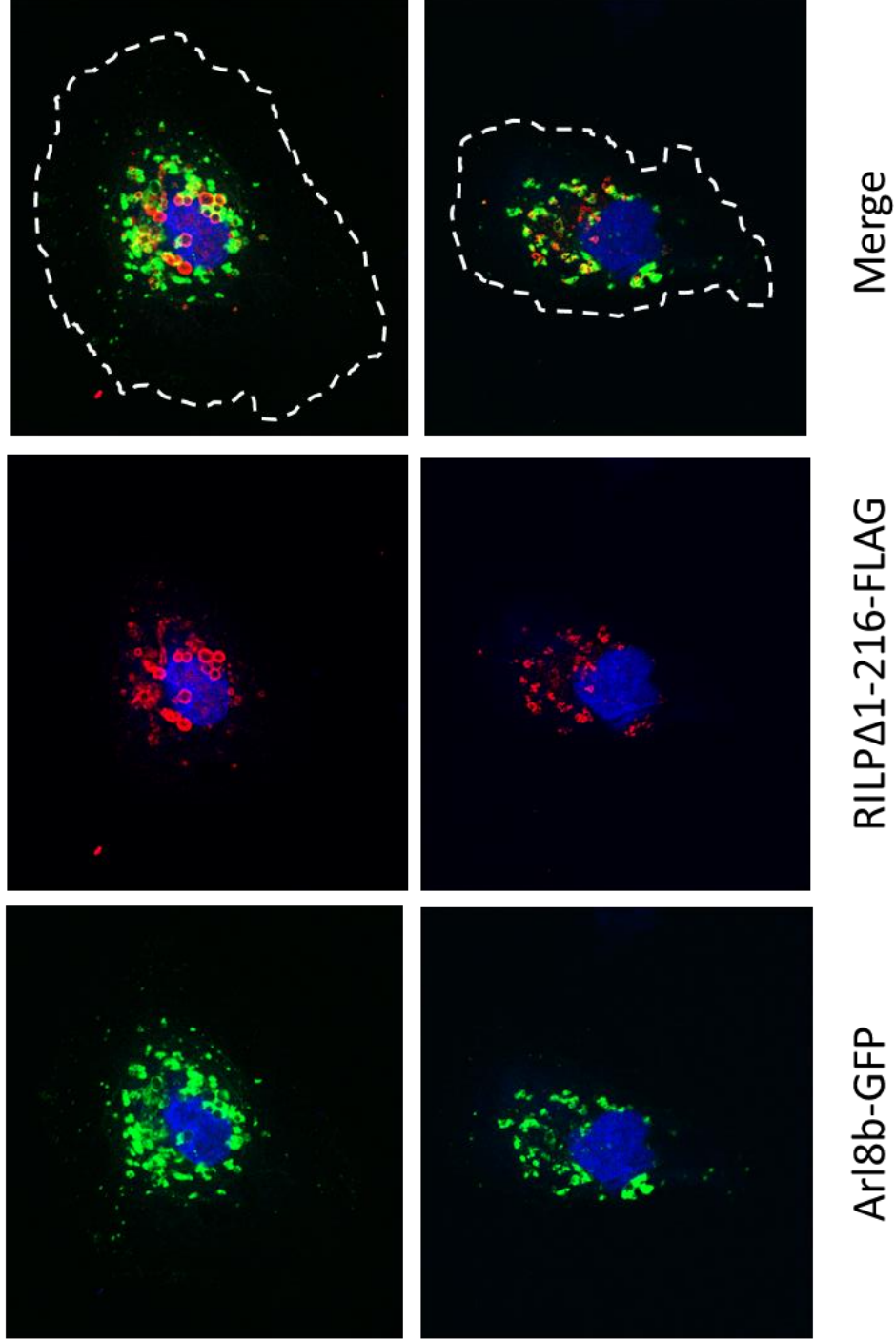
FYCO1 localization is not altered during HCV infection

The Rab7 effector, FYCO1, has been implicated in plus-end directed movement by linking Rab7 to kinesin-1. FYCO1 is found on autophagosomes, late endosomes, and lysosomes and contains domains that allow it to bind to PI3P and LC3-II. It is believed that FYCO1 competes with RILP for binding Rab7 (72). Control and JFH-1 infected cells were transfected with a tagged FYCO1 and stained for either endogenous Rab7 or LC3. FYCO1 strongly co-localized with both Rab7 and LC3-II regardless of the infection status of the cell (Figure 17A&B). Exogenous FYCO1 appeared as large puncta that appeared to decorate the outside of vesicles. Rab7 and LC3 stained these large FYCO1 structures also appearing to decorate the outside of these membranes. There were also many peripherally localized vesicles in FYCO1 transfected cells indicating a linkage to kinesin. However, there did not appear to be a difference in localization of FYCO1-positive vesicles in control cells compared to JFH-1 infected cells.

Discussion

RILP cleavage does appear to reduce the amount of proteins associated with the dynein complex present on cellular membranes in HCV-infected cells. This data is in agreement with Jordens et al. who found that overexpression of an N-terminal truncation of RILP missing amino acids 1-199 could decrease the amount of p50/dynamitin present on membranes from a 100,000xg fractionation (70). This truncation is very similar to the one identified in our lab as that produced when HCV cleaves RILP. By reducing the amount of dynein present on membranes, HCV infection may be priming the cells for organelle movement to the periphery.

Figure 17 Co-localization of FYCO1 with Rab7 and LC3 in HCV-infected cells. Huh-7.5 cells were infected with JFH-1 virus. A) MCherry-FYCO1 was transfected into Huh-7.5 cells. Cells were fixed and stained for endogenous Rab7. Images were collected using MetaMorph software and representative images are shown. Control on pg. 93 and JFH-1 on pg. 94. B) GFP-FYCO1 was transfected into Huh-7.5 cells. Cells were fixed and stained for endogenous LC3. Images were collected using MetaMorph software and representative images are shown.

A.

Mcherry-FYCO1   Endogenous Rab7   Overlay

control

Overlay

Endogenous
Rab7

Mcherry-
FYCO1

JFH-1

Merge

GFP-FYCO1

Endogenous LC3

B.

control

JFH-1
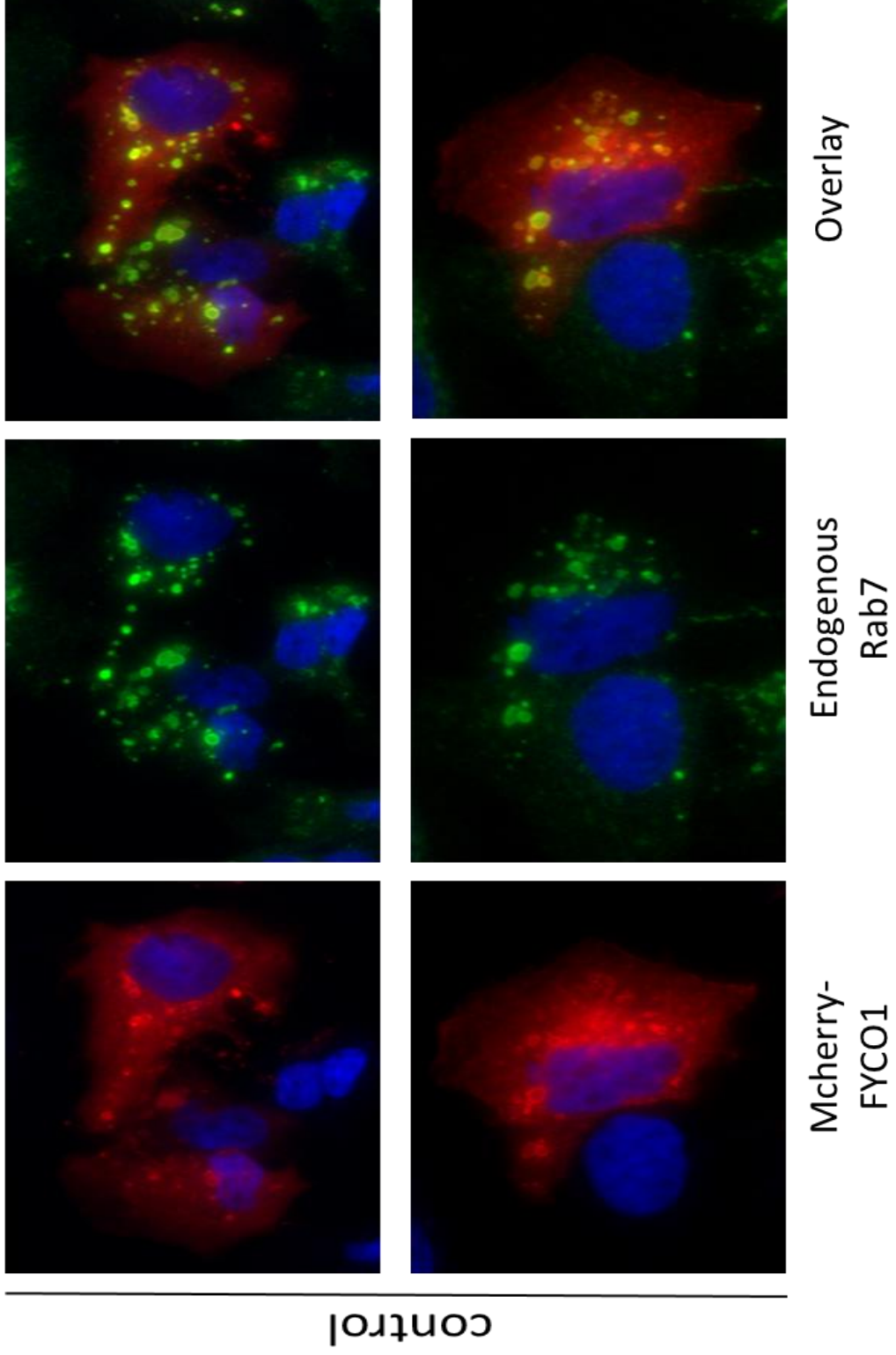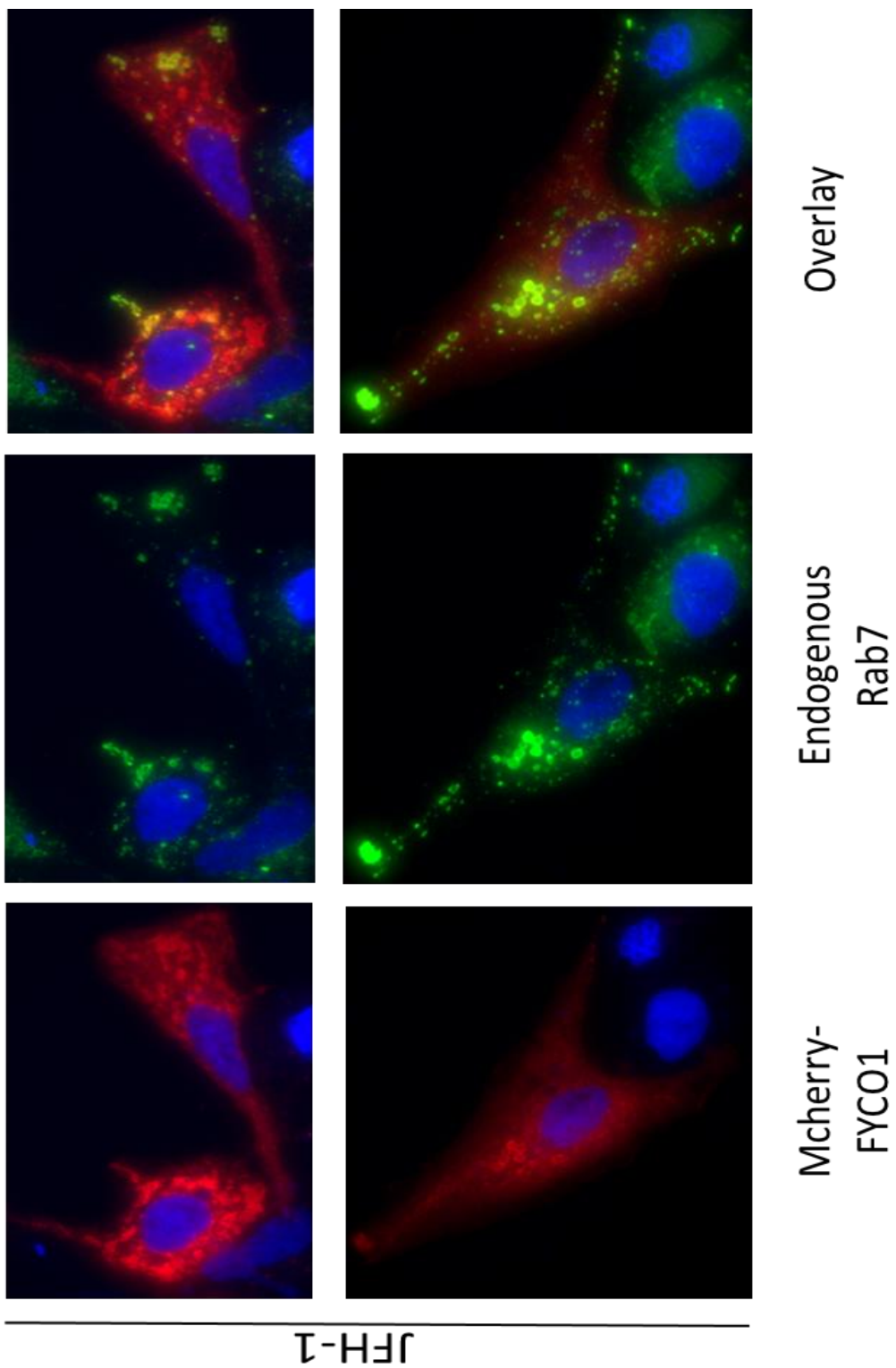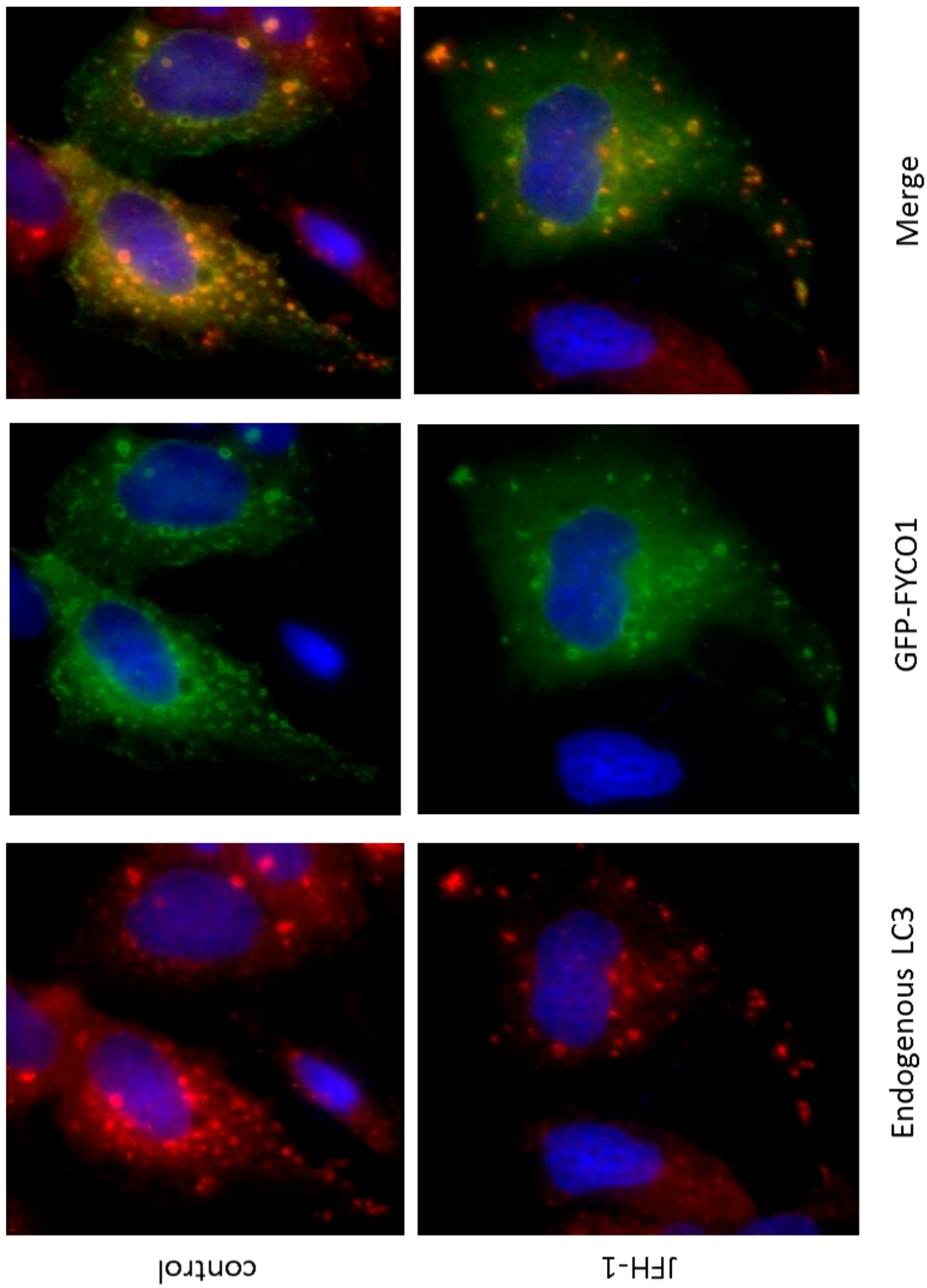
From these experiments, cleavage and/or loss of RILP produced during HCV infection could not be implicated in autophagy or to the movement of Arl8b-positive organelles to the periphery. Potential reasons for no changes in autophagy when manipulating RILP could be the transfection efficiency and lack of sensitivity of western blot though we did select for pools of transfected cells or used selected clones. Additionally, since endogenous RILP is still present in transfected cells, it is unclear what proportion of the transfected RILP or RILP mutants are bound to Rab7 and therefore membranes at any given time. While it may also be surprising that expression of the N-terminal RILP truncation did not move Arl8b-positive vesicles to the periphery, previous studies have produced conflicting data regarding RILP manipulation. For example, Progida et al. did not observe peripheral displacement of late endosomes in RILP knockdown cells and Van der Kant et al. still observed clustering of late endosomes despite abrogating the RILP-dynein interaction (145, 147). Also, there are other effectors that can bind to Rab7 and have known roles in autophagy such as FYCO1, ORP1L, and PLEKHM1 so manipulating RILP alone may not be sufficient to alter autophagy.

While there are no obvious differences in FYCO1 localization comparing control and HCV-infected cells, a more careful analysis of the effect of HCV infection on FYCO1 would have to be undertaken to rule out a role for this effector. For example, it would be important to examine if the interaction of Rab7 with other effectors is increased due to RILP cleavage though this may be unlikely if the C-terminal portion of RILP remains bound to Rab7. While we focused on Arl8b-dependent movement of lysosomes, there might also be peripheral movement of autophagosomes as well. Some of our confocal images suggest that HCV may induce peripheral movement of autophagosomes in addition to lysosomes. It is possible that cleaving RILP might allow autophagosomes to move more readily to the periphery through Rab7-FYCO1. A similar

more peripheral autophagosome distribution was also described in cells overexpressing Arl8b so it is possible that by increasing Arl8b expression during HCV infection, autophagosome transport may also be affected through an unknown mechanism (93).

There is evidence that Arl8b and Rab7-RILP reside together on a subpopulation of vesicles and it is tempting to speculate that HCV infection affects organelle positioning by altering both complexes by cleaving RILP and upregulating Arl8b expression to reduce dynein linkages and increase kinesin linkages respectively. Though RILP cleavage mutants were not sufficient to induce the Arl8b effects seen in lysosomal positioning or autophagy, this may indicate that multiple changes induced by HCV infection are necessary.

Chapter V: Conclusions

Autophagy is an important cellular pathway with many functions in cellular homeostasis, aging, cancer, and the pathogenesis of microbes. The importance of autophagy was recognized this year with the 2016 Nobel Prize in Physiology or Medicine awarded to Yoshinori Ohsumi for discovering essential genes for autophagy in yeast. Since autophagy is known to be important in either promoting or impairing the pathogenesis of viruses, we explored the effect of HCV infection on the autophagic pathway. As described in Chapter 2, we showed that infection with JFH-1, a genotype 2a virus, could decrease autophagic flux. LC3-II levels could not be increased after bafilomycin A1 treatment in infected cells indicating a block in the final step of autophagy when the autophagosome is degraded by the lysosome. We then demonstrated that lack of autophagosome degradation in HCV-infected cells was due to a trafficking defect. Global lysosomal cathepsin activity and maturation was not impaired during HCV infection and autophagosomes and lysosomes from infected cells fused at a normal rate in an in vitro fusion assay. However, in vivo, using the tandem RFP-GFP-LC3 plasmid, autophagosomes from HCV-infected cells retain both RFP and GFP on the LC3-II decorating their membranes displaying yellow fluorescence indicating a lack of lysosomal degradation.

This led to the exploration in Chapter 3 of the role of Arl8b in lysosomal trafficking during HCV infection. The Arl8b GTPase is upregulated nearly three-fold at both the mRNA and protein levels after HCV infection. The localization of transfected Arl8b changes dramatically going from a largely perinuclear cluster of vesicles in control cells to vesicles that are entirely in the periphery of the cell in infected cells. Arl8b decorates vesicles that are positive for LAMP-2 and contain acidic hydrolases both in control and HCV-infected cells. In control cells, Arl8b-positive lysosomes and autophagosomes co-localize in the perinuclear region and this co-

localization is increased when autophagy is induced. In HCV-infected cells, the co-localization between lysosomes and autophagosomes is drastically decreased even when autophagy is stimulated. We established a role for Arl8b in HCV-induced autophagy defects by knocking down Arl8b protein levels which could restore autophagic flux in infected cells to levels seen in control cells.

We also hypothesized that HCV may induce changes in multiple GTPase complexes to coordinate vesicle movement. HCV cleaves RILP uncoupling the Rab7 complex from dynein while at the same time upregulating Arl8b expression to increase linkages to kinesin. In Chapter 4, we verified that Rab7 and Arl8b reside on a subpopulation of vesicles but not exclusively. However, the presence of an N-terminal truncation of RILP that cannot bind to dynein was not sufficient in the experiments performed to cause a block in autophagic flux or move Arl8b-positive vesicles to the periphery.

This is the first study to demonstrate that HCV infection blocks autophagic flux as a result of a trafficking defect caused by Arl8b overexpression in infected cells.

Lysosomal positioning in disease and infection

There is a growing recognition of the importance of lysosomal positioning as a determinant of lysosomal function and a mechanism influencing disease states. Aberrant lysosomal positioning has been implicated in lysosomal storage diseases, Huntington's disease, and cancer. TRPML1 has been shown to move lysosomes to the perinuclear region upon autophagy induction in a Rab7-RILP independent manner (150). Mutations in TRPML1 result in the lysosomal storage disease Mucolipidosis type IV. Many lysosomal storage diseases are characterized by defects in autophagy. In Huntington's disease, expression of mutant huntingtin makes lysosomes accumulate in the perinuclear region of cells which increases autophagic flux.

This enhanced flux results in premature fusion between empty autophagosomes that do not contain cargo and lysosomes which is known to occur in Huntington's (157). Lysosomal function and positioning is also important in cancer progression. Lysosomal hydrolases are often altered in cancer and lysosomes usually move to the periphery of cells where their contents can be secreted into the extracellular space (158). It is thought that lysosomal contents, such as cathepsins, can promote cellular invasion and motility. Arl8b has been shown to play a role in peripheral lysosome movement in prostate cancer. Arl8b was required for protease secretion and for the formation of invasive structures of cancer cells grown in a 3D matrix and knockdown of Arl8b limited tumor growth in a xenograft model in mice (142). Also, our data suggests that even though HCV does not inhibit cathepsin activity, cathepsin B activity was significantly increased in infected cells. While there is one report of increased immature cathepsin B secretion in a Con1, a genotype 1b virus, replicon but this did not hold true for a JFH-1 replicon so this is not likely an explanation for our result (159). Overexpression of cathepsin B has been found in many types of cancers and downregulating its expression can decrease some hallmarks of cancer cells such as increased motility and invasion (129). Increased cathepsin B protein levels have also been associated with hepatocellular carcinoma and is higher levels of the protein are correlated with worse prognosis (160). While we did not explore the mechanism of why cathepsin B activity was increased, it is interesting to speculate that this may be related to cellular changes that could promote cancer progression after HCV infection.

Salmonella typhimurium is the pathogen that has the most similarities to HCV regarding alterations to GTPases. As previously mentioned, S. typhimurium replicates within SCVs which must be prevented from fusing with lysosomes as well as moved to the cell periphery to enable efficient spread of the bacteria. SCV formation requires the microtubule network of the cell and

Rab7 localizes to SCVs (161). Mature SCVs form filamentous structures called Sifs (Salmonella induced filaments) which promote pathogenesis. Salmonella excludes RILP from binding to Rab7 on the Sifs (162). The bacterial effector SopD binds to Rab7 preventing RILP and other effectors from binding (163). Expressing exogenous RILP during *S.* typhimurium infection causes the SCVs to acquire the dynein motor as indicated by the presence of dynamitin and p150glued on the SCVs. This causes SCVs to fuse with lysosomes and intracellular survival of the bacteria is reduced (164). Arl8b localizes to maturing SCVs and is required for the formation of Sifs and cell-to-cell transfer of the bacteria. Arl8b knockdown abrogates peripheral movement of SCVs and Sif formation (94).

Similarly, HCV cleaves RILP removing the dynein motor and upregulates Arl8b providing linkages to kinesin. Knockdown of Arl8b in HCV-infected cells restores autophagic flux hinting that the main role of Arl8b in the context of HCV infection may be to inhibit autophagy by creating a more peripheral distribution of lysosomes so that autophagosomes and lysosomes do not physically contact each other. There are multiple reasons why it might be advantageous for HCV to inhibit the autophagic pathway. If HCV utilizes autophagosomal membranes as part of the replication complexes, then causing an accumulation of autophagosomes by inhibiting their degradation would provide a source of membranes. Additionally, inhibiting autophagy and repositioning lysosomes may also prevent the degradation of, not just autophagosomal membranes, but also components of the replication complex or viral particles if they physically associate with autophagosomes.

HCV and cholesterol

HCV infection is intimately linked to lipid metabolism within hepatocytes. A hallmark of HCV infection is the dysregulation of lipid homeostasis. Most aspects of the HCV lifecycle

depend upon lipids including entry, replication, and virus assembly. The membranous webs where replication takes place are made up of double membrane vesicles as well as cholesterol and sphingolipids (165, 166). Viral assembly takes place in close proximity to lipid droplets where core and other nonstructural proteins, like NS5A, localize. Breakdown of lipid droplets can occur via lipophagy whereby lipid droplets, either by engulfment by autophagosomes or by kiss-and-run interactions with lysosomes, are hydrolyzed to produce free fatty acids or free cholesterol. Inhibition of autophagy by HCV may aid in the viral lifecycle by allowing the accumulation of lipids. However, this increase in lipids does not seem to alter the membrane composition of lysosomes, which does cause autophagy dysfunction in lysosomal storage diseases, since we showed that isolated autophagosomes and lysosomes from HCV-infected cells fuse normally. Additionally, an NS5A-interacting protein, TIP47, is targeted to lipid droplets where viral assembly takes place and then in complex with Rab9 helps target viral particles for egress out of the cell. TIP47 mutants that abolish their Rab9 interaction redirect viral particles to the autophagic pathway and are destroyed (167). This data suggests that viral egress depends upon diversion from the autophagic pathway and that directing HCV particles through this pathway leads to their destruction.

There is also a recent study looking at the effect of cholesterol on autophagosome positioning mediated by Rab7 binding of its effectors RILP, ORP1L (a cholesterol sensor), and PLEKHM1 (recruits the HOPS complex). Their data suggests that the level of endosomal cholesterol may effect autophagosome maturation and transport for lysosome fusion with high levels of cholesterol resulting in retrograde transport of autophagosomes (71). While HCV-induced effects on Arl8b would reposition lysosomes away from perinuclear fusion sites inhibiting the degradative step in autophagy, it is possible that the cleavage of RILP could also

play a role in preventing maturation and movement of autophagosomes regardless of the cholesterol status of a cell.

Future directions

While we have shown that HCV infection inhibits autophagic flux through an Arl8b-dependent mechanism, there are still many questions to ask and avenues to explore. Though autophagosome-lysosome fusion is inhibited, we did not determine whether the autophagosomes remain in an early state or whether they are able to mature into amphisomes in HCV-infected cells. In hepatocytes, it is believed that the majority of autophagosomes fuse with late endosomes to become amphisomes. To assess this, we could look for co-localization of LC3-II with late endosomal markers, like mannose-6-phosphate receptor, though there is much overlap between proteins residing on late endosomes and lysosomes. Also, to more closely examine the late stages of autophagy, the degree of ALR in HCV-infected cells could be assessed. I would predict that since HCV inhibits autophagosome degradation, ALR would be decreased in HCV-infected cells compared to uninfected cells.

It would also be important to assess organelle movement within HCV-infected cells using live cell imaging techniques. Labelled lysosomes could be tracked independently within cells to confirm their peripheral dispersal in HCV-infected cells and the kinetics of movement, including the speed of particles and the amount of retrograde vs. anterograde movement, could be determined. I would predict that HCV-infected cells, at a late stage in infection, would show increased peripheral movement of lysosomes with very little retrograde movement though there may be other dynein-binding proteins, besides RILP, present on lysosomes. Live cell imaging could also be used to assess autophagosome movement within cells and whether they also increase their peripheral localization within infected cells. Arl8b has not been implicated in

autophagosome movement but we cannot rule out that proteins like FYCO1 may play a more prominent role during HCV infection.

Tethering and fusion of vesicles in HCV-infected could also be explored in more detail by examining the HOPS complex. Since it has been reported that Arl8b-SKIP and Rab7-RILP may compete for the HOPS complex, I would expect that there would be increased binding of HOPS complex partners with Arl8b in infected cells. The cleavage of RILP would also abolish HOPS binding in infected cells since the portion that is most likely cleaved contains the domain for HOPS binding. HOPS binding of Arl8b could be examined by immunoprecipitation or co-localization studies based on immunofluorescence of various Vps subunits and Arl8b. It is unclear what effect increased HOPS binding would have in the context of HCV infection though it might increase endosome-lysosome fusion. Another possibility is that viral infection may also affect the localization of the HOPS complex to promote viral particle secretion through the ESCRT pathway. It is currently unclear what the relationship is between HOPS and ESCRT but it is thought that there must be a way to balance sorting of intraluminal vesicles and membrane fusion events (168). It would be interesting to explore whether HCV pushes the balance towards the ESCRT pathway for viral secretion by redirecting HOPS binding.

There are studies exploring the link between autophagy and HCV infection that conclude that autophagy goes to completion in infected cells. It is possible that different stages in infection affect autophagy differently. Protein expression or trafficking may be temporally changed during infection as has been suggested for UVRAG and Rubicon expression during HCV infection. My experiments are usually done at a late time point in infection once almost all the cells in a culture are infected. JFH-1 is also a more cytopathic virus eventually causing cell death at late time points in infection but experiments are done prior to substantial cell death. Different virus strains

or genotypes may also alter autophagy differently in cell culture. A more thorough time course of autophagy changes could be done looking at when post-infection autophagy becomes inhibited and how this correlates with protein expression levels, for example when Arl8b expression is maximal, or virus replication/production.

In conclusion, we have confirmed a role for Arl8b in defective autophagic flux caused by HCV infection. This study sheds light on how viral infection can modulate GTPases to support their pathogenesis and provides some insight into the importance of organelle positioning in cellular function. While HCV is now curable and it may not be worthwhile to seek new drug targets or treatments, the virus can be useful as a tool for illuminating how cells function by studying viral alterations of cellular pathways.

References

1.   **Choo QL, Kuo G, Weiner AJ, Overby LR, Bradley DW, Houghton M.** 1989. Isolation of a cDNA clone derived from a blood-borne non-A, non-B viral hepatitis genome. Science **244:**359-362.
2.   **Gower E, Estes C, Blach S, Razavi-Shearer K, Razavi H.** 2014. Global epidemiology and genotype distribution of the hepatitis C virus infection. J Hepatol **61:**S45-57.
3.   **Lozano R, Naghavi M, Foreman K, Lim S, Shibuya K, Aboyans V, Abraham J, Adair T, Aggarwal R, Ahn SY, Alvarado M, Anderson HR, Anderson LM, Andrews KG, Atkinson C, Baddour LM, Barker-Collo S, Bartels DH, Bell ML, Benjamin EJ, Bennett D, Bhalla K, Bikbov B, Bin Abdulhak A, Birbeck G, Blyth F, Bolliger I, Boufous S, Bucello C, Burch M, Burney P, Carapetis J, Chen H, Chou D, Chugh SS, Coffeng LE, Colan SD, Colquhoun S, Colson KE, Condon J, Connor MD, Cooper LT, Corriere M, Cortinovis M, de Vaccaro KC, Couser W, Cowie BC, Criqui MH, Cross M, Dabhadkar KC, et al.** 2012. Global and regional mortality from 235 causes of death for 20 age groups in 1990 and 2010: a systematic analysis for the Global Burden of Disease Study 2010. Lancet **380:**2095-2128.
4.   **Denniston MM, Jiles RB, Drobeniuc J, Klevens RM, Ward JW, McQuillan GM, Holmberg SD.** 2014. Chronic hepatitis C virus infection in the United States, National Health and Nutrition Examination Survey 2003 to 2010. Ann Intern Med **160:**293-300.
5.   **Lingala S, Ghany MG.** 2015. Natural History of Hepatitis C. Gastroenterol Clin North Am **44:**717-734.
6.   **Zopf S, Kremer AE, Neurath MF, Siebler J.** 2016. Advances in hepatitis C therapy: What is the current state - what come's next? World J Hepatol **8:**139-147.
7.   **Douam F, Ding Q, Ploss A.** 2016. Recent advances in understanding hepatitis C. F1000Res **5**.
8.   **Honda M, Ping LH, Rijnbrand RC, Amphlett E, Clarke B, Rowlands D, Lemon SM.** 1996. Structural requirements for initiation of translation by internal ribosome entry within genome-length hepatitis C virus RNA. Virology **222:**31-42.
9.   **Moradpour D, Penin F, Rice CM.** 2007. Replication of hepatitis C virus. Nat Rev Microbiol **5:**453-463.
10.   **McLauchlan J, Lemberg MK, Hope G, Martoglio B.** 2002. Intramembrane proteolysis promotes trafficking of hepatitis C virus core protein to lipid droplets. Embo j **21:**3980-3988.
11.   **McLauchlan J.** 2009. Hepatitis C virus: viral proteins on the move. Biochem Soc Trans **37:**986-990.
12.   **Wozniak AL, Griffin S, Rowlands D, Harris M, Yi M, Lemon SM, Weinman SA.** 2010. Intracellular proton conductance of the hepatitis C virus p7 protein and its contribution to infectious virus production. PLoS Pathog **6:**e1001087.
13.   **Madan V, Bartenschlager R.** 2015. Structural and Functional Properties of the Hepatitis C Virus p7 Viroporin. Viruses **7:**4461-4481.
14.   **Popescu CI, Callens N, Trinel D, Roingeard P, Moradpour D, Descamps V, Duverlie G, Penin F, Heliot L, Rouille Y, Dubuisson J.** 2011. NS2 protein of hepatitis C virus interacts with structural and non-structural proteins towards virus assembly. PLoS Pathog **7:**e1001278.

15.	**Ma Y, Anantpadma M, Timpe JM, Shanmugam S, Singh SM, Lemon SM, Yi M.** 2011. Hepatitis C virus NS2 protein serves as a scaffold for virus assembly by interacting with both structural and nonstructural proteins. J Virol **85:**86-97.

16.	**Li XD, Sun L, Seth RB, Pineda G, Chen ZJ.** 2005. Hepatitis C virus protease NS3/4A cleaves mitochondrial antiviral signaling protein off the mitochondria to evade innate immunity. Proc Natl Acad Sci U S A **102:**17717-17722.

17.	**Li K, Foy E, Ferreon JC, Nakamura M, Ferreon AC, Ikeda M, Ray SC, Gale M, Jr., Lemon SM.** 2005. Immune evasion by hepatitis C virus NS3/4A protease-mediated cleavage of the Toll-like receptor 3 adaptor protein TRIF. Proc Natl Acad Sci U S A **102:**2992-2997.

18.	**Li S, Yu X, Guo Y, Kong L.** 2012. Interaction networks of hepatitis C virus NS4B: implications for antiviral therapy. Cell Microbiol **14:**994-1002.

19.	**Fiches GN, Eyre NS, Aloia AL, Van Der Hoek K, Betz-Stablein B, Luciani F, Chopra A, Beard MR.** 2016. HCV RNA traffic and association with NS5A in living cells. Virology **493:**60-74.

20.	**Pileri P, Uematsu Y, Campagnoli S, Galli G, Falugi F, Petracca R, Weiner AJ, Houghton M, Rosa D, Grandi G, Abrignani S.** 1998. Binding of hepatitis C virus to CD81. Science **282:**938-941.

21.	**Bartosch B, Vitelli A, Granier C, Goujon C, Dubuisson J, Pascale S, Scarselli E, Cortese R, Nicosia A, Cosset FL.** 2003. Cell entry of hepatitis C virus requires a set of co-receptors that include the CD81 tetraspanin and the SR-B1 scavenger receptor. J Biol Chem **278:**41624-41630.

22.	**Cormier EG, Tsamis F, Kajumo F, Durso RJ, Gardner JP, Dragic T.** 2004. CD81 is an entry coreceptor for hepatitis C virus. Proc Natl Acad Sci U S A **101:**7270-7274.

23.	**Scarselli E, Ansuini H, Cerino R, Roccasecca RM, Acali S, Filocamo G, Traboni C, Nicosia A, Cortese R, Vitelli A.** 2002. The human scavenger receptor class B type I is a novel candidate receptor for the hepatitis C virus. Embo j **21:**5017-5025.

24.	**Zeisel MB, Koutsoudakis G, Schnober EK, Haberstroh A, Blum HE, Cosset FL, Wakita T, Jaeck D, Doffoel M, Royer C, Soulier E, Schvoerer E, Schuster C, Stoll-Keller F, Bartenschlager R, Pietschmann T, Barth H, Baumert TF.** 2007. Scavenger receptor class B type I is a key host factor for hepatitis C virus infection required for an entry step closely linked to CD81. Hepatology **46:**1722-1731.

25.	**Douam F, Dao Thi VL, Maurin G, Fresquet J, Mompelat D, Zeisel MB, Baumert TF, Cosset FL, Lavillette D.** 2014. Critical interaction between E1 and E2 glycoproteins determines binding and fusion properties of hepatitis C virus during cell entry. Hepatology **59:**776-788.

26.	**Benedicto I, Molina-Jimenez F, Barreiro O, Maldonado-Rodriguez A, Prieto J, Moreno-Otero R, Aldabe R, Lopez-Cabrera M, Majano PL.** 2008. Hepatitis C virus envelope components alter localization of hepatocyte tight junction-associated proteins and promote occludin retention in the endoplasmic reticulum. Hepatology **48:**1044-1053.

27.	**Coyne CB, Shen L, Turner JR, Bergelson JM.** 2007. Coxsackievirus entry across epithelial tight junctions requires occludin and the small GTPases Rab34 and Rab5. Cell Host Microbe **2:**181-192.

28.	**Burlone ME, Budkowska A.** 2009. Hepatitis C virus cell entry: role of lipoproteins and cellular receptors. J Gen Virol **90:**1055-1070.

29. **Samreen B, Khaliq S, Ashfaq UA, Khan M, Afzal N, Shahzad MA, Riaz S, Jahan S.** 2012. Hepatitis C virus entry: role of host and viral factors. Infect Genet Evol **12:**1699-1709.
30. **Dubuisson J, Cosset FL.** 2014. Virology and cell biology of the hepatitis C virus life cycle: an update. J Hepatol **61:**S3-s13.
31. **Dorner M, Horwitz JA, Robbins JB, Barry WT, Feng Q, Mu K, Jones CT, Schoggins JW, Catanese MT, Burton DR, Law M, Rice CM, Ploss A.** 2011. A genetically humanized mouse model for hepatitis C virus infection. Nature **474:**208-211.
32. **Blanchard E, Belouzard S, Goueslain L, Wakita T, Dubuisson J, Wychowski C, Rouille Y.** 2006. Hepatitis C virus entry depends on clathrin-mediated endocytosis. J Virol **80:**6964-6972.
33. **Meertens L, Bertaux C, Dragic T.** 2006. Hepatitis C virus entry requires a critical postinternalization step and delivery to early endosomes via clathrin-coated vesicles. J Virol **80:**11571-11578.
34. **Egger D, Wolk B, Gosert R, Bianchi L, Blum HE, Moradpour D, Bienz K.** 2002. Expression of hepatitis C virus proteins induces distinct membrane alterations including a candidate viral replication complex. J Virol **76:**5974-5984.
35. **Gosert R, Egger D, Lohmann V, Bartenschlager R, Blum HE, Bienz K, Moradpour D.** 2003. Identification of the hepatitis C virus RNA replication complex in Huh-7 cells harboring subgenomic replicons. J Virol **77:**5487-5492.
36. **Lohmann V, Korner F, Koch J, Herian U, Theilmann L, Bartenschlager R.** 1999. Replication of subgenomic hepatitis C virus RNAs in a hepatoma cell line. Science **285:**110-113.
37. **Shi ST, Lee KJ, Aizaki H, Hwang SB, Lai MM.** 2003. Hepatitis C virus RNA replication occurs on a detergent-resistant membrane that cofractionates with caveolin-2. J Virol **77:**4160-4168.
38. **Sakamoto H, Okamoto K, Aoki M, Kato H, Katsume A, Ohta A, Tsukuda T, Shimma N, Aoki Y, Arisawa M, Kohara M, Sudoh M.** 2005. Host sphingolipid biosynthesis as a target for hepatitis C virus therapy. Nat Chem Biol **1:**333-337.
39. **Wang C, Gale M, Jr., Keller BC, Huang H, Brown MS, Goldstein JL, Ye J.** 2005. Identification of FBL2 as a geranylgeranylated cellular protein required for hepatitis C virus RNA replication. Mol Cell **18:**425-434.
40. **Boulant S, Targett-Adams P, McLauchlan J.** 2007. Disrupting the association of hepatitis C virus core protein with lipid droplets correlates with a loss in production of infectious virus. J Gen Virol **88:**2204-2213.
41. **Boson B, Granio O, Bartenschlager R, Cosset FL.** 2011. A concerted action of hepatitis C virus p7 and nonstructural protein 2 regulates core localization at the endoplasmic reticulum and virus assembly. PLoS Pathog **7:**e1002144.
42. **Counihan NA, Rawlinson SM, Lindenbach BD.** 2011. Trafficking of hepatitis C virus core protein during virus particle assembly. PLoS Pathog **7:**e1002302.
43. **Masaki T, Suzuki R, Murakami K, Aizaki H, Ishii K, Murayama A, Date T, Matsuura Y, Miyamura T, Wakita T, Suzuki T.** 2008. Interaction of hepatitis C virus nonstructural protein 5A with core protein is critical for the production of infectious virus particles. J Virol **82:**7964-7976.
44. **Tellinghuisen TL, Foss KL, Treadaway J.** 2008. Regulation of hepatitis C virion production via phosphorylation of the NS5A protein. PLoS Pathog **4:**e1000032.

45. **Masaki T, Matsunaga S, Takahashi H, Nakashima K, Kimura Y, Ito M, Matsuda M, Murayama A, Kato T, Hirano H, Endo Y, Lemon SM, Wakita T, Sawasaki T, Suzuki T.** 2014. Involvement of hepatitis C virus NS5A hyperphosphorylation mediated by casein kinase I-alpha in infectious virus production. J Virol **88:**7541-7555.
46. **Huang H, Sun F, Owen DM, Li W, Chen Y, Gale M, Jr., Ye J.** 2007. Hepatitis C virus production by human hepatocytes dependent on assembly and secretion of very low-density lipoproteins. Proc Natl Acad Sci U S A **104:**5848-5853.
47. **Corless L, Crump CM, Griffin SD, Harris M.** 2010. Vps4 and the ESCRT-III complex are required for the release of infectious hepatitis C virus particles. J Gen Virol **91:**362-372.
48. **Dreux M, Garaigorta U, Boyd B, Decembre E, Chung J, Whitten-Bauer C, Wieland S, Chisari FV.** 2012. Short-range exosomal transfer of viral RNA from infected cells to plasmacytoid dendritic cells triggers innate immunity. Cell Host Microbe **12:**558-570.
49. **Ramakrishnaiah V, Thumann C, Fofana I, Habersetzer F, Pan Q, de Ruiter PE, Willemsen R, Demmers JA, Stalin Raj V, Jenster G, Kwekkeboom J, Tilanus HW, Haagmans BL, Baumert TF, van der Laan LJ.** 2013. Exosome-mediated transmission of hepatitis C virus between human hepatoma Huh7.5 cells. Proc Natl Acad Sci U S A **110:**13109-13113.
50. **Pfeifer U.** 1978. Inhibition by insulin of the formation of autophagic vacuoles in rat liver. A morphometric approach to the kinetics of intracellular degradation by autophagy. J Cell Biol **78:**152-167.
51. **Wirth M, Joachim J, Tooze SA.** 2013. Autophagosome formation--the role of ULK1 and Beclin1-PI3KC3 complexes in setting the stage. Semin Cancer Biol **23:**301-309.
52. **Lin MG, Hurley JH.** 2016. Structure and function of the ULK1 complex in autophagy. Curr Opin Cell Biol **39:**61-68.
53. **Gallagher LE, Chan EY.** 2013. Early signalling events of autophagy. Essays Biochem **55:**1-15.
54. **Axe EL, Walker SA, Manifava M, Chandra P, Roderick HL, Habermann A, Griffiths G, Ktistakis NT.** 2008. Autophagosome formation from membrane compartments enriched in phosphatidylinositol 3-phosphate and dynamically connected to the endoplasmic reticulum. J Cell Biol **182:**685-701.
55. **Nakatogawa H.** 2013. Two ubiquitin-like conjugation systems that mediate membrane formation during autophagy. Essays Biochem **55:**39-50.
56. **Ragusa MJ, Stanley RE, Hurley JH.** 2012. Architecture of the Atg17 complex as a scaffold for autophagosome biogenesis. Cell **151:**1501-1512.
57. **Knaevelsrud H, Carlsson SR, Simonsen A.** 2013. SNX18 tubulates recycling endosomes for autophagosome biogenesis. Autophagy **9:**1639-1641.
58. **Hegedus K, Takats S, Boda A, Jipa A, Nagy P, Varga K, Kovacs AL, Juhasz G.** 2016. The Ccz1-Mon1-Rab7 module and Rab5 control distinct steps of autophagy. Mol Biol Cell doi:10.1091/mbc.E16-03-0205.
59. **Bucci C, Thomsen P, Nicoziani P, McCarthy J, van Deurs B.** 2000. Rab7: a key to lysosome biogenesis. Mol Biol Cell **11:**467-480.
60. **Rink J, Ghigo E, Kalaidzidis Y, Zerial M.** 2005. Rab conversion as a mechanism of progression from early to late endosomes. Cell **122:**735-749.
61. **Poteryaev D, Datta S, Ackema K, Zerial M, Spang A.** 2010. Identification of the switch in early-to-late endosome transition. Cell **141:**497-508.

62. **Berg TO, Fengsrud M, Stromhaug PE, Berg T, Seglen PO.** 1998. Isolation and characterization of rat liver amphisomes. Evidence for fusion of autophagosomes with both early and late endosomes. J Biol Chem **273:**21883-21892.

63. **Fader CM, Sanchez D, Furlan M, Colombo MI.** 2008. Induction of autophagy promotes fusion of multivesicular bodies with autophagic vacuoles in k562 cells. Traffic **9:**230-250.

64. **Jager S, Bucci C, Tanida I, Ueno T, Kominami E, Saftig P, Eskelinen EL.** 2004. Role for Rab7 in maturation of late autophagic vacuoles. J Cell Sci **117:**4837-4848.

65. **Gutierrez MG, Munafo DB, Beron W, Colombo MI.** 2004. Rab7 is required for the normal progression of the autophagic pathway in mammalian cells. J Cell Sci **117:**2687-2697.

66. **Sun Q, Westphal W, Wong KN, Tan I, Zhong Q.** 2010. Rubicon controls endosome maturation as a Rab7 effector. Proc Natl Acad Sci U S A **107:**19338-19343.

67. **Liang C, Lee JS, Inn KS, Gack MU, Li Q, Roberts EA, Vergne I, Deretic V, Feng P, Akazawa C, Jung JU.** 2008. Beclin1-binding UVRAG targets the class C Vps complex to coordinate autophagosome maturation and endocytic trafficking. Nat Cell Biol **10:**776-787.

68. **Kochl R, Hu XW, Chan EY, Tooze SA.** 2006. Microtubules facilitate autophagosome formation and fusion of autophagosomes with endosomes. Traffic **7:**129-145.

69. **Johansson M, Rocha N, Zwart W, Jordens I, Janssen L, Kuijl C, Olkkonen VM, Neefjes J.** 2007. Activation of endosomal dynein motors by stepwise assembly of Rab7-RILP-p150Glued, ORP1L, and the receptor betalll spectrin. J Cell Biol **176:**459-471.

70. **Jordens I, Fernandez-Borja M, Marsman M, Dusseljee S, Janssen L, Calafat J, Janssen H, Wubbolts R, Neefjes J.** 2001. The Rab7 effector protein RILP controls lysosomal transport by inducing the recruitment of dynein-dynactin motors. Curr Biol **11:**1680-1685.

71. **Wijdeven RH, Janssen H, Nahidiazar L, Janssen L, Jalink K, Berlin I, Neefjes J.** 2016. Cholesterol and ORP1L-mediated ER contact sites control autophagosome transport and fusion with the endocytic pathway. Nat Commun **7:**11808.

72. **Pankiv S, Alemu EA, Brech A, Bruun JA, Lamark T, Overvatn A, Bjorkoy G, Johansen T.** 2010. FYCO1 is a Rab7 effector that binds to LC3 and PI3P to mediate microtubule plus end-directed vesicle transport. J Cell Biol **188:**253-269.

73. **Kimura S, Noda T, Yoshimori T.** 2008. Dynein-dependent movement of autophagosomes mediates efficient encounters with lysosomes. Cell Struct Funct **33:**109-122.

74. **Jahreiss L, Menzies FM, Rubinsztein DC.** 2008. The itinerary of autophagosomes: from peripheral formation to kiss-and-run fusion with lysosomes. Traffic **9:**574-587.

75. **Kummel D, Ungermann C.** 2014. Principles of membrane tethering and fusion in endosome and lysosome biogenesis. Curr Opin Cell Biol **29C:**61-66.

76. **McEwan DG, Popovic D, Gubas A, Terawaki S, Suzuki H, Stadel D, Coxon FP, Miranda de Stegmann D, Bhogaraju S, Maddi K, Kirchof A, Gatti E, Helfrich MH, Wakatsuki S, Behrends C, Pierre P, Dikic I.** 2015. PLEKHM1 regulates autophagosome-lysosome fusion through HOPS complex and LC3/GABARAP proteins. Mol Cell **57:**39-54.

77. **Jahn R, Scheller RH.** 2006. SNAREs--engines for membrane fusion. Nat Rev Mol Cell Biol **7:**631-643.

78. **Itakura E, Kishi-Itakura C, Mizushima N.** 2012. The hairpin-type tail-anchored SNARE syntaxin 17 targets to autophagosomes for fusion with endosomes/lysosomes. Cell **151:**1256-1269.

79. **Jiang P, Nishimura T, Sakamaki Y, Itakura E, Hatta T, Natsume T, Mizushima N.** 2014. The HOPS complex mediates autophagosome-lysosome fusion through interaction with syntaxin 17. Mol Biol Cell **25:**1327-1337.

80. **Lee JH, Yu WH, Kumar A, Lee S, Mohan PS, Peterhoff CM, Wolfe DM, Martinez-Vicente M, Massey AC, Sovak G, Uchiyama Y, Westaway D, Cuervo AM, Nixon RA.** 2010. Lysosomal proteolysis and autophagy require presenilin 1 and are disrupted by Alzheimer-related PS1 mutations. Cell **141:**1146-1158.

81. **Koike M, Shibata M, Waguri S, Yoshimura K, Tanida I, Kominami E, Gotow T, Peters C, von Figura K, Mizushima N, Saftig P, Uchiyama Y.** 2005. Participation of autophagy in storage of lysosomes in neurons from mouse models of neuronal ceroid-lipofuscinoses (Batten disease). Am J Pathol **167:**1713-1728.

82. **Dennemarker J, Lohmuller T, Muller S, Aguilar SV, Tobin DJ, Peters C, Reinheckel T.** 2010. Impaired turnover of autophagolysosomes in cathepsin L deficiency. Biol Chem **391:**913-922.

83. **Yang Z, Huang J, Geng J, Nair U, Klionsky DJ.** 2006. Atg22 recycles amino acids to link the degradative and recycling functions of autophagy. Mol Biol Cell **17:**5094-5104.

84. **Yu L, McPhee CK, Zheng L, Mardones GA, Rong Y, Peng J, Mi N, Zhao Y, Liu Z, Wan F, Hailey DW, Oorschot V, Klumperman J, Baehrecke EH, Lenardo MJ.** 2010. Termination of autophagy and reformation of lysosomes regulated by mTOR. Nature **465:**942-946.

85. **Hofmann I, Munro S.** 2006. An N-terminally acetylated Arf-like GTPase is localised to lysosomes and affects their motility. J Cell Sci **119:**1494-1503.

86. **Bagshaw RD, Callahan JW, Mahuran DJ.** 2006. The Arf-family protein, Arl8b, is involved in the spatial distribution of lysosomes. Biochem Biophys Res Commun **344:**1186-1191.

87. **Rosa-Ferreira C, Munro S.** 2011. Arl8 and SKIP act together to link lysosomes to kinesin-1. Dev Cell **21:**1171-1178.

88. **Pu J, Schindler C, Jia R, Jarnik M, Backlund P, Bonifacino JS.** 2015. BORC, a multisubunit complex that regulates lysosome positioning. Dev Cell **33:**176-188.

89. **Brocker C, Kuhlee A, Gatsogiannis C, Balderhaar HJ, Honscher C, Engelbrecht-Vandre S, Ungermann C, Raunser S.** 2012. Molecular architecture of the multisubunit homotypic fusion and vacuole protein sorting (HOPS) tethering complex. Proc Natl Acad Sci U S A **109:**1991-1996.

90. **Mrakovic A, Kay JG, Furuya W, Brumell JH, Botelho RJ.** 2012. Rab7 and Arl8 GTPases are Necessary for Lysosome Tubulation in Macrophages. Traffic doi:10.1111/tra.12003.

91. **Saric A, Hipolito VE, Kay JG, Canton J, Antonescu CN, Botelho RJ.** 2016. mTOR controls lysosome tubulation and antigen presentation in macrophages and dendritic cells. Mol Biol Cell **27:**321-333.

92. **Johnson DE, Ostrowski P, Jaumouille V, Grinstein S.** 2016. The position of lysosomes within the cell determines their luminal pH. J Cell Biol **212:**677-692.

93. **Korolchuk VI, Saiki S, Lichtenberg M, Siddiqi FH, Roberts EA, Imarisio S, Jahreiss L, Sarkar S, Futter M, Menzies FM, O'Kane CJ, Deretic V, Rubinsztein**

DC. 2011. Lysosomal positioning coordinates cellular nutrient responses. Nat Cell Biol **13:**453-460.

94. **Kaniuk NA, Canadien V, Bagshaw RD, Bakowski M, Braun V, Landekic M, Mitra S, Huang J, Heo WD, Meyer T, Pelletier L, Andrews-Polymenis H, McClelland M, Pawson T, Grinstein S, Brumell JH.** 2011. Salmonella exploits Arl8B-directed kinesin activity to promote endosome tubulation and cell-to-cell transfer. Cell Microbiol **13:**1812-1823.

95. **Nishikiori M, Mori M, Dohi K, Okamura H, Katoh E, Naito S, Meshi T, Ishikawa M.** 2011. A host small GTP-binding protein ARL8 plays crucial roles in tobamovirus RNA replication. PLoS Pathog **7:**e1002409.

96. **Ait-Goughoulte M, Kanda T, Meyer K, Ryerse JS, Ray RB, Ray R.** 2008. Hepatitis C virus genotype 1a growth and induction of autophagy. J Virol **82:**2241-2249.

97. **Sir D, Chen WL, Choi J, Wakita T, Yen TS, Ou JH.** 2008. Induction of incomplete autophagic response by hepatitis C virus via the unfolded protein response. Hepatology **48:**1054-1061.

98. **Shinohara Y, Imajo K, Yoneda M, Tomeno W, Ogawa Y, Kirikoshi H, Funakoshi K, Ikeda M, Kato N, Nakajima A, Saito S.** 2013. Unfolded protein response pathways regulate Hepatitis C virus replication via modulation of autophagy. Biochem Biophys Res Commun **432:**326-332.

99. **Chakrabarti A, Chen AW, Varner JD.** 2011. A review of the mammalian unfolded protein response. Biotechnol Bioeng **108:**2777-2793.

100. **Huang H, Kang R, Wang J, Luo G, Yang W, Zhao Z.** 2013. Hepatitis C virus inhibits AKT-tuberous sclerosis complex (TSC), the mechanistic target of rapamycin (MTOR) pathway, through endoplasmic reticulum stress to induce autophagy. Autophagy **9:**175-195.

101. **Mohl BP, Tedbury PR, Griffin S, Harris M.** 2012. Hepatitis C virus induced autophagy is independent of the unfolded protein response. J Virol doi:10.1128/jvi.01667-12.

102. **Dreux M, Gastaminza P, Wieland SF, Chisari FV.** 2009. The autophagy machinery is required to initiate hepatitis C virus replication. Proc Natl Acad Sci U S A **106:**14046-14051.

103. **Shrivastava S, Bhanja Chowdhury J, Steele R, Ray R, Ray RB.** 2012. Hepatitis C virus upregulates Beclin1 for induction of autophagy and activates mTOR signaling. J Virol **86:**8705-8712.

104. **Mohl BP, Bartlett C, Mankouri J, Harris M.** 2016. Early events in the generation of autophagosomes are required for the formation of membrane structures involved in hepatitis C virus genome replication. J Gen Virol **97:**680-693.

105. **Su WC, Chao TC, Huang YL, Weng SC, Jeng KS, Lai MM.** 2011. Rab5 and class III phosphoinositide 3-kinase Vps34 are involved in hepatitis C virus NS4B-induced autophagy. J Virol **85:**10561-10571.

106. **Ferraris P, Blanchard E, Roingeard P.** 2010. Ultrastructural and biochemical analyses of hepatitis C virus-associated host cell membranes. J Gen Virol **91:**2230-2237.

107. **Sir D, Kuo CF, Tian Y, Liu HM, Huang EJ, Jung JU, Machida K, Ou JH.** 2012. Replication of hepatitis C virus RNA on autophagosomal membranes. J Biol Chem **287:**18036-18043.

108. **Guevin C, Manna D, Belanger C, Konan KV, Mak P, Labonte P.** 2010. Autophagy protein ATG5 interacts transiently with the hepatitis C virus RNA polymerase (NS5B) early during infection. Virology **405:**1-7.

109. **Ke PY, Chen SS.** 2011. Activation of the unfolded protein response and autophagy after hepatitis C virus infection suppresses innate antiviral immunity in vitro. J Clin Invest **121:**37-56.

110. **Wang L, Tian Y, Ou JH.** 2015. HCV induces the expression of Rubicon and UVRAG to temporally regulate the maturation of autophagosomes and viral replication. PLoS Pathog **11:**e1004764.

111. **Ren H, Elgner F, Jiang B, Himmelsbach K, Medvedev R, Ploen D, Hildt E.** 2016. The autophagosomal SNARE protein syntaxin 17 is an essential factor for the hepatitis C virus life cycle. J Virol doi:10.1128/jvi.00551-16.

112. **Tanida I, Fukasawa M, Ueno T, Kominami E, Wakita T, Hanada K.** 2009. Knockdown of autophagy-related gene decreases the production of infectious hepatitis C virus particles. Autophagy **5:**937-945.

113. **Shrivastava S, Raychoudhuri A, Steele R, Ray R, Ray RB.** 2011. Knockdown of autophagy enhances the innate immune response in hepatitis C virus-infected hepatocytes. Hepatology **53:**406-414.

114. **Shrivastava S, Devhare P, Sujijantarat N, Steele R, Kwon YC, Ray R, Ray RB.** 2016. Knockdown of Autophagy Inhibits Infectious Hepatitis C Virus Release by the Exosomal Pathway. J Virol **90:**1387-1396.

115. **Rautou PE, Cazals-Hatem D, Feldmann G, Mansouri A, Grodet A, Barge S, Martinot-Peignoux M, Duces A, Bieche I, Lebrec D, Bedossa P, Paradis V, Marcellin P, Valla D, Asselah T, Moreau R.** 2011. Changes in autophagic response in patients with chronic hepatitis C virus infection. Am J Pathol **178:**2708-2715.

116. **Gutierrez MG, Master SS, Singh SB, Taylor GA, Colombo MI, Deretic V.** 2004. Autophagy is a defense mechanism inhibiting BCG and Mycobacterium tuberculosis survival in infected macrophages. Cell **119:**753-766.

117. **Moy RH, Gold B, Molleston JM, Schad V, Yanger K, Salzano MV, Yagi Y, Fitzgerald KA, Stanger BZ, Soldan SS, Cherry S.** 2014. Antiviral autophagy restrictsRift Valley fever virus infection and is conserved from flies to mammals. Immunity **40:**51-65.

118. **Paludan C, Schmid D, Landthaler M, Vockerodt M, Kube D, Tuschl T, Munz C.** 2005. Endogenous MHC class II processing of a viral nuclear antigen after autophagy. Science **307:**593-596.

119. **Kim HJ, Lee S, Jung JU.** 2010. When autophagy meets viruses: a double-edged sword with functions in defense and offense. Semin Immunopathol **32:**323-341.

120. **Lennemann NJ, Coyne CB.** 2015. Catch me if you can: the link between autophagy and viruses. PLoS Pathog **11:**e1004685.

121. **Kato T, Date T, Murayama A, Morikawa K, Akazawa D, Wakita T.** 2006. Cell culture and infection system for hepatitis C virus. Nat Protoc **1:**2334-2339.

122. **Koga H, Kaushik S, Cuervo AM.** 2010. Altered lipid content inhibits autophagic vesicular fusion. FASEB J **24:**3052-3065.

123. **Wakita T, Pietschmann T, Kato T, Date T, Miyamoto M, Zhao Z, Murthy K, Habermann A, Krausslich HG, Mizokami M, Bartenschlager R, Liang TJ.** 2005.

Production of infectious hepatitis C virus in tissue culture from a cloned viral genome. Nat Med **11:**791-796.

124. **Blight KJ, McKeating JA, Rice CM.** 2002. Highly permissive cell lines for subgenomic and genomic hepatitis C virus RNA replication. J Virol **76:**13001-13014.

125. **Sumpter R, Jr., Loo YM, Foy E, Li K, Yoneyama M, Fujita T, Lemon SM, Gale M, Jr.** 2005. Regulating intracellular antiviral defense and permissiveness to hepatitis C virus RNA replication through a cellular RNA helicase, RIG-I. J Virol **79:**2689-2699.

126. **Yamamoto A, Tagawa Y, Yoshimori T, Moriyama Y, Masaki R, Tashiro Y.** 1998. Bafilomycin A1 prevents maturation of autophagic vacuoles by inhibiting fusion between autophagosomes and lysosomes in rat hepatoma cell line, H-4-II-E cells. Cell Struct Funct **23:**33-42.

127. **Klionsky DJ, Abdalla FC, Abeliovich H, Abraham RT, Acevedo-Arozena A, Adeli K, Agholme L, Agnello M, Agostinis P, Aguirre-Ghiso JA, Ahn HJ, Ait-Mohamed O, Ait-Si-Ali S, Akematsu T, Akira S, Al-Younes HM, Al-Zeer MA, Albert ML, Albin RL, Alegre-Abarrategui J, Aleo MF, Alirezaei M, Almasan A, Almonte-Becerril M, Amano A, Amaravadi R, Amarnath S, Amer AO, Andrieu-Abadie N, Anantharam V, Ann DK, Anoopkumar-Dukie S, Aoki H, Apostolova N, Arancia G, Aris JP, Asanuma K, Asare NY, Ashida H, Askanas V, Askew DS, Auberger P, Baba M, Backues SK, Baehrecke EH, Bahr BA, Bai XY, Bailly Y, Baiocchi R, Baldini G, et al.** 2012. Guidelines for the use and interpretation of assays for monitoring autophagy. Autophagy **8:**445-544.

128. **Blight KJ, Norgard EA.** 2006. HCV Replicon Systems. *In* Tan SL (ed), Hepatitis C Viruses: Genomes and Molecular Biology. Horizon Bioscience., Norfolk (UK).

129. **Aggarwal N, Sloane BF.** 2014. Cathepsin B: multiple roles in cancer. Proteomics Clin Appl **8:**427-437.

130. **Creasy BM, Hartmann CB, White FK, McCoy KL.** 2007. New assay using fluorogenic substrates and immunofluorescence staining to measure cysteine cathepsin activity in live cell subpopulations. Cytometry A **71:**114-123.

131. **Zaidi N, Maurer A, Nieke S, Kalbacher H.** 2008. Cathepsin D: a cellular roadmap. Biochem Biophys Res Commun **376:**5-9.

132. **Kimura S, Noda T, Yoshimori T.** 2007. Dissection of the autophagosome maturation process by a novel reporter protein, tandem fluorescent-tagged LC3. Autophagy **3:**452-460.

133. **Hailey DW, Lippincott-Schwartz J.** 2009. Using photoactivatable proteins to monitor autophagosome lifetime. Methods Enzymol **452:**25-45.

134. **Cuervo AM, Dice JF, Knecht E.** 1997. A population of rat liver lysosomes responsible for the selective uptake and degradation of cytosolic proteins. J Biol Chem **272:**5606-5615.

135. **Aweya JJ, Mak TM, Lim SG, Tan YJ.** 2013. The p7 protein of the hepatitis C virus induces cell death differently from the influenza A virus viroporin M2. Virus Res **172:**24-34.

136. **Di Paolo G, De Camilli P.** 2006. Phosphoinositides in cell regulation and membrane dynamics. Nature **443:**651-657.

137. **Shin HW, Hayashi M, Christoforidis S, Lacas-Gervais S, Hoepfner S, Wenk MR, Modregger J, Uttenweiler-Joseph S, Wilm M, Nystuen A, Frankel WN, Solimena M,**

De Camilli P, Zerial M. 2005. An enzymatic cascade of Rab5 effectors regulates phosphoinositide turnover in the endocytic pathway. J Cell Biol **170:**607-618.

138. **Chia PZ, Gleeson PA.** 2014. Membrane tethering. F1000Prime Rep **6:**74.

139. **Palmieri M, Impey S, Kang H, di Ronza A, Pelz C, Sardiello M, Ballabio A.** 2011. Characterization of the CLEAR network reveals an integrated control of cellular clearance pathways. Hum Mol Genet **20:**3852-3866.

140. **Settembre C, Di Malta C, Polito VA, Garcia Arencibia M, Vetrini F, Erdin S, Erdin SU, Huynh T, Medina D, Colella P, Sardiello M, Rubinsztein DC, Ballabio A.** 2011. TFEB links autophagy to lysosomal biogenesis. Science **332:**1429-1433.

141. **Kabanova A, Sanseviero F, Candi V, Gamberucci A, Gozzetti A, Campoccia G, Bocchia M, Baldari CT.** 2016. Human Cytotoxic T Lymphocytes Form Dysfunctional Immune Synapses with B Cells Characterized by Non-Polarized Lytic Granule Release. Cell Rep **15:**9-18.

142. **Dykes SS, Gray AL, Coleman DT, Saxena M, Stephens CA, Carroll JL, Pruitt K, Cardelli JA.** 2016. The Arf-like GTPase Arl8b is essential for three-dimensional invasive growth of prostate cancer in vitro and xenograft formation and growth in vivo. Oncotarget doi:10.18632/oncotarget.8832.

143. **Scherer J, Yi J, Vallee RB.** 2014. PKA-dependent dynein switching from lysosomes to adenovirus: A novel form of host-virus competition. J Cell Biol **205:**163-177.

144. **Cantalupo G, Alifano P, Roberti V, Bruni CB, Bucci C.** 2001. Rab-interacting lysosomal protein (RILP): the Rab7 effector required for transport to lysosomes. Embo j **20:**683-693.

145. **Progida C, Malerod L, Stuffers S, Brech A, Bucci C, Stenmark H.** 2007. RILP is required for the proper morphology and function of late endosomes. J Cell Sci **120:**3729-3737.

146. **Wang T, Hong W.** 2006. RILP interacts with VPS22 and VPS36 of ESCRT-II and regulates their membrane recruitment. Biochem Biophys Res Commun **350:**413-423.

147. **van der Kant R, Fish A, Janssen L, Janssen H, Krom S, Ho N, Brummelkamp T, Carette J, Rocha N, Neefjes J.** 2013. Late endosomal transport and tethering are coupled processes controlled by RILP and the cholesterol sensor ORP1L. J Cell Sci doi:10.1242/jcs.129270.

148. **Lin X, Yang T, Wang S, Wang Z, Yun Y, Sun L, Zhou Y, Xu X, Akazawa C, Hong W, Wang T.** 2014. RILP interacts with HOPS complex via VPS41 subunit to regulate endocytic trafficking. Sci Rep **4:**7282.

149. **Schroeder B, Schulze RJ, Weller SG, Sletten AC, Casey CA, McNiven MA.** 2015. The small GTPase Rab7 as a central regulator of hepatocellular lipophagy. Hepatology **61:**1896-1907.

150. **Li X, Rydzewski N, Hider A, Zhang X, Yang J, Wang W, Gao Q, Cheng X, Xu H.** 2016. A molecular mechanism to regulate lysosome motility for lysosome positioning and tubulation. Nat Cell Biol **18:**404-417.

151. **Belyy V, Schlager MA, Foster H, Reimer AE, Carter AP, Yildiz A.** 2016. The mammalian dynein-dynactin complex is a strong opponent to kinesin in a tug-of-war competition. Nat Cell Biol **18:**1018-1024.

152. **Hancock WO.** 2014. Bidirectional cargo transport: moving beyond tug of war. Nat Rev Mol Cell Biol **15:**615-628.

153. **Wozniak AL, Long A, Jones-Jamtgaard KN, Weinman SA.** 2016. Hepatitis C virus promotes virion secretion through cleavage of the Rab7 adaptor protein RILP. Proc Natl Acad Sci U S A **113:**12484-12489.

154. **Amaya C, Militello RD, Calligaris SD, Colombo MI.** 2016. Rab24 interacts with the Rab7/Rab interacting lysosomal protein complex to regulate endosomal degradation. Traffic doi:10.1111/tra.12431.

155. **Khatter D, Raina VB, Dwivedi D, Sindhwani A, Bahl S, Sharma M.** 2015. The small GTPase Arl8b regulates assembly of the mammalian HOPS complex to lysosomes. J Cell Sci doi:10.1242/jcs.162651.

156. **Urnavicius L, Zhang K, Diamant AG, Motz C, Schlager MA, Yu M, Patel NA, Robinson CV, Carter AP.** 2015. The structure of the dynactin complex and its interaction with dynein. Science **347:**1441-1446.

157. **Erie C, Sacino M, Houle L, Lu ML, Wei J.** 2015. Altered lysosomal positioning affects lysosomal functions in a cellular model of Huntington's disease. Eur J Neurosci **42:**1941-1951.

158. **Kroemer G, Jaattela M.** 2005. Lysosomes and autophagy in cell death control. Nat Rev Cancer **5:**886-897.

159. **Taguwa S, Kambara H, Fujita N, Noda T, Yoshimori T, Koike K, Moriishi K, Matsuura Y.** 2011. Dysfunction of autophagy participates in vacuole formation and cell death in cells replicating hepatitis C virus. J Virol **85:**13185-13194.

160. **Ruan J, Zheng H, Rong X, Rong X, Zhang J, Fang W, Zhao P, Luo R.** 2016. Over-expression of cathepsin B in hepatocellular carcinomas predicts poor prognosis of HCC patients. Mol Cancer **15:**17.

161. **Guignot J, Caron E, Beuzon C, Bucci C, Kagan J, Roy C, Holden DW.** 2004. Microtubule motors control membrane dynamics of Salmonella-containing vacuoles. J Cell Sci **117:**1033-1045.

162. **Harrison RE, Brumell JH, Khandani A, Bucci C, Scott CC, Jiang X, Finlay BB, Grinstein S.** 2004. Salmonella impairs RILP recruitment to Rab7 during maturation of invasion vacuoles. Mol Biol Cell **15:**3146-3154.

163. **D'Costa VM, Braun V, Landekic M, Shi R, Proteau A, McDonald L, Cygler M, Grinstein S, Brumell JH.** 2015. Salmonella Disrupts Host Endocytic Trafficking by SopD2-Mediated Inhibition of Rab7. Cell Rep **12:**1508-1518.

164. **Marsman M, Jordens I, Kuijl C, Janssen L, Neefjes J.** 2004. Dynein-mediated vesicle transport controls intracellular Salmonella replication. Mol Biol Cell **15:**2954-2964.

165. **Aizaki H, Lee KJ, Sung VM, Ishiko H, Lai MM.** 2004. Characterization of the hepatitis C virus RNA replication complex associated with lipid rafts. Virology **324:**450-461.

166. **Popescu CI, Riva L, Vlaicu O, Farhat R, Rouille Y, Dubuisson J.** 2014. Hepatitis C virus life cycle and lipid metabolism. Biology (Basel) **3:**892-921.

167. **Ploen D, Hafirassou ML, Himmelsbach K, Schille SA, Biniossek ML, Baumert TF, Schuster C, Hildt E.** 2013. TIP47 is associated with the hepatitis C virus and its interaction with Rab9 is required for release of viral particles. Eur J Cell Biol **92:**374-382.

168. **Solinger JA, Spang A.** 2013. Tethering complexes in the endocytic pathway: CORVET and HOPS. Febs j **280:**2743-2757.